PROCESSING OF REAL AND IMPLIED MOTION

Universiteit Utrecht

Jeannette Lorteije

2006

Functional Neurobiology
Department of Biology, Faculty of Science
Helmholtz Institute
Utrecht University
The Netherlands

ISBN-10: 90-393-4430-2
ISBN-13: 978-90-393-4430-9
Cover photography by Jeroen Warnaar (front) and Frits Kindt (backside)
Print: PrintPartners Ipskamp, Enschede

PROCESSING OF REAL AND IMPLIED MOTION

VERWERKING VAN ECHTE EN GEÏMPLICEERDE BEWEGING

(Met een samenvatting in het Nederlands)

Proefschrift

ter verkrijging van de graad doctor aan de Universiteit Utrecht
op gezag van de rector magnificus, prof. dr. W.H. Gispen
ingevolge het besluit van het college voor promoties
in het openbaar te verdedigen op
vrijdag 22 december 2006 des middags te 12.45 uur

door

Jeannette Agnes Maria Lorteije

geboren op 6 oktober 1977 te Waalre

Promotoren:	Prof. dr. A.V. van den Berg
	Prof. dr. J.L. Kenemans
Co-promotoren:	Dr. R.J.A. van Wezel
	Dr. T. Jellema

Het in dit proefschrift beschreven onderzoek werd uitgevoerd met financiële steun van het Helmholtz Instituut, de Nederlandse Organisatie voor Wetenschappelijk Onderzoek (NWO) en het Federaal Wetenschapsbeleid (België).

CONTENTS

Voor mijn ouders

PROLOGUE

Real motion is defined as a spatial displacement over time of objects or patterns. Implied motion is the dynamic information contained within a static representation of a moving object. To illustrate implied motion, please view the pictures of the horses on this page. Even though the pictures themselves are static, most people will recognize that the horse in the left picture was running at the moment the photograph was taken. The motion direction and maybe even the type of motion (gallop vs. trot or walk) are discernable. On the other hand, the horse on the right is clearly standing still and not implying motion. Many photographers, painters, cartoonist and sculptures successfully use implied motion in their work to evoke a sense of movement in observers, even though conveying motion by a static medium seems a great contradiction. It seems that perception of implied motion must rely on a specialized neural network in the brain, that combines static visual information with real motion processing. Therefore, to understand implied motion processing, it must be studied in combination with real motion processing.

In this thesis, I focus on processing of real and implied motion and their integration. The questions that will be investigated and discussed are how implied and real motion are processed, and where, when and what the functional benefits of integration may be. The studies that are discussed in this thesis will contribute to a further understanding of our brain and visual motion processing in particular.

GENERAL INTRODUCTION

Vision and the visual system

Visual processing starts in the retina, where visual information from the photoreceptors passes through a network of interneurons (bipolar cells, horizontal cells and amacrine cells), which then project onto ganglion cells. Ganglion cells can be divided into two groups: Parvo (P) ganglion cells and Magno (M) ganglion cells. P ganglion cells have sustained responses, small receptive fields, high spatial resolution and most P ganglions are activated by a restricted range of wavelengths of light or are in other words colour selective. M ganglion cells have transient responses, larger receptive fields, are sensitive to low luminance contrasts and are not sensitive to the colour of a stimulus.

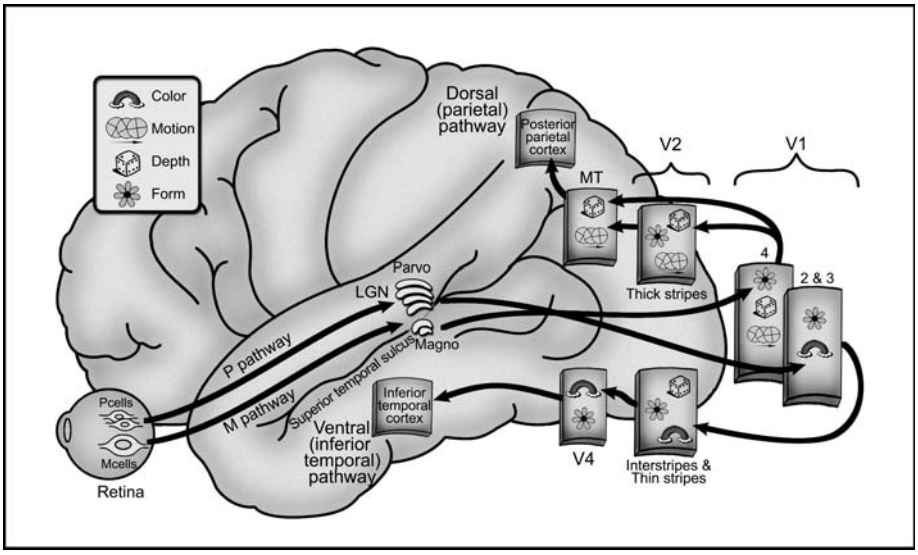

Figure 1
The visual system can be roughly divided into two main pathways, a parvocellular path leading from the retina to V1 and which may continue from V1 as a ventral stream leading towards the inferior temporal cortex; and a magnocellular path leading from the retina to V1 from which it may continue as a dorsal stream towards parietal cortex. (Figure modified from Kandel, Schwartz and Jessell, Principles of neural science, 4th edition.)

Ganglion cells have long axons that are bundled in the optic nerve, which projects onto the lateral geniculate nucleus (LGN). P ganglion cells project onto the parvocellular layers of the LGN, whereas M ganglion cells project onto the magnocellular layers of the LGN. This separation into a magnocellular and parvocellular trajectory is also maintained in the projection from the LGN onto different layers of the primary visual cortex (V1, also called striate cortex or area 17). From V1 onwards, visual information projects onto several extrastriate visual areas. These projections can be divided into two major pathways, a dorsal and ventral stream. These cortical streams, to some extent, seem to maintain the respectively magnocellular and parvocellular division (DeYoe & Van Essen, 1988) (Figure 1). The dorsal visual stream continuous from V1 to V2, V3 and leads to the middle temporal cortex (MT or V5) and further towards the parietal lobe. Since this trajectory leads from V1 in a dorsal direction, it is often referred to as the dorsal visual stream. This pathway is mainly involved in motion perception, stereopsis and spatial information processing. The ventral stream leads from V1 to V2, and further along V4 towards the temporal lobe. Since this trajectory continuous from V1 in a ventral direction, it is referred to as the ventral visual stream. This pathway is mainly specialized in processing colour and form information.

Based on the visual features that both pathways process, the ventral stream is also referred to as the “what” pathway, as it mainly processes information involved in object identification (Ungerleider & Mishkin, 1982). Likewise, the dorsal stream is referred to as the “where” pathway as it seems to be mainly involved in providing spatial information regarding the location and movement of objects (Ungerleider & Mishkin, 1982). Milner and Goodale (Goodale & Milner, 1992; Goodale *et al.*, 2004; Milner & Goodale, 1993) questioned the strict “what-where” dichotomy, and suggested that space and form are processed in both parietal and temporal areas, but for different purposes. In their view, the ventral stream subserves visual ‘perception’, object and scene recognition, and their enduring characteristics. By contrast, the dorsal stream is thought to subserve the visual control of ‘action’ (how to deal with objects). Thus vision for perception (ventral) versus vision for action (dorsal).

All proposed models of the ventral and dorsal division mention that this segregation is not complete and that integration of the two pathways occurs at various stages. Many dorsal and ventral areas are anatomically connected with each other, and visual features belonging to one stream can sometimes be vital for processing in the other stream. For instance, motion of a boundary defined by colour (and not luminance) evokes a response from motion sensitive cells in area MT, even though these neurons do not discriminate between

colours (Gegenfurtner & Hawken, 1996). Furthermore, even though visual processing may be divided across two cortical streams, on the conscious level all this information is again combined to a single united percept. We perceive a blue hopping bird as a blue hopping bird and not as a bird ánd a hopping motion ánd the colour blue as separate components. The question how different visual modalities (and other sensory modalities) are combined to a single percept is known as the binding problem. This thesis will focus on binding of form and motion information by studying implied and real motion. To understand implied motion processing, in relation to real motion processing, and with regard to how and where they may be integrated, a short review of the neural structures underlying real motion processing is required.

Motion perception

Motion perception is an enormous advantage for an organism when it needs to interact with a dynamic environment. As mentioned above, motion is processed along the dorsal stream, leading from area V1 along area V2 and area V3 to the middle temporal (MT) cortex, and further towards the inferior parietal lobe. Especially area MT is known for its crucial role in motion perception. Its primary function is to analyze the direction and speed of object motion in the visual world, as has been shown by a plethora of single-cell studies in monkeys (Britten *et al.*, 1996; Britten *et al.*, 1992; J. H. R. Maunsell & Newsome, 1987; Salzman *et al.*, 1992; S. M. Zeki, 1974, 1978) and imaging studies in humans (Sunaert *et al.*, 1999; Tootell *et al.*, 1995b). Besides motion sensitive, MT neurons can also be orientation selective (Albright, 1984), may be involved in stereopsis (DeAngelis *et al.*, 1998; DeAngelis & Newsome, 1999; DeAngelis & Uka, 2003), may combine motion, orientation and stereopsis information (Xiao *et al.*, 1997), and may play a role in directing eye-movements (Groh *et al.*, 1997).

Area MT is bordered by “satellite” motion regions. In studies using techniques with low spatial resolution (e.g., EEG and several fMRI studies) it is hard to discriminate between MT and surrounding motion processing areas. Therefore in human fMRI studies these areas together are often indicated as the human MT+ complex. From macaque single cell studies more is known about two satellite regions: the medial superior temporal (MST also called V5a) region and the fundus of the superior temporal (FST) region (Desimone & Ungerleider, 1986). Like MT, the more anterior MST area is mainly involved in motion processing, but it differs in the spatial preferences of the neurons. Generally, MST neurons have much larger receptive fields than MT neurons, which may overlap to ipsilateral locations (Desimone

& Ungerleider, 1986). Furthermore, MST neurons are often tuned to complex motion patterns, such as expansion, contraction and rotation (Duffy & Wurtz, 1991) or combinations of these components (Graziano *et al*., 1994), for which MT cells are not or less selective (Lagae *et al.*, 1994). MST is therefore a good candidate for optic flow processing (Smith *et al.*, 2006). Furthermore, in contrast to MT, MST BOLD responses to head centric optic flow can be modulated by visual smooth pursuit, which indicates that this area integrates vestibular and oculomotor information (Goossens *et al.*, 2006).

The other satellite area of MT, area FST, has not been studied as extensively as MT and MST. It has been reported that FST neurons generally have even larger receptive fields than MST neurons and that in comparison to MT and MST, it has a smaller proportion of neurons (30% of total) that respond to motion in particular directions, (Desimone & Ungerleider, 1986). However, a recent macaque fMRI study by Nelissen and colleagues (2006) shows that in fact many FST neurons respond to motion in a directionally selective manner. Area FST has connections with area V4, which is part of the ventral stream, and may thus be sensitive to form and colour as well as motion (Desimone & Ungerleider, 1986). Indeed, FST also seems to be involved in processing two and three dimensional structure from motion (Sereno *et al.*, 2002; Vanduffel *et al.*, 2002) and, even more interestingly for this thesis, together with areas MT, the newly defined lower superior temporal (LST) region and the middle part of the superior temporal polysensory (STP) region, it is involved in processing of directed actions as has been shown for hand movements (Nelissen *et al.*, 2006).

Two seperate motion processing channels?
Even though we as observers might experience low and high speeds as aspects of a continuous spectrum, psychophysical experiments have given rise to the idea of different processing pathways for low and high speeds, i.e., a low temporal frequency channel for motion with low speeds and a high temporal frequency channel that is tuned for motion with high speed (Anderson & Burr, 1985; Smith & Edgar, 1994; Thompson, 1984; Verstraten *et al.*, 1999; Verstraten *et al.*, 1998).

The high temporal frequency channel has transient responses, is tuned for low spatial frequencies and may correspond to motion processing along the dorsal visual pathway, whereas the low temporal frequency channel has sustained responses, is tuned for high spatial frequencies and may lie within the ventral stream. Based on these characteristics it has been postulated that the dorsal high frequency channel processes motion information while the ventral low frequency channel is involved in pattern and shape processing (Kulikowski, 1971;

van de Grind *et al.*, 2001). This ventral pathway may correspond to the dynamic form pathway as postulated by Zeki, for which area V3 may be an important processing stage (Gegenfurtner *et al.*, 1997; S. Zeki, 1993). However, no evidence exists that these channels are anatomically separated. If such segregation exists, the low frequency channel may also be involved in implied motion processing. Therefore, the neural structures underlying processing of slow and fast motion will be examined in chapter 2.

Implied motion

Photographs of people, animals and objects in motion are static images that do not contain real motion. The motion in the photograph (if any) is merely implied. Most people will however recognize motion implied by posture, articulation of arms and legs, and the overall imbalance of a body. Depending on the nature of movement that is implied, many people are even able to identify the type of motion and the direction in which the person or object is heading. Besides postural cues as described above, we can also use conventional cues to recognize implied motion. In cartoons for instance, motion is often indicated by speed lines behind a running person. Developmental studies have shown that young children (kindergarten, preschoolers and first-grade children) can already discriminate between implied moving and implied non-moving objects in pictures (Friedman & Stevenson, 1975). Third-grade children were more apt at interpreting the implied motion information than kindergarten children, which may indicate that at this age a sense of implied motion is still developing although third grade children may also generally perform better in a psychophysical task (Downs & Jenkins, 1996). Interestingly, young children (pre-school, kindergarten and first-graders) identified implied motion more accurately by postural cues than by conventional cartoon indicators of motion, whereas older “children” (grade-6 and college students) used both types of motion cues (Downs & Jenkins, 1996; Friedman & Stevenson, 1975). Recently, is has been shown that macaque MT neurons respond selectively to static cues, e.g., arrows, that the animal through training sessions had learned to associate with real motion, even though this conventional cue would not evoke selective responses from MT before associative learning (Schlack & Albright, 2005). This thesis will focus on implied motion from postural cues whose interpretation, according to the above mentioned studies, is acquired at an early developmental stage. Therefore, postural cues may be widely present in humans as well as other primates and animals, in contrast to conventional cues, for which more specific training seems required.

Two separate fMRI studies investigated the neural sources underlying (postural) implied motion processing in humans (Kourtzi & Kanwisher, 2000; Senior *et al.*, 2000). Interestingly, pictures with implied motion (Figure 2A and C) evoked a stronger BOLD response than pictures without implied motion (Figure 2B and D) in the hMT+ complex, even though this area was thought to be primarily involved in real motion perception. Besides visual responses to implied motion, observation and even imagery of hands expressing implied motion, may induce an increase in corticospinal excitability for the muscles that would be involved in the observed action (Urgesi *et al.*, 2006). Thus, visual implied motion affects even motor and premotor areas.

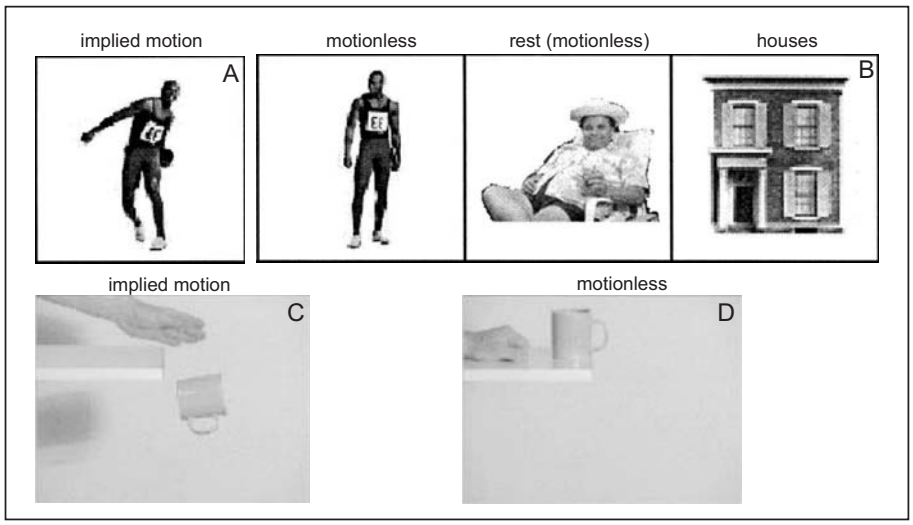

Figure 2
Photographs used in the experiments by Kourtzi and Kanwisher 2000 (above) and Senior *et al*. 2000 (below). Both compared fMRI BOLD responses to pictures of persons and objects with and without implied motion, while Kourtzi and Kanwisher additionally compared responses to implied motion with stimulus classes of other persons (rest) and objects (houses) without implied motion. (Figures printed with permission from the authors.)

Representational momentum

These findings might partly explain the spatial memory shifts that were found by Jennifer Freyd in a series of experiments in the early eighties. In one experiment she presented subjects briefly with one picture of an object or person (Freyd, 1983). This picture was a single frame taken from a movie-clip of that object or person in motion, for instance a person in midair after jumping off a fence. After a short interval, a second picture of that object or person was shown. This second picture could be the same movie frame as the first picture, or it could be slightly further or back in time relative to the first picture. Subjects had to indicate whether the second picture was identical or different from the first picture. Interestingly, subjects identified the second picture faster and more accurately as different when it was backwards in time, and slower and less accurately when it was forwards in time. She concluded that subjects mentally extrapolate the spatial position of the object in the first picture in the direction of its implied motion. In later experiments she called this representational momentum (RM), as a mental reference to physical momentum. RM is not only induced by motion implied in such single frames, but even more effectively by a sequence of isolated frames representing the subsequent stages of a continuous motion (Freyd & Finke, 1984). Also knowledge of the environment surrounding an object (e.g., gravity, friction) or even semantic cues as when words as “bounce” or “crash” are inserted causes or modulates RM effects. For a review on the extensive research that has been performed on RM see (Hubbard, 2005). The spatial displacement in remembered location could suggest involvement of motion processing areas. Activation of hMT+ as revealed by fMRI could be a neural correlate of the implied motion processing giving rise to the spatial memory shift. Furthermore, when MT+ was withheld from coherent firing by application of transcranial magnetic stimulation, the RM effect disappeared (Senior *et al.*, 2002), which indicates the functional necessity of MT+ for RM.

Projection from temporal lobe onto hMT+?

The question arises as to how the static implied motion information arrives in MT+, as this area is part of the dorsal stream, whereas implied motion consists of complex form information that is typically processed along the ventral stream. The ventral stream leads from V1, through V4 toward the end-stage of the ventral stream, the inferior temporal lobe (IT). Area IT contains neurons that are form and/or colour selective. Form preference of IT neurons can be highly specific, and since IT cells often have very large receptive fields, it is often retinotopically independent. Area IT is therefore a crucial stage in object recognition.

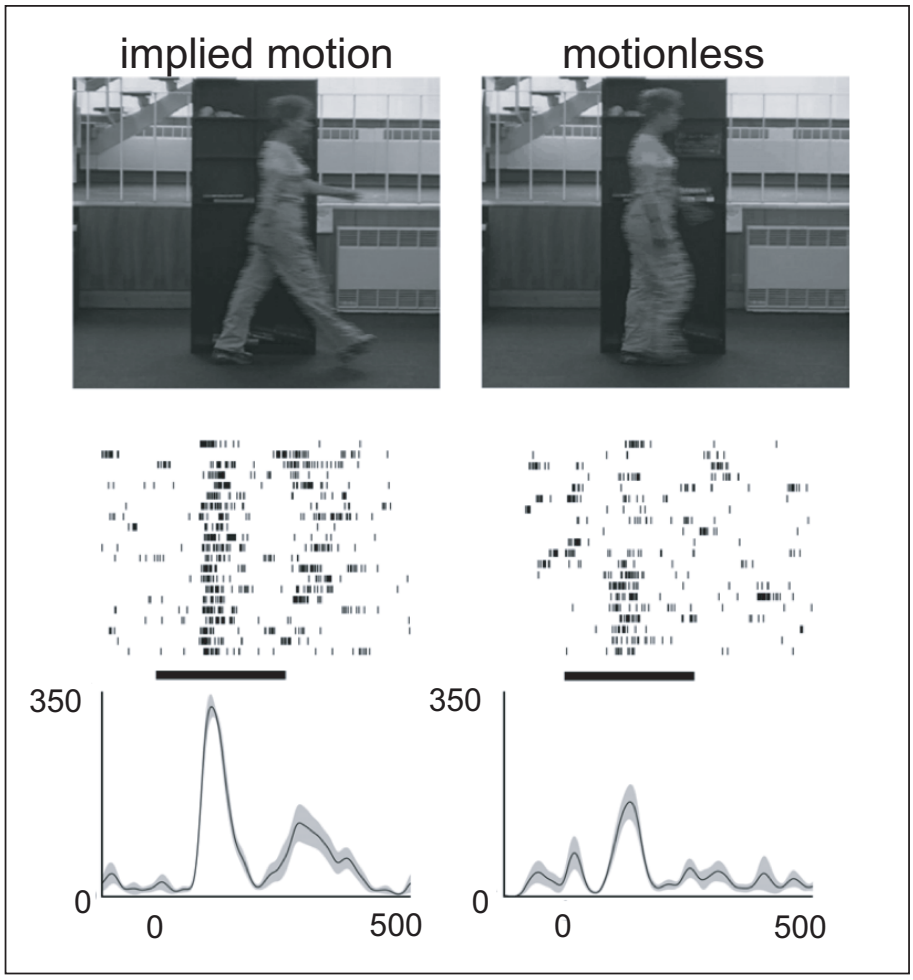

Figure 3
Responses of a single STS cell to a picture with implied motion (top left) and without implied motion (top right) reveal that this cell had a preference for stimuli containing (rightwards) implied motion. The middle figures show the actual action potential occurrence across time (-100 to 500 ms) per repetition. Black bars indicate stimulus presentation duration. Bottom graphs show the average response of the cell to both picture types (spikes/s). (Figure printed with permission from authors: Barraclough *et al*., 2006.)

If implied motion is processed along the ventral stream, how does this information end up in MT+? Area IT may project onto MT+ via a connection along the superior temporal sulcus (STS), during which the implied motion information may even be further processed. Indeed, areas in the Superior Temporal Sulcus (STS) seem to be specialized for the perception of bodily actions and postures in both macaque monkeys (Figure 3) (Barraclough *et al*., 2006; Jellema *et al.*, 2000; Jellema & Perrett, 2003a, 2003b) and humans (Allison *et al.*, 2000).

This proposed ventral-dorsal projection will be investigated in this thesis. The main specific questions that will be discussed are:

1) To what extent is the fMRI activation by implied motion in MT+ correlated with action potential frequencies of individual MT and MST neurons, in other words, are single MT and MST neurons selective for implied motion?

2) What are the temporal properties of the implied motion activation and how do they relate to the temporal properties of real motion processing?

3) Does the implied motion activation contain information regarding the direction of the implied motion, or does it correspond to an overall higher activation of all MT+ neurons?

4) Are the same MT+ neurons involved in both implied and real motion processing, or are different neural populations within MT+ involved in either type of motion?

SYNOPSIS

1. The first chapter considers the temporal properties of implied and real motion responses as recorded by human EEG. Implied motion evokes a response in a cortical region that is also involved in real motion processing, but this implied motion response is delayed compared to the real motion response, suggesting that the implied motion information reaches the motion processing areas via a longer route, probably via the temporal lobe.

2. In the second chapter, interactions between real motion and components of the implied motion VEPs will be investigated in a motion adaptation paradigm in humans. The delayed implied motion component that was identified in the first chapter can be modulated by motion adaptation in a direction specific manner, which is strong evidence that the same neurons process both real and implied motion in a direction selective manner. Furthermore, this chapter not only shows an integration stage of real and implied motion processing, but the direction specific nature of this integration reveals at least one functional benefit of implied motion processing, i.e., to supply the motion system with extra directional motion information of a moving object.

3. In the third chapter, real motion VEPs from an adaptation paradigm will be examined to reveal whether two different systems are present for motion processing; one for slow motion and one for fast motion. Dipole models of the scalp data suggest that high velocity motion is processed mainly by dorsal motion areas whereas low velocity motion is processed by these same dorsal regions as well as by additional ventral stream regions Thus implied motion and low velocity real motion may be processed by similar ventral areas, before a possible convergence with dorsal motion areas.

4. The responses of macaque MT and MST single cells and multi-units to implied motion are discussed in the fourth chapter. Both direct presentation of implied motion Figures in the receptive field of the cells, and modulation of the response to a dynamic noise pattern in the receptive field by implied motion on the fovea are examined. The response selectivity (or in-selectivity) to implied motion of MT and MST neurons is compared to the preferences of cells in the lower bank of the Superior Temporal Sulcus (STS). In contrast to STS, no consistent evidence was found for implied motion processing in MT and MST. Only a small preference for pictures of running vs. standing persons was found in MT, but a comparison with tilted and vertical bars revealed that this difference could be explained by size and orientation of the stimulus and not so much by implied motion.

5. The visual features underlying implied motion activation in MT+ are discussed in the final chapter. The difference in BOLD activation by pictures of humans with and without implied motion were compared to differences in BOLD activation by tilted vs. vertical bars, and by monkeys with and without implied motion within a natural setting. Human forms implying motion and tilted bars evoked stronger BOLD responses in area MT+ than human pictures without implied motion and vertical bars. Responses to monkey pictures were independent of the presence of implied motion. These results indicate that BOLD activation due to implied motion in area MT+ may be due to stimulus features as size and orientation.

Neuro-scientific techniques

Processing of implied and real motion will be investigated by combining the findings from several studies that are described in this thesis, which covered a range of neuro-scientific techniques. The major proportion of studies that will be discussed have used either electroencephalography, fMRI and/or extracellular recordings. Although none of the following chapters in this thesis are focused on psychophysics as a primary research technique, results from studies from others based on psychophysics will often be mentioned. Therefore this technique will be addressed here too.

Psychophysics
Psychophysics is a research method that studies the relationship between physical stimuli and their perception. In a typical psychophysical experiment, subjects report their percept of a stimulus. This report can be used to determine e.g., whether and how fast and correct a subject can detect and/or identify a stimulus, or can discriminate between two stimuli. Psychophysics is a non-invasive method, and describes the subject's own perceptual experience, which makes it especially suited for human research

Electroencephalography (EEG) and visually evoked potentials (VEPs)
Electroencephalography records electrical potentials from electrodes on the scalp, resulting in an electroencephalogram (EEG). The EEG mainly originates from post-synaptic potentials of populations of neurons that are located closely together and lie in the same direction from dendrite to axon, thus forming a neural dipole. The direction of this dipole is dependent on the location of the synaptic connection, also called source. If several neuronal regions are simultaneously active, the EEG represents their combined potential. In conventional EEG recordings, the scalp potential traces are recorded over time. Since the signal to noise ratio of an EEG recording is low, this method is not optimally suited to measure cortical responses to stimuli. Therefore, in an evoked potential paradigm, stimuli are presented

repeatedly and the EEG is cut into segments accordingly to the time of stimulus (or event) onset. Subsequently, the average EEG of these segments can be calculated. Averaging diminishes noise, thus revealing the event related potential (ERP). The EEG response thus recorded after presentation of a visual stimulus is called the visually evoked potential (VEP). The advantage of EEG is its very high temporal resolution, allowing for real-time read-out of fluctuating post-synaptic potentials, bounded only by the digital sample rate. On the downside, the spatial resolution of EEG is low. However, based on the scalp distribution of evoked potentials, the location of the underlying dipole activity can be roughly estimated, for instance with a program as BESA (brain electric source analysis). Even though this model technique has a spatial uncertainty of a few centimeters, it is very suitable to find relative differences between source activity in two or more experimental conditions (e.g., (Jonkman *et al.*, 2004; Kemner *et al.*, 2004; Kenemans *et al.*, 2002).

Functional magnetic resonance imaging (fMRI)
Functional MRI (fMRI) images the proportion of oxygenated vs. deoxygenated hemoglobin in the blood. Since oxygenated haemoglobin is diamagnetic whereas deoxygenated haemoglobin is paramagnetic, this proportion can be read as a slight difference in the MRI signal called the blood oxygenated level dependent (BOLD) response. Caution in interpreting the results obtained from fMRI should be taken as the relationship between neural activity and BOLD response is not well understood (Logothetis & Pfeuffer, 2004). It is generally assumed that neural activity consumes oxygen, which leads to an intitial regional decrease of oxygenated haemoglobin. This initial decrease is quickly overcompensated by an influx of oxygenated blood and activity can thus be measured as an increase in BOLD response. The BOLD response is correlated to local field potentials (which are also the source of evoked potentials) rather than to action potentials, which indicates that the BOLD response represents postsynaptic processes within a region instead of its output (Logothetis *et al.*, 2001). Furthermore, caution in interpreting the BOLD response should be taken as its relationship to regional cerebral blood flow is non-linear. fMRI is particularly popular because of its non invasive character and therefore can be applied in humans. Furthermore, compared to EEG recordings the spatial resolution is high (currently at the millimeter-scale and resolution is still rising). The temporal resolution has improved much with recent developments, but is still on seconds-scale because the blood flow is inherently slow. To the extent that the BOLD response and VEPs represent the same neural processes, they complement each other in spatial and temporal resolution.

Extracellular recordings
Microelectrodes placed inside the brain can record action potentials (spikes) from nearby neurons. Tip size (a few micrometer) and impedance (0.1 to 3 MΩ) determine the specificity of the signal. With smaller tip size and a higher impedance the recording is more likely to isolate the response from a single cell, while larger tips and lower impedances are it is more likely to pick up multi-unit activity from a small group of neurons. Spike sorting software enables identification of single-cell responses within a multi-unit recording. Extracellular recordings have a high temporal resolution, typically around 2000 Hz or more, although often spikes are binned into windows (10 to 100 ms) to represent spike frequency. The spatial resolution is high, as responses from a group of neurons to a single neuron can be measured.

Multi-disciplinary approach
Each technique that was used in this thesis has its own combination of spatial and temporal resolution (Figure 4) and disadvantages and advantages. The above described techniques vary in the way that the data represent the level at which a process takes place. While psychophysics demonstrates the percept of a subject or a group of subjects and EEG and fMRI reveal processes in brain regions, extracellular recordings measure the response from single cells or small groups of clustered cells. In this thesis, the results from experiments that have used different techniques will be combined, to establish a temporal and spatial vision on implied and real motion perception at different neural processing levels.

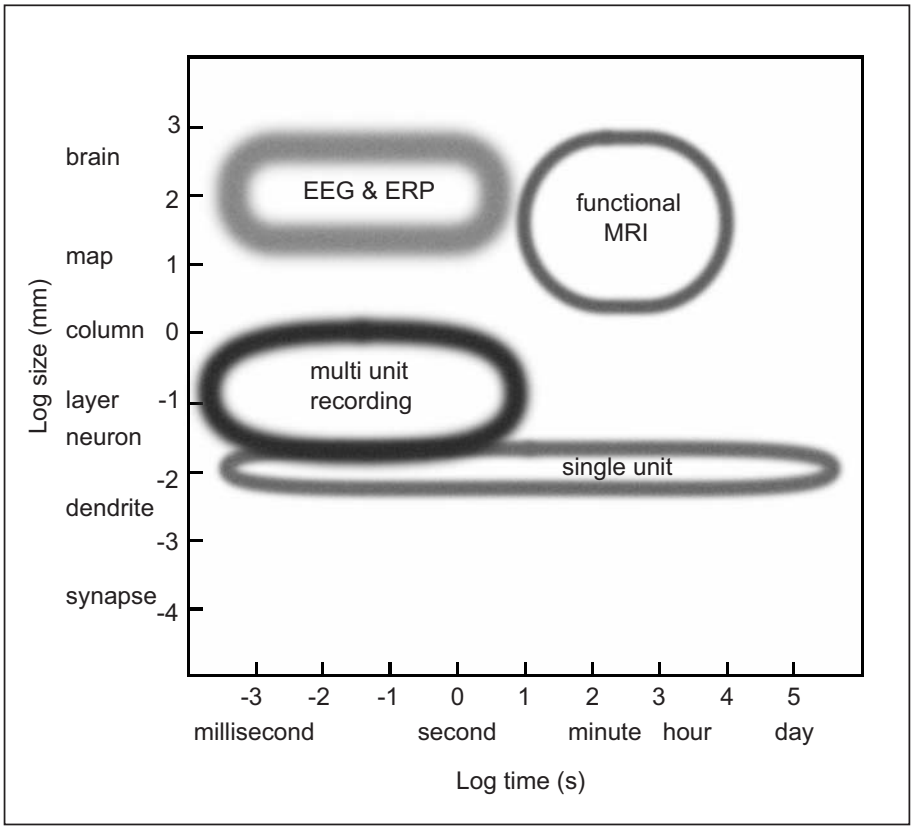

Figure 4
The four techniques that are used in this thesis have distinct spatial and temporal properties. Together they cover a large spatio-temporal area.

CHAPTER 1

DELAYED RESPONSE TO ANIMATE IMPLIED MOTION IN HUMAN MOTION PROCESSING AREAS

Abstract

Viewing static photographs of objects in motion evokes higher fMRI activation in human Middle Temporal complex (MT+) than looking at similar photographs without this implied motion. As MT+ is traditionally thought to be involved in motion perception (and not in form perception), this finding suggests feedback from object-recognition areas onto MT+. To investigate this hypothesis, we recorded extracranial potentials evoked by the sight of photographs of biological agents with and without implied motion. The difference in potential between responses to pictures with and without implied motion was maximal between 260 and 400 ms after stimulus onset. Source analysis of this difference revealed one bilateral, symmetrical dipole pair in the occipital lobe. This area also showed a response to real motion, but approximately 120 ms earlier than the implied motion response. The longer latency of the implied motion response in comparison to the real motion response is consistent with a feedback projection onto MT+ following object recognition in higher-level temporal areas.

Introduction

The accurate perception of motion cues is vital for interacting in a dynamic world. The processing of visual object motion in humans involves neuronal activity in specific brain areas, most notably the middle temporal areas (MT+, also called V5), which are located at the junction of the occipital, parietal and temporal lobes and are part of the dorsal visual pathway (Ungerleider & Mishkin, 1982). It is well established that the primary function of the MT+ complex is to analyze the direction and speed of object motion in the visual world, as shown by a plethora of single cell studies in monkeys (e.g., Britten *et al*., 1992) and imaging studies in humans (*e.g*., *Sunaert et al.*, 1999; Tootell *et al*., 1995).

Implied Motion

In addition to perceiving object motion per se, predicting a moving object's future position is critical for survival, e.g., for evading cars when crossing a busy street, or for aiming at fleeing animals when hunting. Human psychophysical studies have shown that observers extrapolate the remembered position of objects according to the direction of motion implied by form information (Freyd, 1983). Recently, there has been growing awareness that the classical motion sensitive areas do utilize static form information, especially when it implies motion. For example, functional MRI studies have shown a higher BOLD response to photographs of objects that imply motion (e.g., a running athlete or a cup falling from a table), than to photographs without implied motion (e.g., a sitting person or a cup on a table), in the human MT+ complex (hMT+) (Kourtzi & Kanwisher, 2000; Senior *et al*., 2000). Furthermore, when coherent firing in this area is disrupted by application of transcranial magnetic stimulation, the mental extrapolation of the location of an object implying motion disappears, indicating the functional necessity of hMT+ for implied motion perception (Senior *et al*., 2002). Additionally, Krekelberg *et al*., (2003) showed that monkey MT also processes motion implied by the inanimate form information of Glass patterns.

These findings are surprising, since form processing is thought to occur along the ventral pathway (Ungerleider & Mishkin, 1982). It raises the question how (animate) implied motion information arrives in hMT+. If it is via feedback from higher processing centers, then the latency of hMT+ activation should be increased relative to activation by real motion, which typically occurs from 150 to 200 ms after motion onset (Hoffmann *et al*., 2001; Probst *et al*., 1993). To determine the response latency of implied motion and re-establish the response latency of real motion, we used EEG-scans with a high temporal resolution to record the visual evoked potential (VEP) to photographs with vs. photographs without implied motion (Figure 1), as well as to moving stimuli.

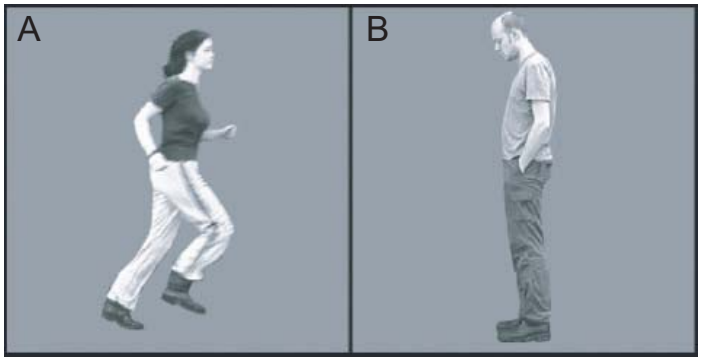

Figure 1
Examples of photographs with implied motion (A) and without implied motion (B), that were used in this study. All photographs were presented at both left and right profile.

Interestingly, both fMRI studies investigating implied motion (Kourtzi and Kanwisher, 2000; Senior *et al*., 2000) found very similar results, even though their paradigms differed at some points, most notably with respect to the moving stimuli used to locate area hMT+. Kourtzi and Kanwisher (2000) used the difference in response to low-contrast moving concentric rings and static rings, while Senior *et al*. (2000) used movie clips of moving objects and the same objects at rest. While the moving rings are standard stimuli for hMT+ activation, the movie clips provide a better comparison to implied motion (the implied motion stimuli were frames taken from these clips). Both methods successfully located area hMT+ in fMRI scans. However, it is not certain what might provide an optimal localization of motion sensitive cortex in spatially poorer EEG recordings. Therefore we used in two different experiments either inanimate motion (random dot patterns: moving vs. static or vs. flicker) and animate motion (movie clip of running person vs. one frame of that movie). Additionally, we were interested in the influence of luminance on the evoked potentials. Therefore, we used luminance uncorrected photographs in the first (inanimate RDP motion) experiment, in contrast to luminance corrected photographs in the second (animate movie clip) experiment.

Methods

Participants
Ten males and nine females participated in the first experiment (luminance- uncorrected implied motion stimuli and RDPs). Five subjects had an excessive number of artifacts in their data and were therefore excluded from VEP analysis, leaving data from seven males and seven females. All were right handed, had normal or corrected to normal visual acuity and were aged between 20 and 31 years. Ten of the participants were naive to the purpose of the study, two females (both authors) and two males were not. Naive and informed subjects only differed significantly in early components of the RDP responses. Since there was no significant difference between the two subject groups in the main condition of this experiment (with vs. without implied motion), no distinction was made between naive and informed participants during analysis.

Three male and four female students participated in the second experiment (luminance corrected photographs and animate motion movie clip). All participants were naive to the purpose of the study, right handed, with normal or corrected to normal visual acuity, and aged between 21 and 32 years.

Naive participants in the first experiment were paid expenses, while subjects in the second experiment participated as part of their course work. All participants had given their written informed consent. Experimental procedures were conducted in concordance with the Declaration of Helsinki (World Medical Association 2000).

Experiment 1: Stimuli and Task
Stimuli were presented within a round aperture (radius of 3.3 degrees, black surround) on a 17 inch monitor (1024 by 780 pixels, 84 Hz) at a viewing distance of 1 m. In the first experiment, two types of grayscale pictures were used: photographs and random dot patterns (RDPs). Photographs showed one of three different human agents either running towards the left or right, or standing still at left or right profile view, against a gray background (edited with Photoshop). Persons in the photographs were six degrees in height. The RDPs had been made by scrambling photographs (with and without implied motion) into dots of 5 by 5 pixels. During the experiment, the RDPs could be moving coherently in left or right direction at approximately 6.8 °/s, they could be stationary, or could be presented in random order as flicker (at 84 Hz).

Stimuli were presented for 500 ms followed by an interstimulus period of 1 s (black screen). To ensure that subjects attended to all stimuli, for both the photograph and RDP conditions, a target-recognition

task was included. When a RDP with dots twice the size of the stimulus dots was presented, participants had to press a button. This RDP could be moving, stationary or flickering with the same parameters as the test RDPs. Also, when a photograph of a person from frontal angle (either running or standing) was presented, subjects had to press the button. Ten percent of all stimuli were targets for these tasks. All subjects detected well above 90% of the control stimuli. The number of false alarms ranged between 0 and 18. No subjects were excluded based on their task performance. Throughout the whole recording session, a red fixation dot was present in the middle of the screen.

Experiment 2: Stimuli and Task

Experiment 2 contained the same gray-scale photographs as used in the first experiment, except that the luminance of the persons (not the background) in the implied photos had been altered to match that of their motionless counterparts. Original luminance of the three motionless and implied pairs in experiment 1 was respectively; 22.3 vs. 23.7, 21.2 vs. 20.5, and 23.2 vs. 23.3 cd/m^2, and was altered to 22.3, 21.7, and 23.2 cd/m^2.

The animate motion movie-clip consisted of 9 frames depicting the same three human agents running from one side of the aperture to the other. Every frame was presented for 70 ms. At this frame-rate the speed of the running person was roughly 9 °/s., which seemed to match the speed expressed in the limb-movements in the clip. Stimuli were presented for 630 ms with a 1000 ms inter-stimulus period. Participants were again requested to push a button when the person in the photographs (not in the movie-clips) was standing or running forwards.

Procedure

Participants were seated in a comfortable chair in a darkened room. All participants received the same instructions regarding the task, and examples of the test stimuli and task stimuli were given prior to the experiment. All were requested to fixate the red dot on the screen and to make eye blinks only in the interstimulus periods. Both experiments were run in Presentation (Neurobehavioral Systems, U.S.).

In experiment 1, RDPs, photographs and task stimuli were presented 720 times in random order, in six fifteen-minute blocks. Due to fatigue, two subjects were unable to complete more than 67% and 90% of the trials, respectively. Since their task performance, and the percentage of rejected artifacts, were within limits, data of these subjects were included in the final analysis.

In experiment 2, movie clips, photographs and task stimuli were presented 400 times in random order, in four seventeen-minute blocks. No subjects needed to be excluded on the basis of their behavioral data or number of artifacts.

Apparatus and Recording
The EEG was recorded from 59 Ag/Cl scalp electrodes. Additional electrodes included one grounding electrode, one electrode on each mastoid, two electrodes above and below the left eye for vertical EOG and one electrode next to each eye for horizontal EOG. Resistance between skin and electrodes was kept below 5 kOhm throughout the experiment. BrainVision Recorder (Brain Products, Germany) was used to sample and digitize the EEG at 1 kHz, filter (high-pass cutoff at 0.03 Hz, low-pass cutoff at 400 Hz, and a 50 Hz notch filter) and stored on hard disk for off-line analysis. Electrode Cz was used as reference during the experiment. All scalp electrodes, including Cz, were offline re-referenced to averaged mastoids for further analysis. For the BESA source analysis all electrodes were re-referenced against the average scalp potential.

Data Reduction and Analysis
BrainVision Analyser was used for data analysis. The EEG was segmented into stimulus locked epochs from 100 ms before to 500 ms after stimulus onset. Segments containing an attention-task stimulus or a (false) response in a test stimulus were removed from further analysis. Epochs including blinks, eye movements (criteria ± 60 μV), or artifacts (±120 μV on any EEG channel) were discarded. Participants for which more than 50% of the segments had been excluded were discarded from further analysis (5 out of 19 participants). Lastly, VEPs were filtered (high-pass cutoff 0.05 Hz, low-pass cutoff 20 Hz, 12 dB/oct) and baseline corrected for 100 to 0 ms before stimulus presentation.

For every participant, VEPs were segmented into 20 ms fragments. The average potentials of these fragments were used to signify differences between responses to the two photograph conditions, between the moving and stationary RDPs, and between the moving and flickering RDPs. A general linear model with repeated measures was performed over all subjects, using condition and electrode location as within, and naivety as between, subjects factor. Greenhouse-Geisser corrected p values < 0.05 were considered significant.

Individual VEPs were used to calculate the grand average VEPs over all subjects. Additionally, the grand average VEP of photographs without implied motion was subtracted from the grand average VEP of photographs with implied motion. Moving minus stationary, and moving minus flickering RDP grand averages were obtained similarly.

Source Localization

To locate the neuronal sources underlying the differences in evoked potentials, brain electric source analysis (BESA 2.2, Scherg & Picton, 1991) was performed. This method modeled location, orientation and strength of equivalent intra-cranial dipole-sources according to the recorded scalp activity. The optimal dipole-solution was found by searching for a minimum in the residual variance (RV) function. To reduce the probability of interacting dipoles (i.e., adjacent dipoles with opposing high-amplitude potential fields), the energy constraint of the BESA model was set to 20% (with the remaining 80% for the RV criterion), thus favoring source solutions with relatively low dipole strengths (Berg & Scherg, 1994). Single dipole pairs were used for source models. The location and orientation of the dipoles were bilateral symmetrically constrained.

Results

Implied Motion

Visually Evoked Potentials

We recorded EEG signals in 14 human subjects that were viewing (luminance uncorrected) photographs of other people in running (implied motion) or stationary (motionless) posture. Examples of the stimuli are presented in Figure 1, a complete description of the visual stimuli and task is given in the method section. Differences between implied vs. motionless conditions were most pronounced at occipital-parietal electrodes (Figure 2). To statistically test differences between conditions, a general linear model with repeated measures was applied to mean amplitudes across 20-ms time segments, with condition (implied and motionless) and electrode position as within subject factors. Significant difference (Greenhouse Geisser p-value < 0.05) in response to photographs with implied motion vs. photographs without implied motion was found from 60 to 100 ms, and from 260 to 320 ms after stimulus onset.

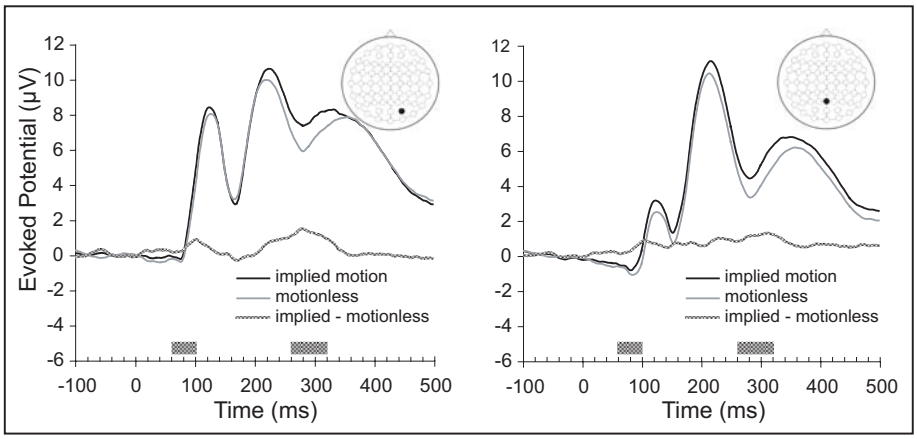

Figure 2

The implied motion effect is maximal from 260 to 320 ms in the luminance uncorrected experiment (N = 14). This is visible as a large deviation between the grand average VEPs to implied motion (black line) and motionless (gray line) at electrode positions PO4 (left panel) and Pz (right panel). The dotted line depicts the difference curve between the implied and motionless VEPs, while the dotted bar highlights the periods during which the two differed significantly (general linear model: condition x electrodes, Greenhouse-Geisser p value < 0.05). From 60 to 100 ms a smaller (but significant) deviation occurred, which might be attributed to a response to low-level stimulus differences, especially luminance.

The first difference was strongest at electrode Pz during a small negative peak. Evoked potentials during this time interval have been shown to reflect luminance (Johannes *et al*., 1995), spatial frequency (Kenemans *et al*., 2000), orientation (Arakawa *et al*, 2000), and size and eccentricity differences (Busch *et al*., 2004), which indicate that this early divergence reflected low-level stimulus differences between the two conditions. For 11 subjects the implied response was more positive than the motionless response. One subject showed a slightly more negative implied motion response, and for two subjects there was no clear difference between the responses to the two conditions.

The second difference (from 260 to 320 ms) between the two photograph conditions was much more pronounced, and was clearly visible at most occipital and occipital-parietal electrodes. A general linear model analysis on a subset of 35 electrodes (5 lateral/medial by 7 anterior/posterior locations) confirmed a significantly different anterior/posterior gradient between these two conditions. The implied motion photographs evoked a more positive potential than the motionless photographs at posterior electrodes, which was clearly noticeable in the grand average and in the individual data of 11 of the 14 subjects. Since activity due to luminance, spatial frequency, orientation, size and eccentricity differences occur much earlier, this divergence between implied and motionless conditions most probably reflected implied motion activity. Subsequently, we refer to this difference as the implied motion response.

Luminance

In a second experiment with seven subjects, the average luminance of the implied motion pictures was adjusted to match their motionless counterparts. Since the first (luminance uncorrected) experiment already revealed that the differences between the implied and motionless responses were maximal at electrode Pz (early difference) and PO4 (late difference), we tested differences between implied and motionless responses at these two electrodes in a paired t-test (Figure 3).

Differences at electrode PO4 were significant ($p<0.05$) from 120 to 140 ms and from 300 to 380 ms after stimulus onset. Differences at electrode Pz were significant from 120 to 160 ms, from 220 to 260 ms, and from 340 to 400 ms. The first difference (120 to 160 ms) is comparable to the 60 to 100 ms difference in the first experiment, while the late difference between 300 and 400 ms is very similar in shape as the 260 to 320 ms difference in the first experiment. As in the first experiment, the first difference was small and difficult to discriminate in comparison to the late response, which was clearly visible as a positive potential in the grand average and in the individual data of 5 out of 7 subjects.

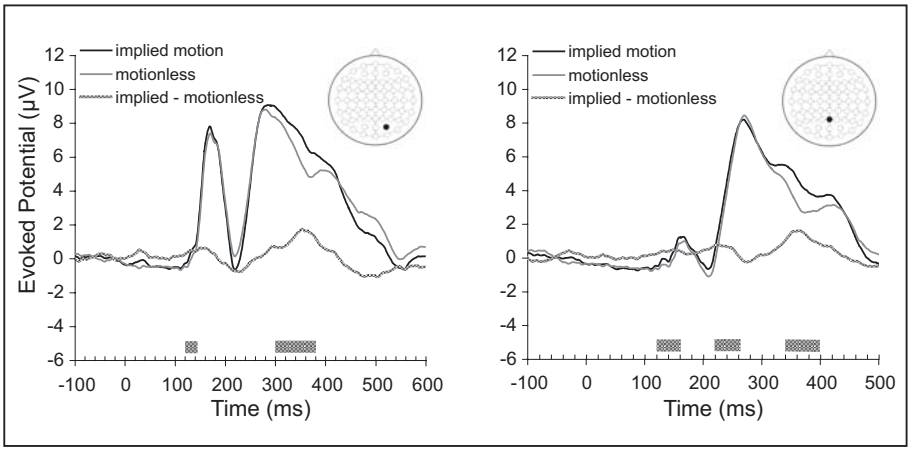

Figure 3
Grand averages for luminance corrected photographs (N = 7) showed the same deviation as luminance uncorrected photographs (Figure 2), albeit at a longer latency. The dotted bars indicate the time periods during which significant differences (paired t-test p-value < 0.05) between implied and motionless potentials occur at electrodes PO4 (left panel) and electrode Pz (right panel).

The longer latencies in this second experiment (when compared to the results of the first experiment) cannot be explained by the luminance adjustment, since only the implied motion photographs were adjusted, while the motionless photographs remained unaltered. Implied and motionless responses in this second experiment had the same response latencies. These longer latencies might thus be attributed to group differences.

Electrode Pz revealed an additional significant difference between implied and motionless responses from 220 to 260 ms after stimulus onset. Since this difference did not occur at electrode PO4, and was absent in the first experiment, it was not taken into account during further analysis.

Implied Motion Source Localization
To estimate the locations of neural sources underlying differences between conditions, dipole modeling (BESA 2.2: Scherg & Picton, 1991; Berg & Scherg, 1994) was performed on the subtraction VEPs: implied motion minus motionless photographs. Source models consisted of single dipole pairs, whose bilateral locations and orientations were mirrored in the midline

Scalp data from the implied minus motionless subtraction grand averages were analyzed for those time periods that the VEPs of the two conditions differed significantly. When the global field power was maximal during these periods, a 3 ms timeframe was chosen for source localization.

For the grand average P80, the global field power was maximal around 98 ms. The model that was fitted at that latency had a residual variance (RV, the percentage of scalp data that the model cannot account for; the lower the RV, the better the model) of 2.47%. The grand average model was then tested on the individual data of 14 subjects at the latency with the lowest RV. The average model fitted the individual data with an average RV of 42.3% (± 6.2 s.e.m.) at an average latency of 89.6 ms (± 2.8 s.e.m.). Individual data was then refitted to obtain the source of P80 activity for each participant (Figure 4). Residual variances ranged between 1.7% and 22% (mean 8.4% ± 1.9% s.e.m.).

Source analysis for the implied motion response (260 to 320 ms) was performed at a latency of 284 ms (when the global field power was maximal) and had a RV of 2.6%. The location of this source was in concordance with an extrastriate source, possibly hMT+. As was done with the 80, the average model was tested on the individual data and refitted per participant to obtain individual sources (Figure 4). For one participant, the refitting revealed a source outside of the brain. This subject was excluded for further source analysis and comparisons. The grand average model fitted the other 13 participants with an average RV of 36.3% (± 5.0 s.e.m.) Residual variances of the refitted individual models ranged between 2.6% and 37.8% (mean 13.2% ± 2.8% s.e.m.).

Luminance Corrected Source Analysis

The late implied motion response (300 to 400 ms) in the luminance-corrected experiment between could also be nicely fitted by a single dipole pair model (RV = 6.4% at a latency of 296 ms). BESA analysis of the grand average data resulted in a dipole model similar to that of the luminance uncorrected data. The model was again tested on the individual data of the seven participants (mean RV 32.9% ± 7.1 s.e.m.) and refitted. Residual variances for the individual sources ranged between 2.7% and 37.8% (mean 12.8% ± s.e.m. 4.1). Individual sources (Figure 4) overlapped with the luminance uncorrected implied motion sources. Three one-way-ANOVAs along three axes revealed that the source locations of both groups did not differ significantly (p-values > 0.05). We thus conclude that luminance does not strongly affect this late implied motion response.

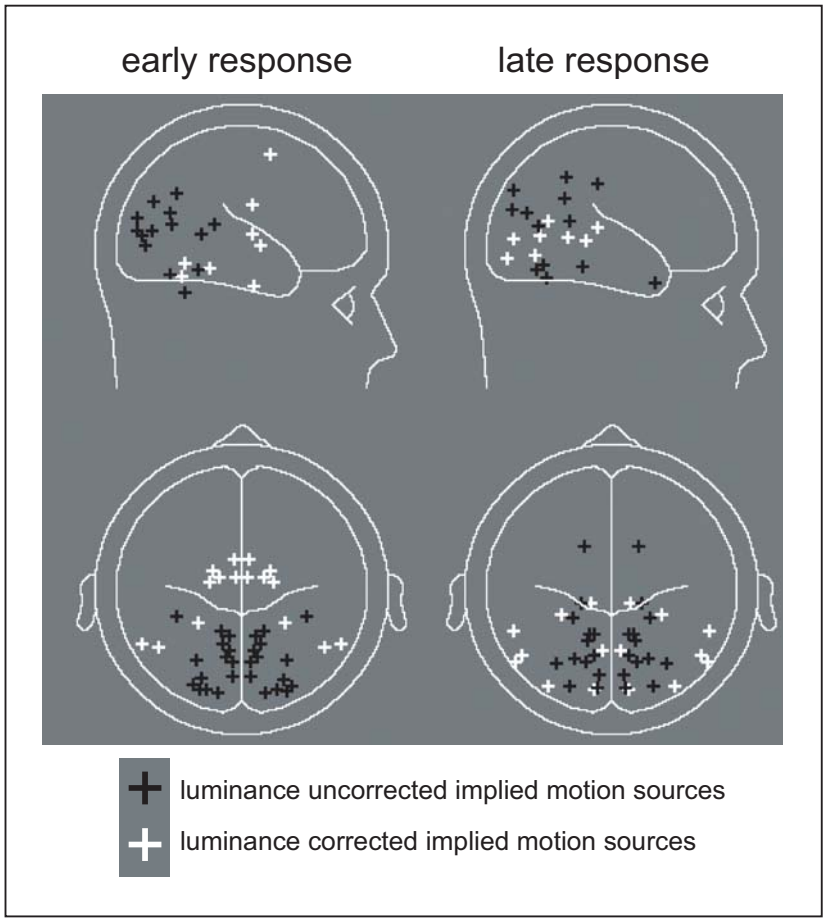

Figure 4
Individual source models for the early implied motion response (60 to 100 ms in luminance uncorrected, and 120 to 160 ms in luminance corrected experiment; left panel) and for the late response (260 to 320 ms in luminance uncorrected, and 280 to 400 ms for luminance corrected experiment; right panel).

The source of the early grand average difference (fitted within a 100 to 160 ms) in response to luminance corrected implied and motionless photographs could not be as clearly established (RV = 24% at a latency of 131 ms) and revealed a much more anterior source than the luminance uncorrected early source. This grand average model fitted the individual data with an average RV of 47.1% at an average latency of 122 ms. Individual sources were refitted (mean RV 13.0 % ± 2.1 s.e.m.).

The luminance corrected sources were located more anterior than the uncorrected sources. Indeed, a one-way ANOVA along the posterior/anterior axis revealed that this difference was significant with a p-value < 0.001. The source locations did not differ significantly (p-values > 0.05) along the other two axis.

Inanimate RDP Motion

Visually Evoked Potentials

Differences in evoked potentials between the moving, static and flickering random dot patterns (RDPs) were clearly visible at the same occipital-parietal electrodes that revealed the implied motion response (Figure 5). The difference in VEPs between coherently moving and flickering RDPs was significant from 120 ms until the end of the stimulus presentation at 500 ms, while the response to a moving and a static RDP differed significantly from 100 to 160 ms and from 180 to 260 ms (repeated measures general linear model; Greenhouse Geisser p-value < 0.05).

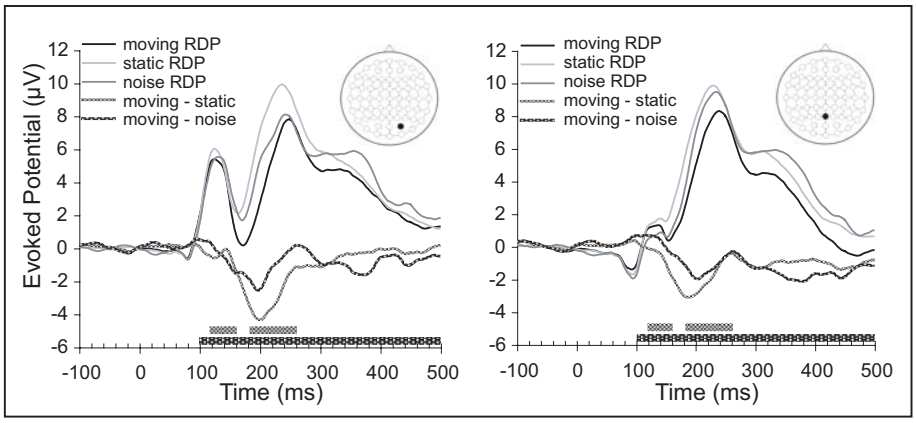

Figure 5

Grand average (N = 14) of evoked potentials to moving, static, and flickering (noise) RDPs differ maximally around 150 to 220 ms. The thick dotted lines and bars represent the difference curves and corresponding significantly differing periods of moving vs. static and moving vs. flickering RDPs. Differences are stronger at electrode PO4 (left panel) than at electrode Pz (right panel).

Source Analysis

Source analysis of the motion vs. static and of the motion vs. noise differences revealed activity of several different sources. To isolate a motion source that could have been responsible for the implied motion response, individual (late) implied motion sources were fitted on the motion data. Best fits were found at an average latency of 140.8 ms (± 5.2 s.e.m.). This latency is close to the 150-200 ms occurrence of the negative peak that was considered to be the direction selective hMT+ response in previous studies (Hoffmann *et al*., 2001; Probst *et al*., 1993). Residual variances of the implied models on the motion data were however still high (32.6% ± 5.4 s.e.m. for motion vs. static, and 29.5% ± 5.2 s.e.m. for the motion vs. noise condition), meaning that either implied and real motion do not share the same source, or that other motion sources are also active during the same period.

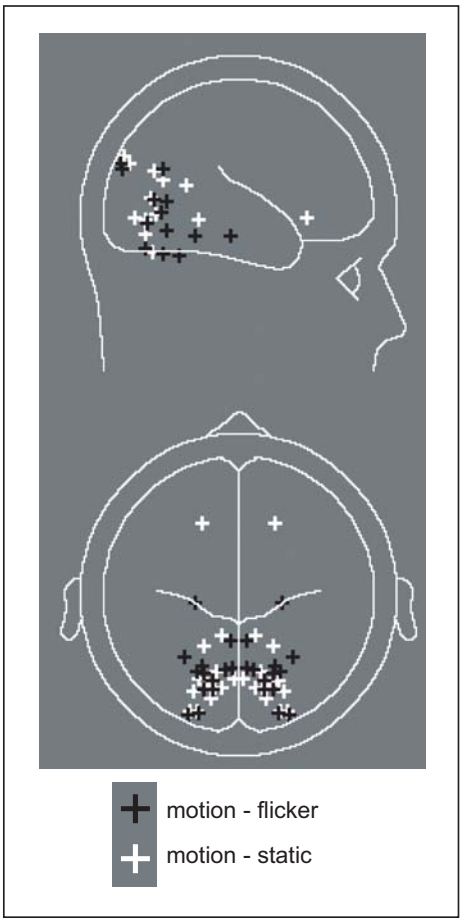

Figure 6
Neuronal sources for motion responses, as established by subtraction of motion vs. flicker (black crosses) and motion vs. static (white crosses) overlap with implied motion sources (Figure 4 right panel).

Next, the individual sources were refitted to obtain the optimal motion sources per individual (Figure 6). The location of the individual implied motion sources were compared with their corresponding motion-static and motion-flicker sources along three axes in a multivariate test. The locations of the implied motion sources did not differ significantly from motion-static and motion-noise positions in multivariate tests (motion-static: Hotelling's trace $F(3,10) = 1.111$, $p = 0.390$; motion-noise: Hotelling's trace $F(3,10) = 2.304$, $p = 0.139$). Apparently, implied motion and real motion sources share a common neural substrate.

Animate Motion

Visually Evoked Potentials

To possibly obtain a more accurate localization of the sources of the VEP to real animate motion, we additionally recorded in a separate experiment the response to movie clips that depicted a human agent running from left to right or vice versa. This experiment was conducted in combination with the luminance corrected experiment, which was described earlier, on seven subjects. The movie clip consisted of 9 frames that were each presented for 70 ms. The onset of the responses to the movie clips (Figure 7) were delayed with about 60 ms compared to the onset of the inanimate RDP motion responses. This difference, however, could be attributed to the stimulus presentation.

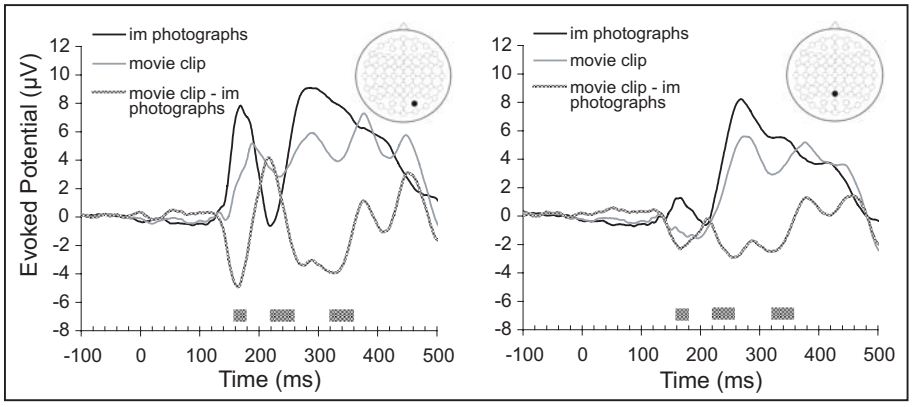

Figure 7

Grand average (N = 7) of evoked potentials to implied motion photographs (luminance-corrected) and to movie clips of a running person. The dotted line depicts the difference curve while the bars indicate time periods during which significant differences between the two conditions occur at electrodes PO4 (left panel) and electrode Pz (right panel).

Motion was visible only after the second frame was presented. In the experiment with the moving RDPs the second frame was shown after 12 ms, whereas for the movie clip the second frame was shown after 70 ms. Additionally, these participants had an overall longer response latency as was visible in the response to the luminance corrected photographs (figure 3), which may also account for this delay.

Differences in potential between implied motion photographs and movie-clips were tested for significance with a repeated measures general linear model. Responses differed significantly from 160 to 180; from 220 to 260; and from 320 to 360 ms (Greenhouse Geisser p-value < 0.05).

Animate Motion Source Localization
As with inanimate RDP motion, the individual implied motion dipole sources were fitted on the difference between the movie clip response and the response to the (luminance corrected) implied motion photographs (without subtraction of the response to the motionless photographs). As movie clips and implied photographs were similar in appearance and presence of implied motion, the difference between the two reflected a pure motion response. The implied sources fitted the data best around 200 ms (mean latency = 198.7 ms ± 14.3 s.e.m.). After subtraction of the 60 ms difference, this motion response is roughly in the same range as we report for the RDPs and as has been reported by others (Hoffmann *et al*., 2001; Probst *et al*., 1993).

Again we used a BESA model to estimate the source location of the animate motion sources. Individual animate motion sources are shown in Figure 8. Implied and animate motion sources were located closely together. The locations of the individual sources were compared along three axes in a multivariate test. This showed that implied motion sources and animate motion sources differed significantly in location (Hotelling's trace $F(3,4) = 15.889$, $p = 0.011$). Univariate analysis revealed that animate motion sources were significantly more posterior than implied motion sources (Greenhouse-Geisser $p = 0.006$, vs. $p > 0.05$ for the other 2 axis).

Conclusion

Based on response latencies and source analysis of both experiments, we conclude that implied motion evokes a delayed response in an area that overlaps with motion sensitive cortex (hMT+).

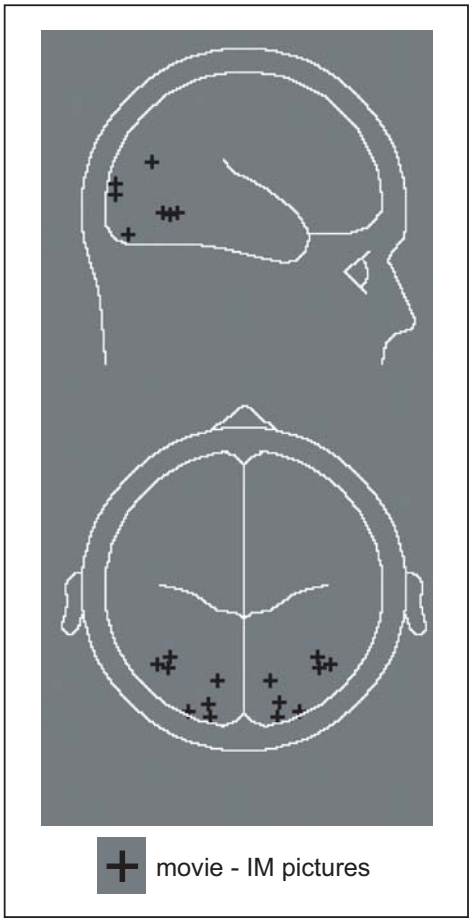

Figure 8
Individual source activity to animate motion was located in the occipital lobe for 5 out of 7 subjects. Even though his area partly overlaps with the locations of the late luminance corrected implied motion sources (Figure 4), individual comparison revealed that animate motion sources were located significantly more posterior compared to the late implied motion sources.

Discussion

Early vs. Late Implied Motion Evoked Potentials
Potentials evoked by photographs of human agents implying motion differed significantly from potentials evoked by photographs of the same human agents without implied motion in two periods: an early period (60 to 100 ms after stimulus onset in the first experiment and 120 to 160 ms in the second experiment), and a late period (280 to 320 ms in the first, and 300 to 400 ms in the second experiment). The early response was much smaller in amplitude than the latter and was barely visible in the grand average VEPs. Furthermore, the timing of the first deviation coincided with VEP responses to luminance (Johannes *et al*., 1995), spatial frequency (Kenemans *et al*, 2000), orientation (Arakawa *et al*., 2000), and size and eccentricity (Busch *et al*., 2004). Therefore we reason that this early response was due to low-level stimulus differences between implied and motionless photographs.

BESA source locations for this early difference were established in both luminance corrected and uncorrected conditions. The luminance corrected sources were more anterior than the uncorrected sources. This indicates that luminance is indeed largely responsible for this early response, but other low-level visual features may still play a role.

In contrast, the late difference in response to implied vs. motionless photographs, which occurred from 260 to 400 ms after stimulus onset, cannot be explained by these low-level image differences as they occur earlier. Although Johannes *et al*. (1995) did find an interaction of luminance and attention from 350 to 750 ms after stimulus onset, this should not affect the responses in the current experiment, as the attention task of the participants was the same for both implied as motionless photographs. Furthermore, we showed that adjusting the luminance of the implied motion photographs to match that of the motionless photographs did not change the implied motion response. In both luminance corrected and uncorrected experiments, this late difference seemed to arise from a specific area in the occipital region. This indicates that the late difference is mainly caused by the presence vs. absence of implied motion in the photographs, and we refer to this difference as the implied motion response.

Delayed Response Latency of Implied Motion compared to Real Motion
The moving vs. stationary RDPs were expected to evoke the largest difference in activity in area hMT+. However, earlier visual areas also show a large difference in response to these stimuli (Qian & Andersen, 1994; Sunaert *et al.* 1999). Therefore, it might be difficult to extract the hMT+ response from just this comparison. Since hMT+ also

responds well to flicker or random noise, the difference in hMT+ activity induced by motion vs. flicker might be expected to be smaller than by motion vs. static. Furthermore, because lower visual areas as V1 discriminate less between motion and flicker (Qian & Andersen, 1994; Sunaert *et al*., 1999), the relative contribution of hMT+ to the subtracted evoked potential should be higher. Therefore, to optimally locate the motion sensitive areas, both static and flickering random dot patterns were compared to moving random dot patterns.

Differences between moving vs. static RDP evoked potentials, and between moving vs. flickering RDP evoked potentials started at respectively 100 and 120 ms after stimulus onset. It has been argued that the initial motion response around 120 ms does not reflect hMT+ activity, as it is not susceptible to direction selective motion adaptation. Instead, the negative peak around 150 to 200 ms is described as a direction selective motion response (Hoffman *et al*., 2001), which can be localized at the hMT+ position (Probst *et al*., 1993). The “motion vs. static”, and the “motion vs. flicker” difference curves in the present study also showed this negative peak. Comparison of this peak with the implied motion response from 260 to 320 ms latency in the first experiment showed that the activation by implied motion was delayed with roughly 90 ms compared to real motion activation. Furthermore, source-modeling showed that when fitting the locations of the individual implied motion sources on the individual RDP motion data in both experiments, these sources gave their best fit around 140 ms, at the onset of the 150-200 peak. This indicates that the area that was involved in implied motion processing, was also involved in RDP motion processing at 140 ms after stimulus onset, 120 ms earlier than the implied motion response.

When fitting individual implied motion sources on their corresponding animate movie clip data, they fitted best around 200 ms. However, to make the speed of the runner in the movie clip as natural as possible, the frame rate in the clip was set to 70 ms. When subtracting the 2nd frame presentation delay of roughly 60 ms (compared to the ±10 ms frame rate of the first experiment and other studies) from this latency, it approaches the RDP motion response of the first experiment and of other studies (Hoffmann *et al*., 2001; Probst *et al*., 1993) at 150 to 200 ms. Additionally, the implied motion response for the subjects that participated in this part of the experiments was also delayed, meaning that these subjects had an overall longer latency. The reason for this overall longer latency remains unclear. Regardless of the overall latencies, the implied motion response for these subjects was delayed by 160 ms compared to the response to animate motion (200 – 60 = 140 ms vs. 300 ms after stimulus onset). However, since these animate motion sources differed in location from the implied motion sources, the inanimate motion sources are a

better indicator of motion response latencies in the area activated by implied motion. Thus, the implied motion response is delayed by approximately 120 ms compared to real motion responses.

Comparison of Neuronal Sources for Implied and Real Motion
Dipole models to explain the RDP motion response revealed sizable overlap between the area that contains the real motion sources and the area that is activated by implied motion. This indicates that implied motion evoked a response from an area in motion sensitive cortex. Comparison of the walking movie clip vs. implied motion stills revealed well-localized motion sources in the occipital lobe. This is consistent with the idea that both the movie and the implied motion activate typical motion areas (e.g., hMT+), but that in addition the movie activates areas more upstream, e.g., parts of V1 that are stimulated by the sequence of energy onsets across the central 6 degrees that constitute the movie of the agent crossing the aperture (Sunaert *et al*., 1999). In sum, both comparisons are consistent with the idea that implied motion activates the same areas in secondary visual cortex as those activated by real motion.

Feedback from Temporal Object Recognition Areas onto Motion Processing Areas
This study showed that the neural response to implied motion in human motion areas is slower compared to the response to real motion, which suggests that the implied motion information arrives at this area via a different, longer pathway. This “feedback” might well arise from the superior temporal sulcus (STS) region, which seems to be specialized for the perception of bodily actions and postures in both macaque monkeys (Jellema & Perrett, 2002) and humans (Allison *et al*., 2000). Of particular interest for the current study is that cells in the anterior part of the macaque STS respond to specific articulated body movements and postures, whether executed by an actor or expected to happen on the basis of the immediately preceding perceptual history (Jellema & Perrett, 2003a), or when implied by the articulation of limbs in a static body posture (Jellema & Perrett, 2003b). This view is in agreement with Senior (2000), who, besides the response in hMT+, reported a difference in BOLD response for the implied vs. motionless conditions in temporal regions, and with Kourtzi and Kanwisher (2000), who showed additional implied motion activation in the STS.
The current EEG study however does not clearly demonstrate activity in temporal regions following implied motion. The early response from 60 to 100 ms seems too early for STS activity, and individual sources were not consistently found at temporal locations. Since the STS is thought to discriminate between implied and motionless responses, it contains cells responsive to either or both conditions. The difference in response to both conditions might thus be smaller than the

difference in response in hMT+. Furthermore, the response from the STS might overlap in time with responses related to stimulus onset and low-level stimulus differences in other areas, which might obscure the STS response. This might explain why the temporal activation did show up in both fMRI studies, which can easily differentiate between responses from different areas, but not in the spatially poorer EEG.

Role of form feedback onto motion processing areas
Basically, the processing of visual form and motion are thought to occur along two different neural pathways: motion along the dorsal, and form along the ventral pathway (Ungerleider & Mishkin, 1982). However, in an observers' percept, the two are combined. Feedback processes as described in the current study may contribute to this combined percept. Implied motion may activate posture dependent neurons in the temporal cortex, which in turn may activate hMT+ neurons that are sensitive to motion in the same direction as was implied. This activation would enhance the percept of that particular motion. Thus, implied motion would cause the static object to 'jump out' from other static objects that do not possess implied motion cues. At the same time it would 'prepare' the observing agent for the type and direction of motion that is most likely to happen next. This would be particularly advantageous when the observer itself is in motion or making eye-movements, or when detecting an animate object in an inanimate moving surrounding, for instance a rabbit in rustling, tall grass. Further, studies on representational momentum have shown that implied motion distorts an observers' memory for the location of an object in the direction of the implied motion (Freyd, 1983). Thus, implied motion may help to predict the motion path and future position of an object.

CHAPTER 2

ADAPTATION TO REAL MOTION REVEALS DIRECTION SELECTIVE INTERACTIONS BETWEEN REAL AND IMPLIED MOTION PROCESSING

Abstract

Viewing static pictures of running humans evokes neural activity in dorsal motion sensitive cortex. To establish whether this response arises from direction-selective neurons that are also involved in real motion processing, we measured the visually evoked potential to implied motion following adaptation to static or moving random dot patterns. The implied motion response was defined as the difference between evoked potentials to pictures with and without implied motion. Interaction between real and implied motion was found as a modulation of this difference response by the preceding motion adaptation. The amplitude of the implied motion response was significantly reduced after adaptation to motion in the same direction as the implied motion, compared to motion in the opposite direction. At 280 ms after stimulus onset, the average difference in amplitude reduction between opposite and same adapted direction was 0.5 μV on an average implied motion amplitude of 2.0 μV. These results indicate that the response to implied motion arises from direction-selective motion-sensitive neurons. This is consistent with interactions between real and implied motion processing at a neuronal level.

Introduction

Visual motion is processed in specialized areas of the visual cortex, most notably in medio-temporal and medio-superior-temporal cortical area MT/MST, which is part of the dorsal visual pathway (Ungerleider & Mishkin, 1982). It has been shown that the human MT/MST complex also shows a higher BOLD signal in response to photographs of objects in motion (for instance a cup falling off a table or an athlete throwing a ball) than to photographs of the same objects at rest (cup on the table, athlete sitting) (Kourtzi & Kanwisher, 2000; Senior *et al.*, 2000). This is an interesting finding, since form information was generally thought to be processed along the ventral visual pathway (Ungerleider & Mishkin, 1982) and not in MT/MST. A visually evoked potential study revealed that this implied motion response is visible as a positive potential at occipital and occipito-parietal electrodes from 260 to 400 ms after stimulus onset (Lorteije *et al.*, 2006). This response is delayed with approximately 100 ms compared to the response to real motion in the same area. These findings suggest that MT/MST receives feedback from higher-level visual areas where animate form is analysed, possibly in temporal cortical areas.

Although these studies show that animate implied motion evokes a response in motion sensitive areas, it still remains unclear whether the same direction-selective neurons in MT/MST are involved in both real motion and animate implied motion processing. The use of direction-selective adaptation with real motion makes it possible to evaluate whether the implied motion response arises from the same directionally selective neurons that also process real motion.

Numerous studies using different techniques have shown that a prolonged exposure to motion in one direction alters the response of direction-selective neurons to a subsequent motion stimulus in that direction. Single cell studies in monkeys have shown that most MT neurons are tuned to a specific motion direction (Maunsell & Newsome, 1987; Zeki, 1978). After exposure to motion in this preferred direction, the cell's response to motion in the same direction is attenuated (Kohn & Movshon, 2003; Van Wezel & Britten, 2002b). Human psychophysical studies have shown that after being adapted to motion in one direction, the subjects' perceived direction of motion shifts away from the adapted direction (Levinson & Sekuler, 1976; Schrater & Simoncelli, 1998). Adaptation to one motion direction can even result in the perception of an illusionary motion in the opposite direction, i.e., a motion after effect (Mather *et al.*, 1998). Furthermore, functional MRI revealed a decreased response to motion in the human MT+ complex when it is preceded by motion adaptation in the same direction (Huk *et al.*, 2001). This decrease did not occur when the preceding adaptation occurred in the opposite direction.

Bach and Ullrich showed that components of the motion visually evoked potential (VEP) can be modulated by motion adaptation, especially a positive peak around 110 to 130 ms after stimulus onset (P1) and a negative peak around 180 ms after stimulus onset (N200) (Bach & Ullrich, 1994). Comparison of motion VEPs with 8 different directions deviating from the adapted direction revealed that especially the N200 could be modulated by motion adaptation in a direction specific manner (Hoffmann *et al.*, 2001), i.e., VEPs to motion directions approaching the adaptation direction were much stronger attenuated than VEPs to motion in opposite directions of the adapted direction. In another study with a similar paradigm it has been shown that the N200 is not only direction specific, but also speed specific (Heinrich *et al.*, 2004). This indicates that this negative response reflects, at least partly, MT/MST activation.

To test the hypotheses that motion sensitive neurons are also responsive to implied motion, and that this interaction is directionally selective, we recorded VEPs to implied motion after three different types of adaptation: 1) a static random dot pattern (RDP), 2) a RDP moving in the same direction as the implied motion, 3) a RDP moving in the opposite direction as the implied motion. The advantage of this paradigm is that the implied motion test stimuli are always the same, only the preceding adaptation by real motion varies.

In addition to a direction invariant attenuation of the implied motion response caused by motion adaptation vs. static adaptation, we found direction specific adaptation effects. Most notably, the positive implied motion peak around 280 ms was reduced after motion adaptation in the same direction compared to static adaptation and adaptation in the opposite direction. These results provide evidence that the same motion direction-selective neurons process both real and implied motion.

Methods

Subjects
Twelve female and eleven male human subjects participated in this study. All of the participants were naive to the purpose of the study. They had given written informed consent and were paid expenses. The experiment was conducted in accordance with the declaration of Helsinki (World Medical Association 2000). Recordings from five subjects had to be discarded due to excessive eye-movements or noise, leaving data from ten males and eight females. These remaining 18 subjects were aged between 19 and 26 years (average 22.1 ± 0.4 s.e.m. years) and reported normal or corrected to normal visual acuity. One male was left handed, all other subjects were right handed.

Stimuli
Stimuli were presented within a round aperture (radius of 4.3°, black surround) in the middle of the screen. Participants were asked to fixate on a red square (0.2°x0.2°) in the centre of the screen during trials and to refrain from eye-blinks during the test-stimulus.

Trials consisted of an adaptation phase (2000 ms), a variable inter-stimulus-interval (ISI, ranging from 500 to 600 ms) and a test-stimulus (500 ms) (Figure 1). Three types of adaptation were used: a static random dot pattern (RDP), a leftward moving RDP, and a rightward moving RDP. These different conditions were presented in separate recording blocks to enable top-up adaptation. To ensure strong adaptation at the first trial, every block was preceded by 17 seconds of adaptation.

The duty cycle (test duration as a percentage of the total trial duration) of the test stimulus ranged between 16% and 17%, dependent on the length of the variable ISI. At duty cycles higher than 20%, test periods containing real motion could cause adaptation effects resulting in an invalid “unadapted” baseline (Bach & Ullrich, 1994). Even though the test periods in the current study did not contain real motion, implied motion may cause similar adaptation effects. However, with this duty cycle the unadapated baseline condition was valid.

In the adaptation phase, participants viewed a RDP that consisted of black and white dots (0.1°x0.1°) against a gray background. The dot density was 2% of the total background surface: 1% white and 1% black dots. Average luminance of the RDP was 38 cd/m^2. The RDPs either moved coherently to the right or left at 6.8 °/s, or remained stationary. The final frame of the adapting RDP remained static during the ISI and remained on screen as a static background during the test-stimulus. At the onset of the next adaptation period,

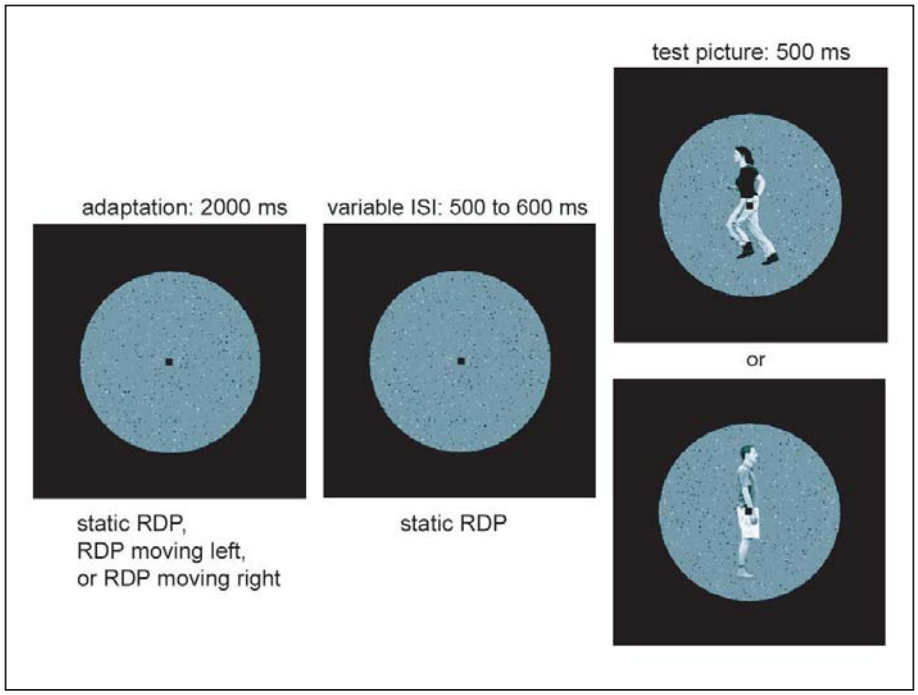

Figure 1
Trials consisted of an adaptation period, a variable interstimulus interval (ISI) and a test period. During the adaptation period, the RDPs could move to the left or right, or remain static for baseline recordings. However, during the ISI and the test period, the RDP remained static in the background. The test period did not contain any real motion onset, only motion implied by the pictures. The human agents in the (static) test pictures either expressed implied motion (top picture) or did not express implied motion (bottom picture). The running/viewing directions for both implied and implied motionless pictures could be to the left or right. The implied motion response was established as the subtraction VEP of the evoked potentials to pictures with implied motion minus the evoked potentials to pictures without implied motion.

the RDP was refreshed. Only one sequence of dot motion was shown, in left or right moving order, such that the background for test-stimuli preceded by the same direction of adaptation motion was always the same.

The test stimulus consisted of pictures of human agents profiled toward the right or left. The human agents either expressed implied motion (running, Figure 1 top panel) or did not express implied motion (standing still, Figure 1 bottom panel). During the test, the RDP remained static. The test contained no real motion, only motion

implied by the pictures. These photographs, that were stills from digitally recorded movie-clips, showed one of three different persons (two male, one female). Persons in the photographs were 6° in height. To diminish the influence of luminance on the VEP, the average luminance of the persons (not the background) in the implied motion photographs was adjusted to match that of their implied motionless counterparts.

The difference between the average response to implied motion stimuli minus the average response to stimuli without implied motion was calculated for every subject. This subtraction potential eliminates responses to processes that are common in both conditions, such as stimulus onset or face recognition, and thus mainly reflects the implied motion response. Therefore, whenever we speak about “the implied motion response”, we refer to this subtraction potential.

The photographs were presented randomly in both directions. The adapted motion could thus be in the same or opposite direction as the implied motion or as the profiled direction of the images without implied motion. Direction of motion in the RDP and direction of implied motion in the picture were combined in the analysis as *same* or *opposite* when they were in the same or opposite direction, respectively. Every condition was presented 240 times.

Experimental Procedure
Participants were seated in a comfortable chair in a darkened room. They sat in front of a 17-inch computer monitor with a screen resolution of 1024x768 pixels, 85 Hz, at a viewing distance of 85 centimeter. The experiment was run in Presentation (Neurobehavioral Systems, Albany, California) and consisted of six blocks of 25 minutes. Blocks were separated by breaks of at least 3 minutes, to prevent fatigue and transfer of adaptation from motion blocks onto other blocks. Blocks were presented in a weighted ACBBCA order, with A and B being motion adaptation blocks in either left or right direction (varying across subjects) and with C being stationary adaptation blocks.

A detection task was included to ensure that participants attended to all stimuli. The target stimuli were photographs in which the person was shown from frontal angle, either running or standing. Participants had to press a button upon detection of a target. The number of targets was six percent of the total number of trials and they were presented at random. All eighteen subjects detected well above 97% of the attention task stimuli. Five subjects reported a single false alarm, when no target had been presented.

The EEG was recorded from 59 Ag/Cl ring electrodes, which were mounted in an elastic cap (Braincap, Brain Products, Germany). Scalp electrodes were distributed according to the 10/10 system. Additional electrodes included two electrodes above and below the left eye to record the vertical EOG, two electrodes on the outer canthi of both eyes for horizontal EOG and one grounding electrode. Additionally, two electrodes were applied on both mastoids. Resistance between skin and electrodes was kept below 2 kOhm throughout the experiment. BrainVision Recorder (Brain Products, Germany) was used to sample and digitize the EEG at 1 kHz, filter (high-pass cutoff at 0.03 Hz, low-pass cutoff at 400 Hz, and a 50 Hz notch filter) and stored on hard disk for off-line analysis. Electrode Cz was used as reference during the experiment. All scalp electrodes, including Cz, were offline re-referenced to averaged mastoids for further analysis.

Data analysis

BrainVision Analyser (Brain Products, Germany) was used for data analysis. The EEG was segmented into stimulus locked epochs of 600 ms (100 ms before to 500 ms after stimulus onset). Segments containing an attention task stimulus (or a false response to a test stimulus) and blinks or eye-movements (criteria were > 100 µV or < -100µV), or artifacts (criteria were > 120 µV or < -120 µV on any EEG channel) were excluded from further analysis. VEPs were filtered (high-pass cutoff 0.05 Hz, low-pass cutoff 20 Hz, 12 dB/oct) and baseline corrected (for 100 ms to 0 ms before stimulus onset). For every subject, the average response per condition was calculated. The difference between the average response to implied motion stimuli minus the average response to stimuli without implied motion stimuli was calculated for every subject.

In an earlier evoked potential study (Lorteije *et al*., 2006), differences in potential between responses to photographs with and without implied motion were most pronounced at occipito-parietal electrodes. EEG potentials evoked by real motion were clearly visible at the same electrodes (Bach & Ullrich, 1994; Heinrich *et al*., 2004; Hoffmann *et al*., 2001; Lorteije *et al*., 2006). For this reason, we selected 17 occipital and parietal electrodes for further analysis on peak amplitudes (P7, P5, P3, P1, Pz, P2, P4, P6, P8, PO7, PO3, POz, PO4, PO8, O2, Oz, and O1, for locations see N150 panel in Figure 4A).

Source Analysis

To locate the neuronal sources underlying the differences in evoked potentials, brain electric source analysis (BESA 2.2 (Scherg & Picton, 1991)) was performed on the baseline implied motion grand averages. For each peak, the grand average was calculated over the subjects that were selected for that specific peak in the previous peak amplitude analysis. The analysis included data from all scalp electrodes

and not only the 17 posterior ones. BESA modeled location, orientation and strength of equivalent intra-cranial dipole-sources according to the recorded scalp activity. Grand average peak latencies were established for the P100, the N150 and the P280 as the latencies at which one of the 17 electrodes reached the maximum amplitude for that peak. The optimal dipole-solutions were found by searching for a minimum in the residual variance (RV) function at those latencies To reduce the probability of interacting dipoles (i.e., adjacent dipoles with opposing high-amplitude potential fields), the energy constraint of the BESA model was set to 20% (with the remaining 80% for the RV criterion), thus favoring source solutions with relatively low dipole strengths (Berg & Scherg, 1994). Single dipole pairs were used for source models. The location and orientation of the dipoles were bilateral symmetrically constrained.

Results

Implied motion VEP

The focus of analysis was on 17 occipital, temporal and parietal electrodes that most probably reflected responses from visual motion areas. Three peaks in the implied motion response could be discriminated at these locations (Figure 2): two positive peaks at approximately 100 and 280 ms after test-stimulus onset (P100 and a broad P280), and one negative peak around 150 ms after test-stimulus onset (N150). Comparison of the implied motion VEPs after the three different adaptation conditions showed that the P100 was attenuated due to motion adaptation (static vs. same and opposite), but this modulation was not dependent on the direction of the motion. In contrast, the P280 was clearly reduced in amplitude after adaptation in the same, but not after adaptation in the opposite direction. The negative peak did not show any modulation due to motion.

The amplitude of each peak after static adaptation was calculated for every subject. The amplitude in this static condition had to be large enough to reveal possible modulation in the moving adaptation conditions. Therefore, the maximum of each peak after static adaptation was established for every subject by automatic detection of global maxima for each of the 17 channels in Analyzer. The mean potential over the period of 10 ms before to 10 ms after the maximum was chosen as peak amplitude. Since the scalp distribution varied across subjects (especially due to left or right hemisphere dominance), the electrode at which this highest amplitude was found could vary across subjects.

The P100 was established as the peak amplitude between 40 and 120 ms after stimulus onset, for every subject. Likewise, the N150 was located between 100 and 200 ms, and the P280 was located within the 240 to 340 ms range. Subjects that had a positive amplitude < 1.5μV, or a negative amplitude > -1.5μV in the static adaptation condition were not included in further analysis for that specific peak.

Using this rule, 14 out of 18 subjects were included for the P100 analysis, 18 for the N150, and 15 for the P280. Additionally, one subject was excluded for the P280 analysis as she had a much stronger negative peak coinciding in time with the P280 (-4.9 μV at P7 vs. 2.2 μV at Pz).

The average maximum of the p100 was 2.6 μV (±0.2 μV s.e.m.) for the static adapted condition vs. 1.9 μV (±0.2 μV s.e.m.) for opposite adapted and 1.7 μV (±0.3 μV s.e.m.) for same adapted conditions. The P280 had an average maximum of 2.0 μV (±0.2 μV s.e.m.) for the static adapted condition, 1.7 μV (±0.3 μV s.e.m.) for the opposite adapted, and 1.2 μV (±0.3 μV s.e.m.) for the same adapted condition.

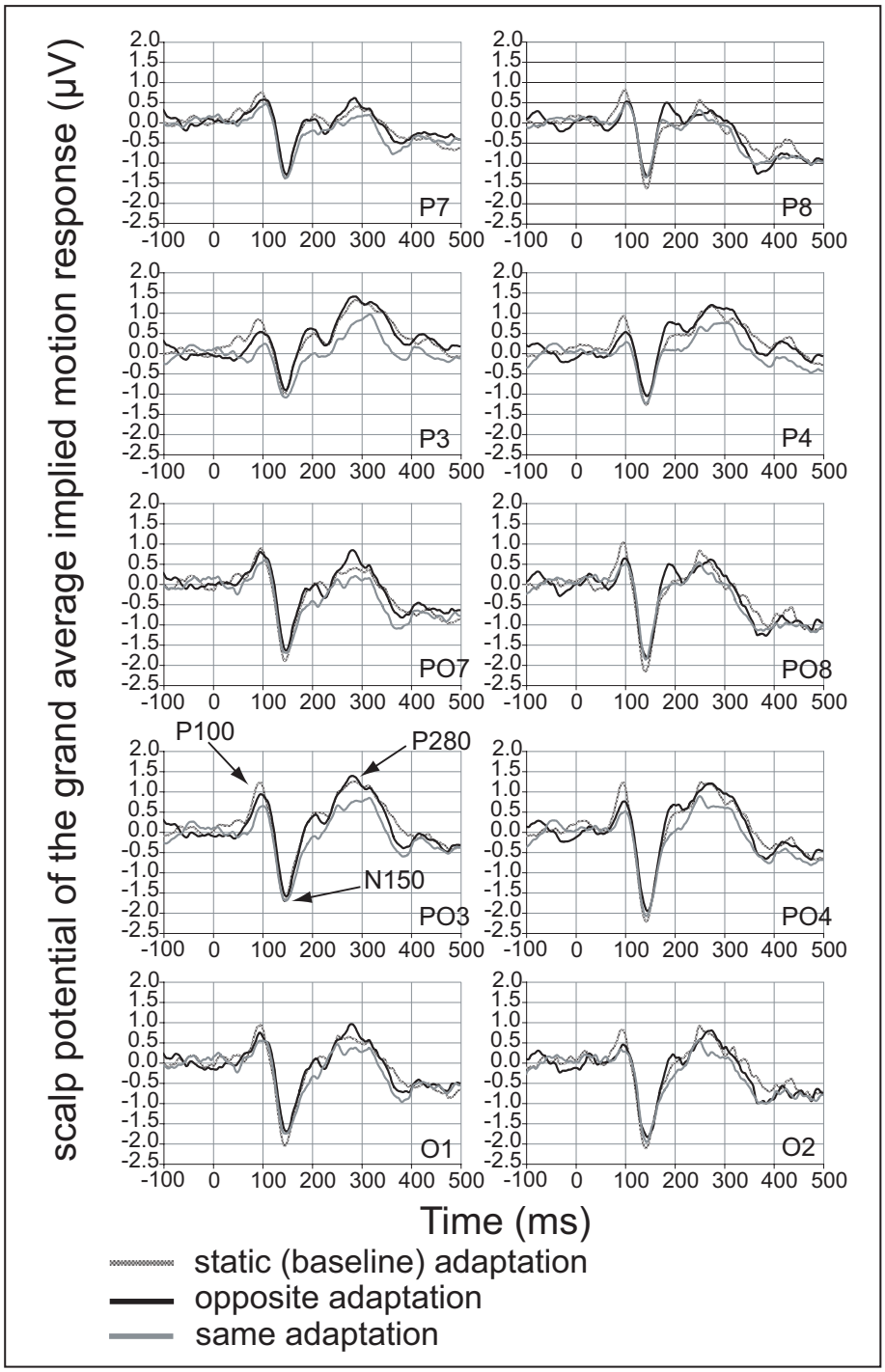
scalp potential of the grand average implied motion response (μV)
P7
P8
P3
P4
PO7
PO8
P100
P280
N150
PO3
PO4
O1
O2
Time (ms)
static (baseline) adaptation
opposite adaptation
same adaptation

Figure 2 (previous page)
Grand Averages (N=18) of the implied motion response after three types of adaptation at ten electrode positions. Clearly visible are the positive peak around 100 ms (P100), the negative peak around 150 ms (N150), and the much wider positive peak around 280 ms (P280) after stimulus onset, which are indicated with arrows for electrode PO3.

The average maximum amplitude of the N150 was -3.3 μV (±0.4 μV s.e.m.) for static adapted, -3.2 μV (±0.4 μV s.e.m.) for opposite adapted and –3.3 μV (±0.4 μV s.e.m.) for same adapted conditions.

Non-directional adaptation effects
The evoked potentials to implied motion after adaptation to a moving RDP (regardless of direction) were calculated. The amplitudes for these VEPs were obtained from the same electrodes that provided the amplitudes for the static RDP condition. A paired t-test revealed that the amplitudes of the P100 and P280 after motion adaptation differed significantly from the same peaks after static adaptation (p-values were 0.000 and 0.001 respectively), whereas the N150 did not change significantly (p-value was 0.628).

Direction specific adaptation
To establish direction specific adaptation effects, the motion adaptation trials were separated into adaptation in the same direction as the implied motion, and adaptation in the opposite direction as the implied motion. The amplitudes of all three peaks after the three adaptation conditions were compared in a repeated measures ANOVA. Adaptation had a significant effect on the P100 and the P280 (Greenhouse-Geisser corrected p-values were 0.001 and 0.002 respectively), but not on the N150 (Greenhouse-Geisser corrected p-value was 0.813). Individual amplitudes after adaptation in the opposite and same direction were normalized by dividing by the corresponding individual amplitudes after static adaptation (Figure 3). Paired t-tests revealed that only the amplitude of the P280 was significantly different after adaptation in the same vs. opposite direction (p-value was 0.036, p-values of P100, and N150 were 0.516 and 0.261, respectively).

Scalp distributions and source localization
To estimate the locations of neural sources underlying implied motion responses Brain Electric Source Analysis (Berg & Scherg, 1994; Scherg & Picton, 1991) was performed on the scalp distribution of the baseline grand averages for the P100 and the P280 peaks (Figure 4A). Source models consisted of single dipole pairs, whose bilateral locations and orientations were mirrored in the midline.

Sources were estimated at the grand average peak latencies, i.e., 99 ms for the P100, 145 ms for the N150, and 282 ms for the P280 (Figure 4B). The P100 arose from sources in the occipital lobe. Residual variance (RV, the percentage of scalp data that the model cannot account for; the lower the RV, the better the model fits the data) of this dipole model was only 3.7%. The sources responsible for the N150 were also located in the occipital lobe, though located slightly more anterior than the P100. RV for the N150 was 1.1%. The dipole pair which fitted the P280 was located even more anterior, towards the temporal lobe compared to the other peaks, with a RV of 6.8%.

Dipole solutions for the individual data were located in the same way as the grand average sources were established, at the individual peak latencies. However, source locations varied across subjects. The x, y and z positions of the individual source locations were compared in a multivariate test. Since not all participants passed the criteria to be included in analysis for all three peaks (± 1.5μV amplitude), only the source solutions for subjects which were included in analysis for all three peaks were compared statistically. Individual peak locations of 12 subjects were compared in a multivariate analysis, with the three peaks as within subject factors and the x, y and z positions as measures. Locations of the three peaks did not differ significantly (Hotelling's trace $F(6,38) = 1.1$, $p = 0.356$). Univariate tests for the three different coordinates did not reveal significantly different positions for the three peaks either (Greenhousse Geisser corrected p values for x, y, and z coordinates were 0.49, 0.17 and 0.72 respectively).

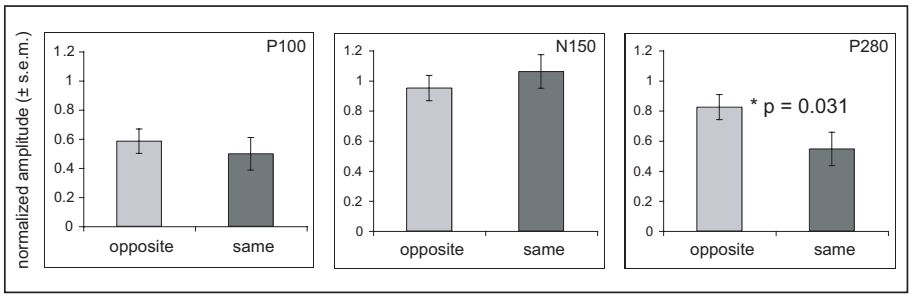

Figure 3
Normalized average maximum amplitudes for three typical implied motion peaks after adaptation to real motion in either the same or opposite direction as the implied motion. Paired t-tests revealed that only the amplitude of the P280 was significantly different for the two motion adaptation directions.

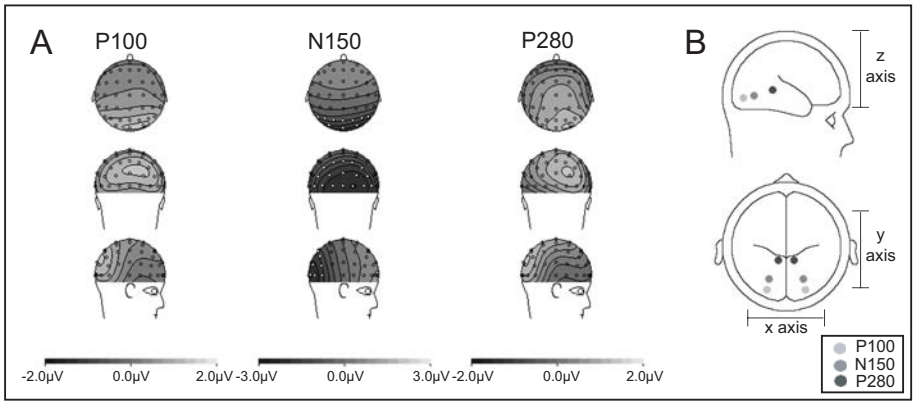

Figure 4

(A) The potential distributions across the scalp of the P100, the N150 and the P280 vary, as is visible in these maps of the grand average implied motion responses at three peak latencies. Note that the scale of the N150 map is larger, as the amplitude of this response was larger than that of both positive peaks. The 17 electrodes that were included in the amplitude analysis are marked with white dots in the N150 maps. (B) Source analysis was performed on the scalp maps. The P100 and N150 are located in the occipital lobe, whereas the P280 seems to be located more anterior, towards the temporal lobe. However, due to inter-individual variation statistical analysis on the individual source locations revealed that these source locations were not significantly different.

Discussion

Interactions between real and implied motion
The current experiment revealed that adaptation to real motion modulated responses to animate implied motion. The modulation consisted of an attenuation of the amplitude of the early component of the evoked potential (P100), which did not depend on the direction of adapting motion, and an attenuation of the later component (P280), which did depend on congruency of adapting motion and implied motion directions. These peaks are in concordance with those found in an earlier study (Lorteije *et al*., 2006). In that study, dipole source analysis suggested that the later component (P280) originated from motion sensitive cortex. However, even though real and animate implied motion responses appeared to arise from the same cortical area, this does not necessarily mean that they are processed by the same neurons. Here, for the first time, we have provided evidence that is consistent with interactions at neuronal level between real and animate implied motion processing.

Source localizations
Source analysis for the grand average P100, N150 and P280 showed a trend from posterior locations for the P100 towards a more anterior location for the P280, with the N150 in the middle. However, individual locations overlapped and comparison of the source locations for individual subjects did not reveal any significant differences in locations between these peaks. This means that the performed analysis lacked the spatial resolution or statistical strength to discriminate between the three sources. However, the modulation by motion adaptation of the three peaks differed, which indicates that they do arise from different neural populations.

Non-directional adaptation
The amplitude of the P100 peak was attenuated after adaptation with a moving RDP. This modulation is indifferent to the direction of the motion. An earlier study (Lorteije *et al*., 2006) has hypothesized that this response arises from early visual areas in response to low-level stimulus features such as luminance, spatial frequencies and orientation. The current results revealed that this peak actually originated from motion or flicker sensitive neurons, which also responded to non-directional features of implied motion. The P100 found in the current study coincides in time with the early phase of the P1 component that was found by Di Russo and colleagues (Di Russo *et al*., 2001) in their study on early components of the VEP. By combining VEP recordings with fMRI scans, they established that the early phase (80 to 110 ms) of this P1 arose from dorsal extrastriate cortex, most probably V3, V3a and adjacent middle occipital gyrus. Besides the temporal congruency of the P1 in Di Russo's study and

the implied motion P100, the source location found for the latter also resembles that of the former, even though the spatial resolution of the current study is low.

Direction specific implied motion response
Implied motion typically evoked a positive peak that was maximal around 280 ms after stimulus onset. The amplitude of this peak was significantly attenuated after adaptation to real motion in the same direction as the implied motion, compared to adaptation to real motion in the opposite direction. It has been suggested that this implied motion response is not caused by low-level stimulus differences between the images with vs. images without implied motion, such as luminance, orientation and spatial frequency (Lorteije *et al*., 2006). In the current paradigm, those features cannot explain the directionally selective adaptation, as the test stimuli were equal for both conditions, only the preceding adaptation direction differed. This strongly suggests that the P280 arises, at least partly, as a response to implied motion from motion-sensitive neurons that are directionally tuned. Dipole source analysis of this peak suggests that it arose from an extrastriate area deep between the occipital and temporal lobes, but the spatial resolution was not high enough to reveal the true anatomical source of this response. However, based on the direction-selective motion-sensitive behavior and combined with the implied motion activation found with fMRI (Kourtzi & Kanwisher, 2000; Senior *et al*., 2000), MT/MST is a plausible candidate for evoking the P280 implied motion response. Recently however, Orban and colleagues defined cortical areas in macaque monkeys rostrally of MT/MST, that like MT/MST responded to real motion, but also to actions implied in static pictures which MT/MST did not respond too (Nelissen *et al.*, 2006). These areas included the lower superior temporal (LST), the fundus superior temporal region (FST) and the middle of the superior temporal polysensory region (STPm). All three are located near the MT/MST complex and may therefore be part of the human MT/MST complex in previous fMRI studies on implied motion (Kourtzi & Kanwisher, 2000; Senior *et al*., 2000). It may thus well be that the P280 arose from human homologues of macaque LST, FST and STPm instead of MT/MST.

The N150
The negative peak around 150 ms was not modulated by motion in either direction selective or direction independent manner. This suggests that the N150 is a response to implied motion arising from neurons that are not involved in real motion processing. Even though this N150 overlaps in time with the N200 evoked by real motion onset, the N150 originates from a different neural population and should not be mistaken for the N200.

Since we established the implied motion response as the difference in response to pictures with minus pictures without implied motion, the N150 may reflect low-level stimulus differences between the two picture conditions irrespective of the presence or absence of implied motion, e.g., size, orientation and spatial frequency. These stimulus features cannot explain the direction-selective P280, but may be responsible for the N150.

In contrast, the P100 that preceded the N150 could be modulated by real motion, i.e., its amplitude was reduced after motion adaptation, regardless of direction. Interestingly, this adaptation of an early visual process is not inherited by the process underlying the N150. There are two explanations for this discontinued adaptation. Firstly, it could mean that the neural process that underlied the N150 did not follow the neural process responsible for the P100 in the hierarchy of the visual system. Instead, the N150 might have represented neural processing that was part of a parallel visual path. Secondly, even when the total response from an earlier process (P100) was diminished due to adaptation, gain control mechanisms could have enabled further processes (N150) to respond as vigorously as before adaptation by responding to the ratio of the output of the adapted process rather than to the total strength of the output.

Role of the Superior Temporal Sulcus in implied motion processing
The latency of the implied motion response (240 to 300 ms) was longer than that of real motion, which typically has a latency of 150 to 200 ms (Bach & Ullrich, 1994; Heinrich *et al*., 2004; Hoffmann *et al*., 2001; Lorteije *et al*., 2006). This indicates that implied motion is not processed along the dorsal visual path, as real motion is, but arrives at motion processing areas via a longer route, possibly as a projection from temporal form areas. The implied-motion sensitive VEP contains contributions from motion-sensitive neurons across the complete spectrum of directional selectivity. Therefore, direction-selective adaptation of the VEP is only possible if the feedback input to its underlying generator is also direction-selective.

A good candidate for providing a directionally selective projection is the superior temporal sulcus (STS) region, which seems to be specialized for the perception of bodily actions and postures in both macaque monkeys (Barraclough *et al*., 2006; Jellema *et al*., 2000; Jellema & Perrett, 2003a, 2003b) and humans (Allison *et al.*, 2000). Cells in the anterior part of the macaque STS respond to specific articulated body movements and postures, whether executed by an actor, or expected to happen on the basis of the immediately preceding perceptual history (Jellema & Perrett, 2003b), or when implied by the articulation of limbs in a static body posture (Jellema & Perrett, 2003a). Importantly, the vast majority of these cells shows selectivity

for the direction of the articulation with respect to the observer, while only a minority will respond to an articulation irrespective of its direction (Jellema & Perrett, 2006).

Barraclough and colleagues showed that neurons in the upper bank, lower bank and fundus of rostral STS and inferotemporal cortex are selective to the degree of articulation (Barraclough *et al*., 2006). Interestingly, neurons that responded stronger to static images of walking persons were more responsive to a movie in which a person was walking forwards vs. backwards, whereas neurons that were more responsive to images of standing postures responded stronger to walking backwards vs. walking forwards.

Thus, populations of STS neurons could provide the information needed for a direction specific implied motion response in motion sensitive areas. Evoked potentials arising from the STS responses to faces and objects occur as a negative peak around 170 ms (Itier & Taylor, 2004a, 2004b). However, it is very unlikely that the N150 found here was STS based. Instead it arose from a much more occipital source. Since similar numbers of STS neurons respond to images with and images without implied motion, the net implied motion response from the STS population would approach zero (Barraclough *et al*., 2006). This might explain why the STS response was not visible in our EEG recordings

Shared neural structure for implied and real motion
The direction specific interaction of implied and real motion processing may play an important role in visual processing. We showed that an image of a person or object expressing implied motion activates direction-specific motion-sensitive neurons. A strong activation might lead to illusory motion perception. Such a phenomenon has been described by e.g., Freyd (Freyd, 1983) in psychophysical experiments. Freyd showed that observers extrapolate the remembered position of objects according to the implied direction of motion, referred to as Representational Momentum (RM). When MT/MST is withheld from coherent firing by application of transcranial magnetic stimulation, the RM effect disappears (Senior *et al.*, 2002), which indicates the functional necessity of MT/MST for RM. Our results suggest that rather than this complete disruption of MT/MST, a more subtle adaptation of direction selective motion neurons might also eliminate the RM effect.

Note that RM has many forms and can be induced by several stimulus features, including postural cues which were present in the current study, but also by for instance an inducing motion sequence (Freyd & Finke, 1984). Also knowledge of the environment surrounding an object (e.g., gravity, friction) or even semantic cues as inserting inducing words as “bounce” or “crash” causes or modulates RM effects. For a review on the extensive research that has been performed on RM see (Hubbard, 2005).

The sharing of neural structures for real and implied motion processing is in concurrence with a MEG study by Amorim and colleagues that revealed a common substrate in the right centro-parietal region for rotational RM and imaginary rotation (Amorim *et al.*, 2000). These authors found the same scalp distribution for imagining a virtual sea horizon rotate and for the RM effect induced by a rotating virtual sea horizon, which indicates that they are processed in the same cortical area. It would be interesting to use an adaptation paradigm as used in the current paper to establish whether those two effects are processed by the same (rotation direction–selective), or by different populations of neurons in the same area.

Function of direction specific implied motion processing
A weak activation of motion sensitive cortex by animate implied motion might not lead to illusory motion, but it could still lower the action potential threshold of neurons with a specific direction tuning, thus making the motion sensitive area more sensitive for motion in the implied motion direction. In natural scenes, a moving animate figure expresses both form cues (implied motion) and real motion cues. The extra activation of motion areas by implied motion would make the viewer more susceptible to the motion of the moving figure, which is especially relevant when the background is also moving. The animate moving figure would thus jump out of the background motion. Furthermore, we often get an intermittent view of a continuous action due to distractions such as occluding objects or blinking of the eyes. To be still able to infer the course of the action in such situations, it would be extremely useful if the fragmented images of articulated body postures would somehow contribute to the action representation and the perceived motion. The direction-selective interaction between real and animate implied motion processing as described in this study, could well provide for this.

CHAPTER 3

DISENTANGLING NEURAL STRUCTURES FOR PROCESSING OF HIGH AND LOW SPEED MOTION

Abstract

Both psychophysical and electrophysiological studies on motion adaptation suggest the existence of at least two separate motion pathways or channels. One channel is tuned to low speeds, while the other is tuned to a broader range of high speeds, that partly overlaps with the low speed channel. However, it remains unclear whether these two different channels are represented by two different cortical areas or by subpopulations within one cortical area.

To investigate this, we recorded evoked potentials at 59 scalp locations to the onset of a slow (3.5°/s) and fast (32°/s) moving pattern. These test patterns were preceded by an adapting pattern, moving at either the low or high speed in the same or opposite direction as the test motion. Additionally, baseline potentials were recorded for slow and fast moving test patterns after adaptation to a static pattern. Comparison of adapted responses with baseline responses revealed that the N2 peak around 180 ms after test stimulus onset was modulated by the preceding adaptation. This modulation depended on both direction and speed.

Source localization of the baseline potentials revealed that different cortical areas were involved in slow and fast motion processing. Areas responsible for processing motion at high speeds were more dorsal, medial and posterior compared to the neural structures underlying processing of slow motion. The neural structures that were modulated by direction independent motion adaptation were also different for slow and fast speeds. However, the direction dependent component of this modulation by adaptation occurred in the same area for both speeds. For both speeds, neural structures that could be adapted in a directionally specific manner were found to be significantly more dorsal compared to neural structures that were adapted in a direction independent manner.

These results show that within dorsal motion sensitive cortical areas, direction dependent motion information at high and low speeds is processed by different neural (sub)populations. In the ventral stream we also found evidence for areas selectively processing motion at low speeds (and not high speeds), that are less direction dependent.

Introduction

Motion processing is vital for most animals to interact with a dynamic environment, whether for detecting moving prey, predators or partners, for crossing streets without being hit by a car, or to intercept a moving object. Even though we as observers might experience low and high speeds as aspects of a continuous spectrum, human psychophysical experiments have given rise to the idea of two separate motion processing pathways, one channel that is tuned to low temporal frequencies and high spatial frequencies (low speeds) and one channel that is tuned to a large bandwidth of high temporal frequencies and low spatial frequencies (high speeds) (Anderson & Burr, 1985; Gegenfurtner & Hawken, 1996; Kulikowski & Tolhurst, 1973; Smith & Edgar, 1994; Thompson, 1984; van de Grind *et al.*, 2001), but see also a recent model of van Boxtel and colleagues (van Boxtel *et al.*, 2006) that shows that a single motion channel may explain speed perception in similar experiments.

Several human psychophysical studies used motion adaptation to study characteristics of these two channels. More specifically, these studies focused on the motion aftereffect (MAE: for a review see (Mather *et al.*, 1998)), a visual illusion caused by motion adaptation. After prolonged exposure (i.e., at least several seconds) to a pattern moving in a single direction, a static pattern may be experienced as moving in the opposite direction as the adapting motion. Interestingly, speed of the adapting pattern and refresh rate of the test pattern interact. Whereas low speeds are capable of evoking a MAE on static test patterns or patterns at low refresh rates (static MAE), fast motion evokes a MAE on patterns with high refresh rates (dynamic MAE) (Verstraten *et al.*, 1999; Verstraten *et al.*, 1998). These results show that the different channels for low and high speed motion can be adapted separately. The divergence between both channels does not simply reflect a difference in processing of two extremes of a single continuous speed range, but these studies show a sharp turnover point at approximately 20 Hz. Furthermore, it is even possible to perceive a transparant MAE after simultaneous adaptation with a transparent fast and slow moving pattern, when the test pattern consists of combined low and high temporal frequencies (van der Smagt *et al*., 1999).

Recording of visually evoked potentials (VEPs) with electro-encephalography (EEG) has become a valuable tool for studying physiological structures underlying motion processing. Motion onset evokes a typical negative peak with a latency of 150 to 200 ms which is often referred to as N2 or N200 (Hoffmann *et al.*, 1999; Kubova *et al.*, 1995; Lorteije *et al.*, 2006; Niedeggen & Wist, 1998; Probst *et al.*, 1993). Motion adaptation was used to study the

processes underlying this N2. Preceding motion onset with an adapting motion resulted in a decrease of the N2 amplitude, which is evidence that this peak mainly reflects motion processing (Bach & Ullrich, 1994). Part of this reduction was direction dependent, it occurred for test directions approaching the adapting motion direction, but not for test directions opposing the adapting direction (Bach & Hoffmann, 2000; Heinrich & Bach, 2003; Hoffmann *et al.*, 2001). Heinrich and colleagues (Heinrich *et al.*, 2004) combined low and high adaptation speeds with low and high test speeds in the opposite or same directions. Adaptation was not only direction dependent, but also speed specific. This reduction was in accordance with the speed dependence of the MAE and provided physiological evidence for the existence of two separate speed channels. However, since they used only 3 electrodes in their recordings, the authors could not perform a source localization to establish whether the two channels involved different anatomical regions.

To investigate whether a two-channel system is divided across anatomical structures, we recorded direction specific adaptation of the N2 at low and high speeds in an experiment similar to the work of Heinrich *et al*., but instead of 3 scalp electrodes, we recorded VEPs from 59 scalp positions. Together, these electrodes showed the distribution of the N2 across the scalp, for slow and fast baseline recordings, as well as adapted N2s and difference potentials between conditions. The scalp distribution of a VEP is dependent on the location and orientation of the underlying neural structures in the brain. Brain electric source analysis (BESA) modeling can be performed on these distributions to estimate the relative location of the cortical areas responsible for these scalp distributions.

In accordance with Heinrich's findings, we observed a direction and speed dependent reduction of N2 amplitude following adaptation. Source analysis revealed that the un-adapted baseline N2 differed in source location for low and high speeds. Furthermore, motion adaptation modulates different areas for low and high speeds. The direction independent part of this adaptation revealed an anterior/posterior and medial/lateral difference in source activity for low and high speeds. However, the separate direction-selective component of this adaptation occurred in overlapping areas for both speeds. For both speeds, neural structures that could be adapted in a directionally specific manner were found to be significantly more dorsal compared to neural structures that were adapted in a direction independent manner.

Methods

Subjects
A total of 17 subjects participated in this study, 6 males and 11 females. One male and one female author participated as subjects, all other 15 subjects were naive as to the purpose of the study. All participants gave their written informed consent and the purpose of the experiment was explained to them after the recordings. Naive subjects were paid expenses. Experiments were in accordance with the declaration of Helsinki (World Medical Association 2000) and the protocol was approved by the ethical committee of the faculty of Social and Behavioural Sciences of Utrecht University.

All subjects reported normal or corrected to normal visual acuity and all subjects were right handed except for one female. The average age was 22.2 (± 1.2 s.e.m.).

Stimuli
Stimuli were presented using Presentation software (Neurobehavioral Systems, Albany, California) on a 19 inch LaCie electronblue IV monitor (1024 by 768 pixels) with a refresh rate of 85 Hz at a distance of 57 cm. The stimuli and their presentation were made to match those used by Heinrich and colleagues (Heinrich *et al*., 2004).

A random pixel array (RPA) with a pixel size of 0.04° moved within a round aperture of 24° diameter. Contrast of the RPA was 73%, at which the space average luminance was 18 cd/m2. A fixation target of 3° diameter was presented in the middle of the aperture.

The RPA could move in either leftwards or rightwards direction at 3.5°/s (slow) or at 32°/s (fast). These speeds matched those used in Heinrich's experiment and were chosen because they were within the speed ranges that are processed by mostly slow or by exclusively fast motion processing channels respectively (van de Grind *et al*., 2001; van der Smagt *et al*., 1999; Verstraten *et al*., 1999; Verstraten *et al*., 1998).

Trials were presented in a cyclic design, starting with an adaptation period of 2200 ms followed by an inter stimulus interval (ISI) of 500 ms and finally a test period of 300 ms. During the adaptation period the RPA could move at either low or high speed in left or right direction, or could remain stationary for the baseline recordings. The duty cycle of the test stimulus (test duration as a percentage of the total trial duration) was 10%. At duty cycles higher than 20%, test periods containing motion could cause adaptation effects resulting in an invalid "unadapted" baseline (Bach & Ullrich, 1994). With a 10% duty cycle the unadapted baseline condition in this study was truly unadapted.

Trials were presented in single-adaptation-type blocks (200 trials per block, except for one subject who was presented with only 150 trials per block). This “top-up” adaptation ensured a deep adaptation state throughout each block. To ensure a deep adaptation at the first trials of each block, every block was preceded by 30 seconds of non-stop adaptation. Subjects were instructed to take a short brake of at least 3 minutes between blocks to prevent fatigue and transfer of adaptation onto the next block. Blocks were presented in a counterbalanced block design, e.g., slow left adaptation, fast right adaptation, a double baseline block, fast left adaptation, and slow right adaptation. The condition that was presented in the first block (and that decided the order of the following blocks), was counterbalanced between subjects.

During the ISI, the RPA remained stationary for 500 ms and started moving again at the onset of the test period. The test pattern could move either fast or slow and rightwards or leftwards, regardless of the adaptation speed and direction. Since responses to left and rightward motion cannot be distinguished in the motion VEP, trials were not discriminated on test motion direction per se. Instead, trials were grouped according to the congruence of the adaptation and test direction, i.e., test motion in either the same or the opposite direction as the adaptation direction (Table 1).

adaptation speed	*test speed*	*test direction compared to adaptation direction*
static (baseline)	fast	baseline fast
	slow	baseline slow
fast	fast	opposite
		same
	slow	opposite
		same
slow	fast	opposite
		same
	slow	opposite
		same

Table 1
Combinations of direction and speed of the adaptation and test motion resulted in 10 conditions (right column).

Recordings
The recordings were performed in a darkened room. A chin rest was placed in front of the monitor to ensure that subjects remained at a viewing distance of 57 cm throughout the recordings. The EEG was recorded from 59 Ag/Cl ring electrodes, which were mounted in an elastic cap (Braincap, Brain Products, Germany). Scalp electrodes were distributed according to a 10/10 system. Additional electrodes included two electrodes above and below the left eye to record the vertical electro-oculogram (EOG), two electrodes on the outer canthi of both eyes for horizontal EOG and one grounding electrode. Resistance between skin and electrodes was kept below 4 kOhm throughout the experiment. BrainVision Recorder (Brain Products, Germany) was used to sample and digitize the EEG at 1 kHz, to filter (high-pass cutoff at 0.03 Hz, low-pass cutoff at 400 Hz, and a 50 Hz notch filter) and to store the data on hard disk for off-line analysis. Electode Cz was used as reference during the recordings. Data was re-referenced offline to the average scalp potential for further analysis.

VEP Analysis
BrainVision Analyser (Brain Products, Germany) was used for data analysis. The EEG was segmented into stimulus locked epochs of 500 ms (100 ms before to 400 ms after test stimulus onset). Segments containing blinks or eye-movements (criteria were > 100 µV or < -100 µV), or artifacts (criteria were > 120 µV or < -120 µV on any EEG channel) within a time window of 100 ms before to 100 ms after the test period, were excluded from further analysis. For every subject, the average evoked potential per condition was calculated. Finally, average VEPs were filtered (high-pass cutoff 0.05 Hz, low-pass cutoff 20 Hz, 12 dB/oct) and baseline corrected (i.e., VEPs from all scalp electrodes were offset corrected so that their average potential from 100 ms to 0 ms before stimulus onset was 0µV).

EEG potentials evoked by motion are most pronounced at occipital and occipito-parietal electrodes (Bach & Ullrich, 1994; Heinrich *et al*., 2004; Hoffmann *et al*., 2001; Lorteije *et al*., 2006; Probst *et al*., 1993). For this reason, 8 posterior electrodes were selected for analysis on peak amplitudes (PO7, PO3, POz, PO4, PO8, O2, Oz, and O1, see Figure 4 for scalp locations of these electrodes). For every subject the N2 peak values and corresponding latencies were established at these electrode locations. Since the N2 is often lateralized to left or right hemisphere across subjects (Andreassi & Juszczak, 1982), for every subject the 2 electrodes (or single electrode if slow and fast motion responses are maximal at the same electrode position) with maximal N2 amplitude for slow and for fast motion were selected for further analysis. To assess modulation of this N2,

the baseline N2 needed to be strong enough. Therefore an acceptance criterion was set. Only subjects with both high and low speed baseline N2 amplitudes more negative than –2 μV were included in further analysis. Only one subject was excluded based on this criterion.

Source Analysis

To locate the neuronal sources underlying fast and slow motion processing, brain electric source analysis (BESA 2.2 (Scherg & Picton, 1991)) was performed. The analysis included data from all scalp electrodes (not just the 8 posterior ones). BESA modeled location, orientation and strength of equivalent intra-cranial dipole-sources according to the recorded scalp activity. The optimal dipole-solution was found by searching for a minimum in the residual variance (RV) function in a 3 ms window at the baselines' fast and slow latencies (either for grand average or for individual subjects). To reduce the probability of interacting dipoles (i.e., adjacent dipoles with opposing high-amplitude potential fields), the energy constraint of the BESA model was set to 20% (with the remaining 80% for the RV criterion), thus favoring source solutions with relatively low dipole strengths (Berg & Scherg, 1994). Single dipole pairs were used for source models. The location and orientation of the dipoles were bilateral symmetrically constrained.

Results

N2 amplitudes

In the baseline condition (adaptation to a static pattern) test motion patterns evoked a N2 at occipital electrodes, for both high and low speeds. These slow and fast baseline N2 amplitudes were established for all subjects as the most negative amplitudes at one of the eight posterior electrodes within a latency window of 150 to 210 ms after stimulus onset. In order to establish modulation of the N2 amplitudes due to adaptation, the baseline N2 peak amplitudes needed to be large enough. For one subject the amplitude of the slow baseline N2 was above the acceptance criterion of -2 μV (-0.4 μV for slow and -2.1 μV for fast). Data from this subject were excluded from further analysis. The average baseline peak amplitudes of the remaining 16 subjects were –4.8 μV (± 0.5 s.e.m.) at an average latency of 192 ms (± 3.6 s.e.m.) for slow and -8.6 μV (± 0.9 s.e.m.) at a latency of 190.4 ms (± 3.2 s.e.m.) for fast motion.

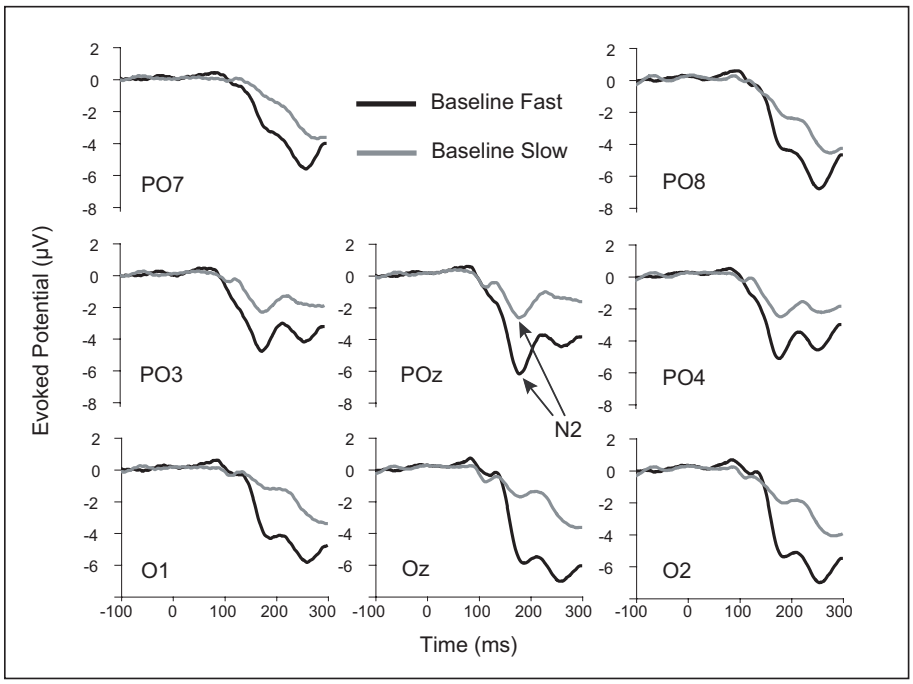

Figure 1

The N2s within the grand average baseline evoked potentials at 8 posterior electrodes are stronger for fast test motion (black line) than for slow test motion (gray lines). For both speeds the N2 had a maximum amplitude at electrode POz at a latency of 180 ms after test stimulus onset. The N2 is indicated with arrows for electrode POz.

The average evoked potential for both slow and fast baseline tests across 16 subjects was calculated (Figure 1). The N2 was visible at all posterior electrodes, but was strongest at electrode POz. The response to fast motion was stronger than the response to slow motion, at all electrodes. Interestingly, the VEPs do not fall back to baseline level after the N2, but remain negative and even show another negative peak around 250 ms after stimulus onset.

Peak amplitudes for these grand average VEPs were estimated. The peak N2 was –2.1 μV for the slow baseline and –6.1 μV for the fast baseline. The maximum N2 of both speeds occurred at electrode POz at a latency of 180 ms after stimulus onset.

For both fast and slow tests after both fast and slow adaptation, the grand average evoked potentials for motion in the same and opposite direction as the adaptation direction were calculated. At electrode POz (which had the strongest baseline N2), modulation of the N2 due to adaptation was clearly visible for conditions with congruent adaptation and test speed (Figure 2, A & D). The results showed two different effects of adaptation. First there was a global attenuation of VEPs adapted in both opposite and same direction as the test direction vs. the baseline VEPs. Second, the motion onset VEP that was adapted in the same direction as the test direction was much stronger attenuated than the motion onset VEP that was adapted in the opposite direction, which means that modulation due to adaptation was partly direction selective.

In both conditions with incongruent adaptation and test speed (Figure 2, B & C), adaptation effects were nearly absent. Only for fast tests following slow adaptation the same adapted N2 was slightly attenuated compared to the baseline and opposite adapted VEPs.

For 16 subjects, the N2 amplitudes for low and high test speeds after all adaptation conditions were established at the 2 electrodes (or single electrode if slow and fast motion responses for the baseline condition were maximal at the same electrode position) at which the individual slow and fast baseline N2s were at maximum, in a latency window of 20 ms before to 20 ms after the latency of the baseline N2.

Individual N2 amplitudes after adaptation were normalized by dividing by the corresponding slow or fast baseline amplitudes. Thus the modulation due to adaptation averaged over our population of subjects of slow and fast N2 amplitudes could be compared (Figure 3).

First, adaptation resulted in a direction independent amplitude reduction across most adaptation conditions compared to the baseline amplitudes. N2 amplitudes of all adaptation conditions were compared

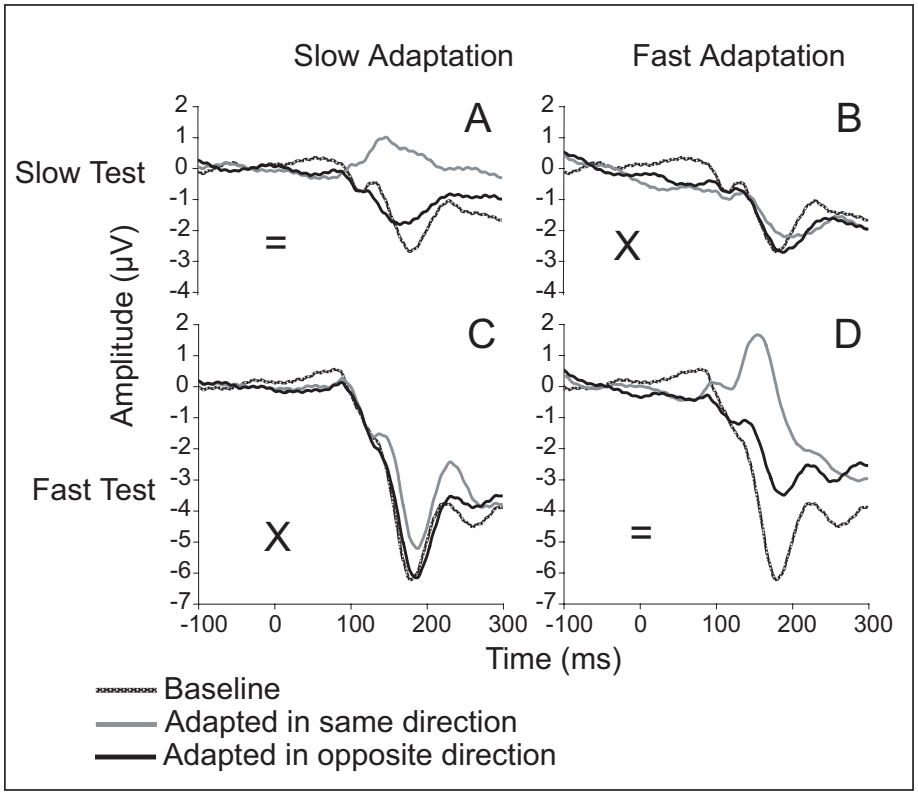

Figure 2
The N2s of slow and fast test motion are modulated by the preceding adaptation when the adapting and test motion are of congruent speed (=), but less so when the speeds of the adaptation and test differ (X). This modulation is stronger for test motion in the same direction as the adapting motion (grey lines) than for test motion in the opposite direction as the adapting motion (black lines), compared to the baseline responses (dotted lines).

to the corresponding fast or slow baseline in a paired T-test. Indeed, almost all adapted N2s were significantly reduced compared to the baseline N2 ($p < 0.01$) except for the fast test N2 which was preceded by a slow adaptation in the opposite direction, although this condition tended towards significance ($p = 0.060$).

Second, when the adapting and test motion had congruent speeds, differences in reduction between test motion in the same vs. opposite direction as the adaptation direction were found (Figures 3A and 3D). Paired t-tests were performed to statistically test the difference between these same and opposite adapted N2 amplitudes. For both slow and fast N2s adapted by congruent speeds these differences were significant ($p < 0.001$).

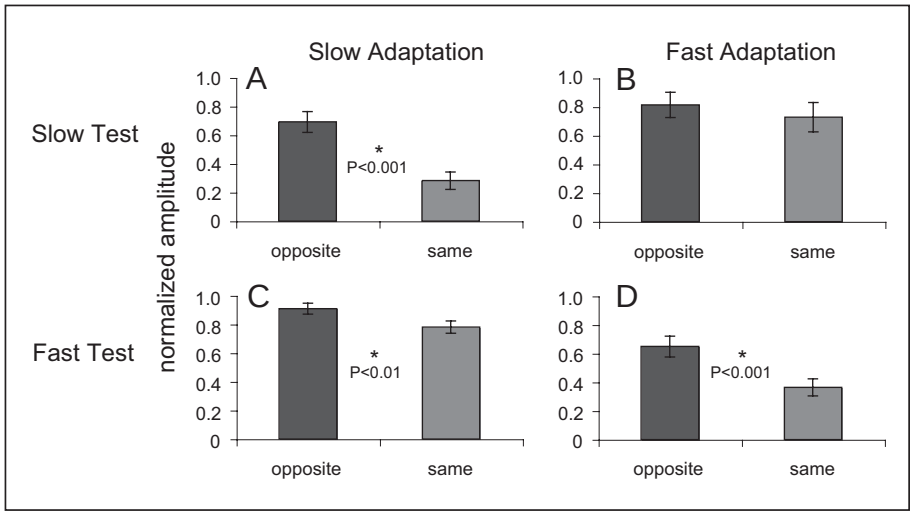

Figure 3
The average normalized N2 amplitudes for slow and fast test speeds after adaptation at slow or fast adaptation speeds in the same or opposite direction as the preceding adaptation. Amplitudes were normalized for each subject by dividing through the corresponding slow or fast baseline N2 amplitude. Asterisks indicate significant differences in amplitude between opposite and same motion.

In contrast to the data from Heinrich (Heinrich *et al.*, 2004), the amplitude to high speed onset after slow adaptation (incongruent speeds) was also significantly different between the same vs. opposite direction ($p < 0.01$, Figure 3C). However, this cross-speed adaptation was much weaker than the congruent-speed adaptations, as the N2 of the same direction was reduced by only 14% compared to the N2 of the opposite direction test. In contrast, N2 reduction was 59% and 44% for respectively slow tests and fast tests after congruent speed adaptation. Only for the low speed test after high speed adaptation there was no significant difference in amplitude between directions (Figure 3B).

In the previous analysis the electrode that was chosen to perform the calculations could be different for fast and slow tests. Therefore we also compared N2 amplitudes for same and opposite test for a single electrode at which the baseline grand average N2 for both speeds was strongest (POz), and also for the average N2 across all 8 posterior electrodes. Both comparisons showed the same significant differences between same and opposite directions. Again, for both slow and fast N2s adapted by congruent speeds these differences were significant ($p < 0.001$), while the amplitude to high speed after slow adaptation (incongruent speeds) was also significantly different between the same vs. opposite direction ($p < 0.01$).

Source analysis of baseline N2s

For both unadapted baseline grand averages, the scalp distribution in a 3 ms window around the peak amplitude latency (180 ms for both speeds) was established (Figure 4). The response to fast motion was stronger than the response to slow motion. Further, the scalp distribution of the high speed response had a much sharper gradient than the wider low speed scalp potential distribution.

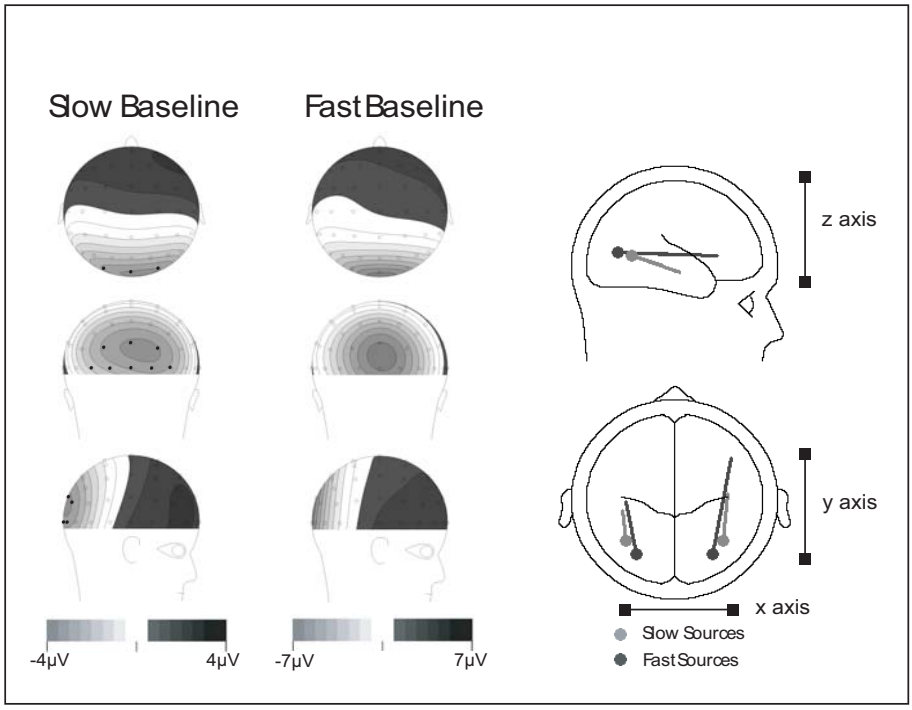

Figure 4

The grand average scalp maps of the slow and fast baseline VEPs at 180 ms after stimulus onset (left and middle panel) formed the basis for source localization of these baseline responses (right panel). Dots indicate the location of the dipole sources (dark grey high and light grey low speeds). The direction of the lines originating from these dots indicate the positive direction of the dipoles, while their relative strength is represented by their length and size. Sources for fast motion were more posterior, more medial and slightly more dorsal than slow motion sources. X, y and z axes are shown in the right hand panel. The 8 posterior electrodes that were used in N2 amplitude analysis are marked with black dots in the scalp distribution map of the slow baseline response.

These scalp distributions were used for source modeling of the neuronal sources underlying the N2s. The data could be well fitted in a symmetrical dipole model. The residual variance (RV) was the percentage of the scalp data which could not be explained by the model. Therefore, the lower the RV, the better the model fitted the data. The RV for the slow baseline source model was 2.7%, and the RV for the fast baseline source model was 1.9%, which means that both were excellent fits.

Source analysis revealed that the high speed N2 arose from neural structures that were located posterior, dorsal and medial from the areas that underlies the low speed N2 (Figure 4). To statistically test this trend, source analysis was performed on the individual N2 scalp distributions at the corresponding individual latencies. Scalp data of two subjects did not deliver valid source localization for the slow motion condition, i.e., sources were located in the neck. Source locations of these subjects were excluded from statistical analysis that compared locations for fast and slow baseline N2s and those that compared locations of the slow baseline N2 with (slow) adapted sources. Individual x, y and z coordinates (see Figure 4 for an explanation of these axes) for slow and fast motion onset were compared in a multivariate test (repeated measures ANOVA) with speed (2) as within subjects factor and coordinates (3) as measures. The difference in location for the baseline response of the two speeds was significant (for N = 14, Hotelling Trace $F(3,11) = 5.108$, $p = 0.019$). A univariate test revealed that this difference was not significant for any of the three axes separately (Greenhouse-Geisser corrected p values were respectively 0.055, 0.067 and 0.080 for x, y and z axis), which means that the significant deviation between the two conditions should be attributed to a combination of differences along the three axes.

Source analysis of N2 adaptation

Although the differences in baseline N2 sources reflect different activated motion areas, they reflect non-motion processing as well. To more specifically isolate motion processing, the VEP that was adapted by motion in the same direction was subtracted from its corresponding baseline VEP (i.e., with the same speed), for low and high test speeds (Figure 5). Only tests with the same speed as the preceding adaptation were included in this subtraction, and cross speed adaptations were excluded. This difference reflected the maximum adaptation, encompassing both direction specific and speed specific components. Source locations of the grand average of these difference potential showed the same trend as the baseline sources along the x and y axis, but not along the z axis, the high speed N2 arose from neural structures that were located posterior and medial, but ventral from the areas that processed the low speed N2.

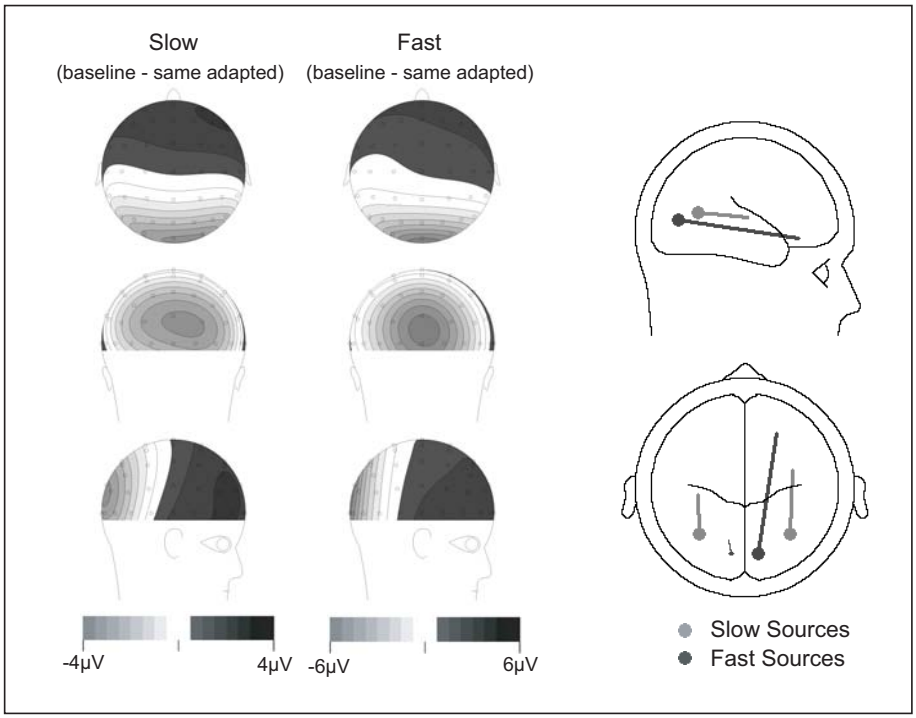

Figure 5
Grand average scalp maps and source localizations for baseline VEPs – VEPs adapted in the same direction, identified the cortical regions underlying the maximum adaptation for low and high speeds. Differences along the x and y axis were statistically significant. (Same conventions as figure 4.)

RV for the slow source solution was 1.2%, RV for the fast source model was 0.8%. Multivariate analysis on the individual sources revealed that locations were indeed significantly different (N = 16, Hotelling Trace F(3,13) = 6.462, p = 0.007). Univariate analysis indicated that differences were significant along the x axis (Greenhouse-Geisser p = 0.025) and along the y axis (Greenhouse-Geisser p = 0.001) but not along the z axis (Greenhouse-Geisser p = 0.345). The slight differences between this pattern of results and that for the baseline N2 suggests that the latter does reflect more than adaptable motion-dependent responses.

Direction independent adaptation
The baseline minus same subtraction reflects both direction dependent and independent motion-dependent responses, which could well originate from different areas, the geometrical average of which is estimated as the baseline minus same adapted source. To reduce the direction specific contribution of the adaptation and to focus

more on the speed dependent part of the adapted N2, we subtracted the opposite adapted N2 from the baseline N2. Since directionally dependent responses would be present in both N2s, they would be strongly reduced in the subtraction N2. This N2 would then mainly reflect a non-directional adaptation component. Source localization revealed that these direction independent components were even stronger divided for responses to slow and fast motion (figure 6). The RV for the slow source model was 2.73%, and the RV for the fast model was 5.17%. Individual sources were again established to statistically quantify this difference. For one subject in the fast condition and one subject in the slow condition, no reliable sources could be obtained. Therefore these subjects were excluded for statistical comparisons regarding these sources.

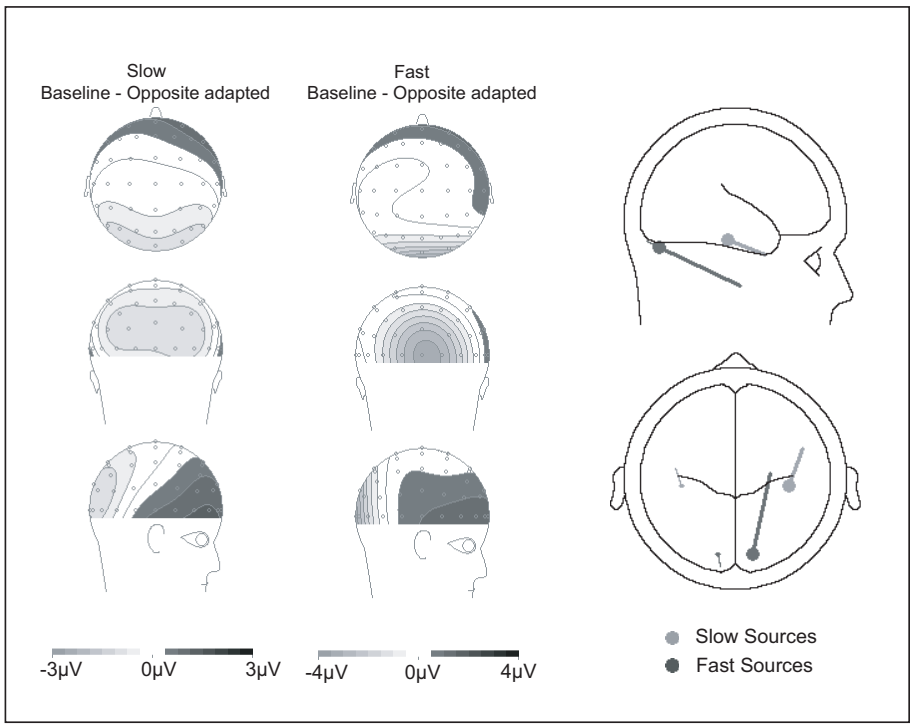

Figure 6
Grand average scalp maps and source localizations for baseline VEPs – VEPs adapted in the opposite direction revealed significant differences in neural structures for direction independent adaptation. Adapted regions for the N2 evoked by low speeds were significantly more anterior and lateral compared to adapted regions for N2s evoked by high speeds. (Same conventions as figure 4.)

Sources of the remaining subjects were compared, again in multivariate and univariate tests, and revealed a significant difference in location between responses to slow and fast speeds (multivariate, N = 14, Hotelling Trace F(3,11) = 7.842, p = 0.004). Locations differed along the x and y axis, but not along the z axis (Greenhouse-Geisser p values were respectively 0.013, 0.007 and 0.373).

Source analysis of direction dependent N2 adaptation
To investigate whether direction selective processing occurs in different areas for low and high speeds, the difference potentials between tests in opposite vs. same direction as the adaptation were established for both low and high speeds (Figure 7). These difference potentials included only tests with the same speed as the preceding adaptation, excluding cross speed adaptations. Since this subtraction eliminated common components of the opposite and same adapted response, only the N2 components that were directionally adapted were reflected (as those are present in the opposite adapted response, but not in the same adapted response).

Source localization of the grand average difference potential was performed for the same latency window as the baseline model (180 ms for both speeds). BESA analysis revealed that directionally selective adaptation arose from the same or from closely located areas for both slow and fast speed processing. The RV for the slow source model was 2.8%, and the RV for the fast model was 1.7%. Multivariate analysis on the individual sources revealed that they did not differ in location for high or low speeds (N = 16, Hotelling Trace F(3,13) = 0.496, p = 0.691). The combination of direction dependent and independent adapted sources seems to be consistent with a geometrical average as reflected in the baseline minus same adapted estimated source.

Individual locations of the sources underlying the N2 direction specific adaptations for low and high speeds were compared with the locations of the baseline N2 sources in multivariate and univariate tests. For both high and low speeds, locations of baseline N2 activation and of N2 adaptation differed significantly (N = 16 high speed: Hotelling Trace F(3,13) = 4.163, p = 0.029, low speed: Hotelling Trace F(3,13) = 10.627, p = 0.001). Fast sources differed significantly along the x and y axis, but not along the z axis (Greenhouse-Geisser p-values were respectively 0.035, 0.028 and 0.123). Slow sources differed significantly along the y and z axis (Greenhouse-Geisser p values < 0.001), but not along the x axis (Greenhouse-Geisser p = 0.524).

Comparison of directionally dependent and independent N2 adaptation
The direction independent N2 adaptation revealed different sources for slow and fast motion processing, but the direction dependent N2

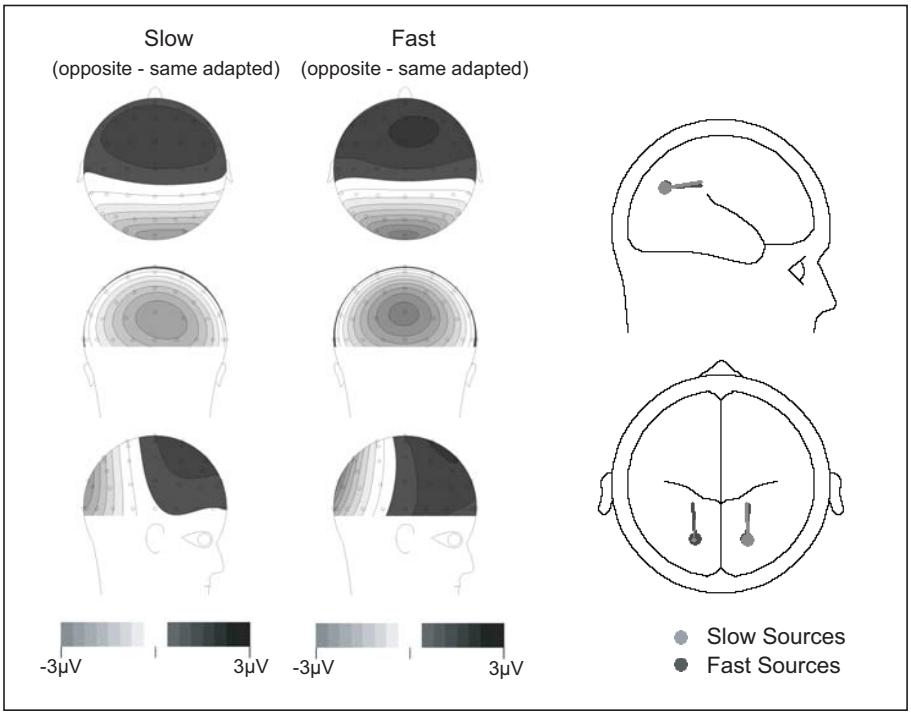

Figure 7
Grand average scalp maps and source localizations for VEPs adapted in the opposite direction – VEPs adapted in the same direction, revealed no differences in neural structures for direction dependent adaptation. (Same conventions as figure 4.)

adaptation occurred at the same location for both speeds. To test whether these two adaptation conditions were anatomically separate, we compared for both speeds the location of the two direction dependent and independent N2 adaptation. For both high and low speeds, multivariate tests revealed that direction dependent and independent adaptation of the N2 occurred at different locations (N = 15, fast: Hotelling Trace $F(3,12) = 8.553$, $p = 0.003$), slow: Hotelling Trace $F(3,12) = 5.349$, $p = 0.014$). For high speed, this difference occurred mainly along the z axis (Greenhouse-Geisser p-value = 0.002), but also along the x and y axis (Greenhouse-Geisser p values were 0.035 and 0.037 respectively). For low speed this difference was only significant for the z axis (p value = 0.001) and not along the x and y axis (Greenhouse-Geisser p values were 0.291 and 0.204 respectively).

Discussion

Direction and speed specific N2 adaptation
EEG potentials evoked by the onset of slow and fast moving RPAs were recorded. These test RPAs were preceded by an adaptation period during which a RPA was presented that could 1) remain static for the unadapted baseline conditions, 2) move at high speed (32°/s), 3) move at low speed (3.5°/s). The moving RPAs could move in the same or opposite direction as the test RPA. The two speeds were chosen based on psychophysical studies of the MAE, according to which motion at these speeds is processed respectively by strictly high temporal frequency channels and mainly low temporal frequency channels (van der Smagt *et al*., 1999; Verstraten *et al.*, 1999; Verstraten *et al.*, 1998). VEPs contained a typical negative peak between 150 and 200 ms, which was named the N2. Amplitudes and source estimates of N2s evoked by slow and fast motion after different adaptation conditions were compared.

The N2 was followed by an extra negative peak that peaked at approximately 250 ms after stimulus onset. This peak may correspond to a parieto-occipital negativity that occurs about 300 ms after stimulus onset and has been shown to represent subjective perception of visual motion perception, irrespective of the physical properties of the stimulus (Haarmeier & Thier, 1998). In contrast to the current study, this peak was much less pronounced in Heinrichs results (Heinrich *et al.*, 2004), even though visual stimulation and instructions in both studies were closely matched and the N300 is thought to be less dependent on the physical characteristics of motion. In this paper, we focus on modulation of the N2 by motion adaptation.

The amplitude of the N2 was modulated by the preceding adaptation, which indicates that this peak mainly reflects motion processing, as has been shown in several studies (Bach & Ullrich, 1994; ffytche *et al.*, 2000; Hoffmann *et al.*, 2001; Lorteije *et al.*, 2006; Muller *et al.*, 2004; Niedeggen & Wist, 1998). In concurrence with the results from Heinrich (Heinrich *et al.*, 2004), modulation of the test N2 depended on both the speed and direction of the adapting motion.

However, in addition to the direction specific adaptation for conditions with congruent adaptation and test speed that were found by Heinrich, a much smaller but significant direction specific adaptation was found for fast speeds that were preceded by a slow adaptation. Only slow speeds that were preceded by fast adaptation did not contain this direction specific adaptation.

The results that were congruent with Heinrichs results (Heinrich *et al.*, 2004) indicate separate processing of slow and fast motion. However, the additional direction specific attenuation of the fast motion response by slow motion adaptation revealed that the speed ranges of the two channels are not completely distinct. Instead, the high speed evoked N2 arose from direction-selective neural structures that were also involved in direction selective processing of slow motion. In contrast, the low speed N2 arose mainly from direction-selective neurons that were not involved in direction-selective processing of fast motion. Psychophysical data has revealed that the suggested low speed motion channel has a tuning range for speeds below ~20°/s and peaking around 3°/s, while the suggested high speed motion channel has a higher range from below 1°/s up to 80°/s (Curran & Benton, 2006; van de Grind *et al.*, 2001; Verstraten *et al.*, 1998). Due to this overlap, a single intermediate speed can evoke a transparent MAE on a test pattern containing both slow and fast moving dots (Curran & Benton, 2006). This explains why the high frequency channel could be slightly adapted by slow motion, while the low frequency channel could not be adapted by fast motion. This cross-speed N2 reduction is much smaller in amplitude than the congruent-speed N2 reductions. Thus, it may have been insignificant in Heinrichs work, while the congruent reductions found in that study were. The current study used more electrodes for a more optimal N2 recording and a larger number of participants, which probably gave it enough statistical power to detect this smaller reduction.

Different cortical areas are involved in processing of low and high speeds

Source localization of the baseline responses to fast and slow motion revealed that their corresponding N2s arose from different areas. The current study lacked the spatial landmarks that could reveal the exact anatomical areas from which the N2s arose. However, the spatial resolution was high enough to differentiate between neural structures underlying the N2 responses to low and high speed motion. Sources contributing to the N2 response to slow motion onset were found more anterior, lateral and slightly more ventral than sources underlying the N2 response to fast motion onset.

These relative locations are very interesting, as the large anterior/posterior difference is opposite of what could be expected based on extracellular recordings in macaques, which revealed that neurons in the posterior primary visual area (V1) detect directional differences at lower speeds than neurons in relatively more anterior middle temporal region (MT) (Churchland *et al.*, 2005; Mikami *et al.*, 1986). Additionally, macaque area MT shows a stronger fMRI BOLD response when presented with fast motion (> 8°/s) than when presented with slow motion (< 4°/s) (Nelissen *et al.*, 2006). Also in humans BOLD

responses in visual areas have been compared, but only for a range of speeds up to 9°/s (Singh *et al.*, 2000). From human psychophysical studies we know that speed tuning of low and high speed channels overlaps in this speed range. We are not aware of any fMRI study that compares speed preferences of visual areas across a speed range that can discriminate between responses from both channels, from nearly zero to at least 25°/s.

It has been proposed that the dorsal, mainly magnocellular, visual pathway is the anatomical correlate of the broadly tuned transient high frequency channel. The ventral, mainly parvocellular, visual pathway may correspond to the sustained low temporal frequency channel. These suggestions might be an explanation for the separation between statica and dynamic MAEs (van der Smagt *et al.*, 1999; Verstraten *et al.*, 1998). Furthermore, it could explain the different binocular rivalry stages for low and high speed motion perception (van de Grind *et al*., 2001), and the interaction between color and motion processing (Gegenfurtner & Hawken, 1996). However, physiological data comparing speed tuning simultaneously in different brain regions was lacking, until now. It would be very interesting to specify at a higher spatial resolution, for instance with fMRI, which brain areas of the ventral and dorsal pathways are involved in motion processing and for which speeds they are tuned, even though a technique as fMRI lacks the temporal resolution to discriminate which areas are responsible for the N2 peak.

It should be noted that the static adaptation that was used as a baseline condition in these experiments may not be completely unadapted, since static patterns may also adapt motion channels, especially the low speed channel (van de Grind *et al.*, 2004). This implies that the amplitude of the baseline response used here, may have been lower than for a true unadapted motion response, especially for the low speed condition, which means that the direction independent adaptation effect described below may have been even stronger than described here. However, this should not affect the size of the direction dependent adaptation, nor strongly effect the source localizations of any condition.

Slow and fast motion adaptation occurs in different areas
Difference potentials reflecting responses from adapted areas were calculated by subtraction of the maximally adapted potentials (same speed and same direction) from baseline potentials. This subtraction eliminates responses from areas that were not adapted, leaving only responses from areas that were adapted. These areas differed for slow and fast speeds along the x and y axis, and showed nearly the same pattern as the baseline sources; fast adaptation occurred more medial and posterior than slow motion adaptation, only the dorsal/ ventral divergence lacked.

Direction independent adaptation
To investigate which motion sensitive areas were adapted by motion adaptation per se, for both speeds, the scalp distribution of the N2 that was adapted with the same speed but in the opposite direction was subtracted from the corresponding baseline scalp distribution. Sources for direction independent N2 adaptation for slow test motion were significantly more anterior and lateral compared to sources for fast test motion. These results show that different neural structures are involved in processing motion with low and high speeds. The anterior/lateral location of the slow sources may correspond to cortical regions in the temporal lobe, whereas the occipital sources responding to fast motion could represent early visual areas.

Direction dependent adaptation component
To establish which areas were adapted in a direction dependent manner, for both speeds the scalp distribution of the N2 that was adapted in the same direction with equal speed was subtracted from the scalp distribution with opposite direction and equal speed. Sources underlying this subtraction scalp distribution were compared for slow and fast test motion and did not differ in location. This may perhaps partly be attributed to the low spatial resolution of VEP source modeling and the fact that the direction specific N2 reduction is a much weaker signal than the unsubtracted baseline N2 and the more optimal subtraction of the same adapted N2 from the baseline N2 as fewer neurons are (as a consequence) represented in the signal. However, the spatial resolution was high enough to discriminate between these sources of direction dependent adaptation and the sources of the direction independent adaptation, which indicates that the spatial resolution and signal strength are indeed strong enough for reliable source estimates and that at least one area processes direction at both low and high speeds.

The N2 amplitude reduction due to adaptation already revealed that speed tuning of the fast motion channel was broad and overlapped with tuning of the slow motion channel. Therefore, it could be argued that the fast motion channel contributes to both fast and (perhaps in a lesser extent) slow adapted N2s, thus “pulling” the source estimates for both speeds together.

Note that these sources were obtained from the difference potential of the opposite and same adapted N2s, and though this difference is similar in strength, the absolute response from this area to low and high speeds may differ. Based on the dorsal location of these sources, they may represent dorsal motion areas such as area MT+.

Disentangling direction dependent and independent motion processing for both speeds

For N2s in response to both slow motion and fast motion, source locations for direction independent adaptation were significantly more ventral compared to source locations for direction dependent adaptation. This ventral dorsal segregation is very interesting as the cortical visual system is generally assumed to be divided into two major pathways. First, a dorsal visual stream that is mainly involved in motion perception, stereopsis and spatial information processing, and that is therefore often referred to as the "where" pathway (Ungerleider & Mishkin, 1982). Second, a ventral visual stream that is mainly specialized in processing colour and form information, which can be used for object identification, and is therefore often referred to as the "what" pathway (Ungerleider & Mishkin, 1982). The transient response characteristics of the dorsal pathway vs. the sustained response characteristics of the ventral pathway suggest that the division across the two cortical streams may correspond to a division in earlier stages of visual processing that are divided across respectively a magnocellular and a parvocellular route (DeYoe & Van Essen, 1988). The transient vs. sustained response characteristics indicate that this division may underlay the separate low frequency and high frequency channels.

However, the present data do not support such a simple slow-to-ventral and fast-to-dorsal mapping. For both speeds, direction-dependent adaptation was found dorsally, suggesting fast-to-dorsal and slow-to-dorsal mapping. Direction-independent adaptation still allows for a specific slow-to-ventral mapping. For high speed, the direction independent adapted areas were also more medial and posterior compared to direction dependent adapted regions. This may suggest that, for high speeds, the former represents activation in early visual areas, such as V1, whereas the latter arises from region further along the dorsal motion processing pathway.

For N2s evoked by low speed, the cortical areas that were adapted in a direction independent manner were more ventral than the areas that were adapted in a direction dependent manner. Furthermore, these direction independent areas arose from more temporal areas compared to their high speed counterparts.

These findings suggest a division of motion processing along a direction independent ventral pathway for low speeds, and a direction dependent dorsal pathway for high and low speeds. Since N2 amplitudes were modulated in a combined speed and direction dependent manner, this reveals that dorsal visual areas may process both low and high speeds, but that this process occurs separately within different neural populations. These populations may occupy

the same areas, as the current source models predict, or areas that are located closely together and cannot be discriminated by BESA source analysis. Furthermore, as revealed by the N2 amplitude reduction, the fast motion channels is broadly tuned and may also process the low speed used here. Thus, directionally dependent sources for both speeds may have been "pulled" together by the high speed sources.

Our results are in concurrence with a division of motion processing across a dorsal and ventral pathway that is well known in literature. Based on their respectively transient vs. sustained responses, it has been postulated that the dorsal high frequency channel processes motion information while the ventral low frequency channel is involved in pattern and shape processing (Georgeson, 1985; Kulikowski, 1971; van de Grind *et al.*, 2001). This idea corresponded to work by Probst *et al.*, who showed that both motion onset and pattern reversal (which is a direction independent "motion" stimulus) evoked an N2 peak. Sources for pattern onset were more anterior and medial compared to sources for motion onset (Probst *et al.*, 1993). Source activity due to motion onset as recorded with magneto-encephalograms (MEG) also reveals temporal occipital sources, but with the most prominent peaks occurring between 200 and 300 ms (Amano *et al.*, 2006), which is later than the N2 peak as recorded with EEG.

As has been suggested by van de Grind *et al*., this ventral motion pathway may be vital for obtaining structure from motion (van de Grind *et al*., 2001). This ventral pathway may correspond to the dynamic form pathway as postulated by Zeki, for which area V3 may be an important processing stage (Gegenfurtner *et al*., 1997; S. Zeki, 1993). Even though direction dependent adaptation mainly affected the N2 components arising from the dorsal visual pathway, this does not necessarily rule out any direction sensitivity in the ventral stream. Direction sensitivity may be much stronger in the dorsal stream, thus "pulling" the direction dependent sources toward the dorsal stream.

We have shown, for the first time, physiological evidence that motion with low speed is processed along the ventral pathway, whereas the dorsal motion processing pathway has a much larger range of speed tuning, and is divided into two neural populations.

CHAPTER 4

NO EVIDENCE FOR ANIMATE IMPLIED MOTION PROCESSING IN MACAQUE AREAS MT AND MST

Abstract

In this study we investigated animate implied motion processing in macaque motion sensitive cortical neurons. We recorded cell responses in middle temporal (MT) and medial superior temporal (MST) cortical areas to static photographs of humans or monkeys, which were running or walking in two opposite motion directions. These responses were compared to responses to photographs of the same humans and monkeys standing or sitting still. We also investigated whether the implied motion direction that elicited the highest response was correlated to the preferred direction for moving random dot patterns. In the first experiment the pictures were presented inside the cell's receptive field, and in the second experiment the pictures were presented at the fovea, while a dynamic noise pattern was presented at the cell's receptive field location. For both experiments, the results show that the responses of MT and MST neural populations do not discriminate between pictures with moving agents and pictures that do not imply motion. An analysis of each unit separately also showed no evidence for modulation of activity by the implied motion content of the stimuli. Response preferences for human implied motion reflected preferences for low-level visual features such as orientation and stimulus location. Furthermore, no correlation was found between the preferred direction for implied motion and the preferred direction for moving random dot patterns. In a separate experiment we show that cells in anterior regions of the superior temporal sulcus (STSa) respond differentially to the implied versus motionless stimuli that we used in this study, which confirms processing of implied motion in STSa. Our results show no evidence for such object information related modulation in macaque MT and MST.

Introduction

A static photograph of an object or person in motion can evoke a strong sense of motion due to the content of the picture. A possible reason for this implied motion sensation could be that a snapshot of e.g., a running person is associated with real motion. There is recent evidence from single cell recordings in macaque monkeys that associative learning induced plasticity can already take place in the low-level motion processing middle temporal (MT) region (Schlack & Albright, 2006). Furthermore, human fMRI studies have shown that static photographs depicting an object or person in motion evoke a higher BOLD response in area MT and its satellites than photographs of the same objects or persons without this implied motion (Kourtzi and Kanwisher, 2000; Senior *et al*., 2000).

We tested whether individual neurons in macaque MT and medial superior temporal (MST) are sensitive to implied motion as expressed by animate agents in static pictures. Responses in single cells in macaque areas MT and MST may give some indication whether the implied motion responses found in human fMRI studies are correlated to firing rates of individual neurons in macaque areas MT and MST. However, it is much more important that it allows us to investigate several new aspects of implied motion processing. First of all, single unit recordings allow us to compare temporal response properties of implied and real motion in the same cell. There is evidence from human EEG studies that implied motion responses in dorsal motion processing areas are delayed compared to responses to real motion (Lorteije *et al*., 2006). This would suggest that object motion information that is processed via the ventral visual stream (DeYoe & Van Essen, 1988; Goodale & Milner, 1992; Ungerleider & Mishkin, 1982) is fed back via the anterior superior temporal sulcus (STSa, also called rostral STS) onto dorsal motion areas. Specific cells in this part of the STS are specialized for the perception of bodily actions and postures both in macaque monkeys ((Barraclough *et al*., 2006; Jellema *et al.*, 2000; Jellema & Perrett, 2003a, 2003b) and humans (Allison *et al.*, 2000). These cells typically have response latencies of about 80-110 ms (Barraclough *et al*., 2006). Neurons in areas MT and MST have response latencies to real motion stimuli of about 50-70 ms (Perge *et al*., 2006; Azzopardia *et al*., 2003; Raiguel *et al*., 1999; Schmolesky *et al*., 1998; Lagae *et al*., 1994). If single neurons in MT and MST show implied motion related activity, which is relayed via object information processing cells in STSa, than we might observe that as a delayed activity in the responses of MT and MST neurons.

Several other new aspects of implied motion processing can also be studied by single unit recordings in MT and MST. First, since most MT neurons are strongly tuned for the direction of real motion, direction preferences for real and implied motion can be compared. Second, modulation of MT responses to real motion by implied motion information can be studied. And third, it is possible to determine whether implied motion information can only modulate neural responses when presented within the receptive field of the MT cell, or whether it is a more global modulation that is affecting neural responses even when implied motion information is presented outside the receptive field. This might seem inplausible at first sight, because MT neurons are known to have distinct retinotopic receptive fields. However, neurons in STSa typically have large receptive fields. The latter respond to visual objects in either a viewer-centered or object-centered manner (Jellema & Perrett, 2006). A feed-back projection from object-centered or viewer-centered STSa neurons with large receptive fields and invariance for the position and size of the stimulus, may thus induce modulation of MT neurons regardless of the position of the agent inside or outside of the MT neurons' receptive field.

To investigate implied motion responses at the neuronal level, we measured single and multi-unit activity in areas STSa, MT and MST of awake macaques while pictures of humans and monkeys with and without implied motion, as well as controls for low-level visual features (tilted and vertical bars, and scrambled pictures.) were presented. First we recorded responses from STSa cells to pictures with and without implied motion. Some of these neurons responded selectively to either implied or motionless stimuli, which agreed with results from earlier studies (N. E. Barraclough *et al.*, 2006a; Jellema & Perrett, 2006). This experiment in STSa validates our methods. In the second experiment we investigated responses to pictures depicting the humans and monkeys with and without implied motion and control stimuli (bars and scrambled pictures) from MT and MST neurons.

In a third experiment, MT neuron responses to the onset of a dynamic noise pattern within the receptive field were recorded, while pictures with and without implied motion were presented at the fovea. Dynamic noise consists of motion energy at a broad range of speeds and in all directions, and typically evokes activity above spontaneous level in MT cells (Britten *et al*., 1993; Britten and Newsome, 1998; van Wezel and Britten, 2002a). Studies on attentional modulation of MT and MST neurons often use this type of stimuli, because it provides more sensitivity to pick up modulatory effects (Maunsell and Treue, 2006). Presentation of the implied and motionless stimuli on the fovea enabled the animals to clearly perceive the pictures, while low-level differences between conditions in the receptive field were removed.

Our experiments revealed that even though STSa cells responded selectively to implied motion, in areas MT and MST implied motion did not evoke different neuronal responses compared to motionless stimuli that could be attributed to the implied motion content of the pictures. Nor did the presence of implied motion modulate responses to real motion in a dynamic noise pattern.

Methods

Experiment 1 was performed in accordance with the guidelines of the UK Animals (Scientific Procedures) Act 1986 at the School of Psychology, University of St. Andrews, UK. Experiments 2 and 3 were conducted at the Department of Functional Neurobiology, Utrecht University, The Netherlands. Housing, surgical procedures, recording, handling and all other procedures used in experiment 2 and 3 were approved by the Animal Use Committee (DEC) of Utrecht University, and procedures followed national and international guidelines.

Experiment 1: STS recordings

STS cell visual responses were recorded in one, nine year old, adult male rhesus macaque (*Macaca mulatta*). Using standard techniques (Perrett *et al.*, 1985, Barraclough 2006), recording chambers were implanted over both hemispheres to enable electrode penetrations to reach the STS. Cells were recorded using tungsten microelectrodes. The animal was trained to fixate during the recording and its eye position (± 1°) was monitored (IView, SMI, Germany). A Pentium IV PC with a Cambridge electronics CED 1401 interface running Spike 2 recorded eye position, spike arrival and stimulus on/offset times. Presentation commenced when the animal fixated within 3° of a yellow dot presented centrally on the screen for 500 ms. To allow for blinking, deviations outside the fixation window lasting shorter than 100 ms were ignored. Fixation was rewarded with the delivery of orange juice. Spikes were recorded during the period of fixation. If the animal looked away for longer than 100 ms, spike recording and presentation of stimuli stopped until the animal resumed fixation for at least 500ms. Stimuli consisted of colour pictures of humans and monkeys, with and without implied motion as well as controls for low-level visual features (Figure 1A). Pictures were presented foveally for 125 ms with a 500 ms interval. Cell responses were recorded in a 100ms window starting at cell response latency (3sds above the spontaneous activity measured in a 50ms window before the onset of the stimulus). If no latency was detected then the window was fixed at 50ms after stimulus onset.

For each electrode penetration, x-ray photographs were taken coronally and para-sagitally. The positions of the tip of each electrode and its trajectory were measured with respect to the intra-aural plane and the skull's midline. Using the distance of each recorded neuron along the penetration, a 3-dimensional map of the position of the recorded cells was calculated. Additionally, histology was performed. Coronal sections were taken at 1 mm intervals over the anterior-posterior extent of the recorded neurons.

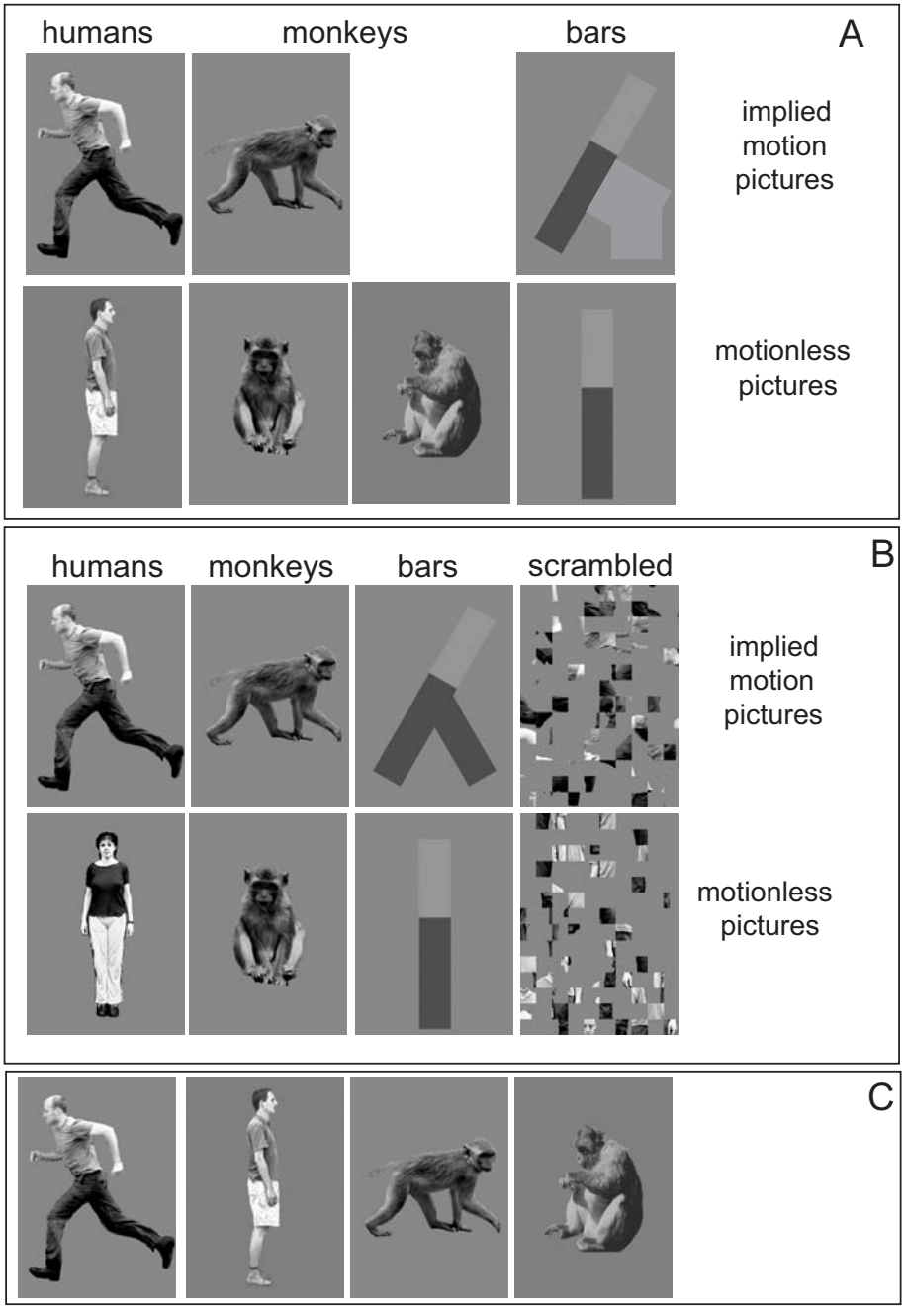
humans
monkeys
bars
A
implied motion pictures
motionless pictures
humans
monkeys
bars
scrambled
B
implied motion pictures
motionless pictures
C

Figure 1 (previous page)
Examples of stimuli used in three experiments. Pictures representing humans and monkeys with and without implied motion were used in all experiments. The implied motion pictures were identical in both experiments (profiled towards left or right), but the angle at which the pictures were taken differed and could be frontal or sideways, profiled to left and right. Experiment 1 used both frontal and sideways implied motionless pictures for the monkey condition, but only sideways views for human pictures without implied motion (A). In experiment 2, both monkeys and humans without implied motion were presented profiled frontally (B), but from a sideways profile for experiment 3 (C). To control for low-level stimulus features control stimuli were added in experiment 1 and 2. Bar stimuli could be vertical to match implied motionless pictures, or tilted towards left or right to match implied motion pictures. Bars were presented with a side bar in experiment 2, to eliminate a falling implied motion. Furthermore, scrambled versions of the figures were used as control stimuli in experiment 2.

Alignment of sections with the x-ray co-ordinates of the recording sites was achieved using the location of microlesions and injection markers on the sections. Anatomical data show that the cells presented in this study were recorded in STSa, which is the region of cortex in the upper bank, lower bank and fundus of the STS that lies rostral to the fundus of the superior temporal area (FST).

Experiments 2 and 3: MT and MST recordings

Experimental procedures
Data from two adult rhesus macaque (*Macaca mulatta*) males were recorded. Before the experiments, each monkey was implanted surgically with a head-holding device, a search coil for measuring eye movements using the double induction technique (Malpeli, 1998; Reulen & Bakker, 1982), and a stainless-steel recording cylinder placed over a craniotomy above the left occipital lobe. For one animal, a second cylinder was placed dorsally over a craniotomy above the parietal/occipital region. The surgical procedures were performed under N_2O/O_2 anaesthesia supplemented with isoflurane. After recovery, the monkeys were trained to fixate a rectangular spot (0.4° by 0.4°). During experiments, each monkey sat in a primate chair 57 cm from a 19 inch monitor. The framerate of the monitor was 120 Hz in experiment 1 and 100 Hz in experiment 2. Eye movement recordings were sampled at 500 Hz. For accurate fixation, the monkeys had to maintain their viewing direction within a virtual fixation window around the fixation point (1° radius). While correctly fixating, the monkey was rewarded with water or juice every second during the reverse correlation recordings, and after every stimulus presentation during the implied motion recordings.

Electrophysiological recordings
Extracellular single and multi unit recordings were carried out using standard methods. During experimental sessions, a parylene-insulated tungsten microelectrode (0.1–2 MΩ impedance) was inserted manually through a guide tube and then manipulated by a micropositioning controller. Cortical areas MT and MST were identified by the recording position and depth, the transition between grey matter, white matter and sulci along the electrode track, and by its functional properties. For MT these were the prevalence of direction-selective units, the similarity in direction tuning for nearby single-unit recordings, the receptive field size according to eccentricity and the change of direction tuning along the electrode penetration. For MST the functional properties were large receptive fields overlapping the fixation point and also on the ipsilateral side, and selectivity for complex motion patterns. One monkey is currently being used in other experiments and therefore anatomical confirmation of the recording sites is lacking. In the other monkey the anatomical positions were checked with structural MRI scans of the brain with an electrode inserted at the location of the recordings.

Action potentials from single and multi units were isolated with a window discriminator (BAK Electronics Inc., USA) for recordings in one monkey and with online spike sorting software (ASD, Alpha Omega, US) for the other animal. Spike times were registered at 0.5 ms resolution for on-line analysis and data storage, using a Macintosh G4 computer with a National Instruments PCI 1200 data acquisition board. As a search stimulus we used either moving random dot patterns or the pictures that were used in this study. Position and size of the receptive fields were handmapped by projecting a light bar on a dark monitor while the monkey was fixating the fixation dot. Direction tuning for real motion was established using a motion reverse correlation paradigm (Borghuis *et al*., 2003; Perge *et al*., 2005a, 2005b). A moving random pixel array rapidly switched between 8 possible directions. The delay between successive steps was 10 or 8.3 ms, with a stepsize of 0.12° corresponding to velocities of 12°/s and 14.4 °/s, respectively. The random pixel array was centered at the cells' receptive field. In experiment 1 the size of the random pixels array was similar to the size of the picture stimuli (8.5° x 11.5°). In experiment 2 the size of the random pixel array was matched to the excitatory receptive field size. It has been shown that the preferred direction determined with this reverse correlation paradigm is very strongly correlated with the preferred direction measured conventionally with handmapping or with presenting moving random pixel arrays in different directions at long durations (in the range of seconds) (Borghuis *et al*., 2003).

Experiment 2: stimulus presentation

In experiment 2, stimuli were presented at the centre of the receptive field against a black background (Figure 2A). Stimuli were colour pictures of humans or monkeys with implied motion, running towards left or right, or without implied motion, standing or sitting face forwards (Figure 1B). Additionally, pictures of bars that do not convey implied motion and scrambled pictures were presented as controls for low-level orientation, position and size effects. In the human pictures series, three different human agents were used either with or without implied motion, while the monkey pictures only showed one animal without implied motion and one animal with implied motion in both directions. Bars also included only one type of tilted bar (in both directions) and one type of vertical bar. Since the implied motion or tilted bar stimulus could be to the left or to the right, whereas the implied motionless or vertical bar stimulus was only in one direction, the first condition is presented twice as many times as the latter. Each stimulus was repeated 10 to 20 times depending on the quality and duration of the isolation. All MT and MST units were tested with the human pictures, and 80% of the recordings also included monkey pictures and bars.

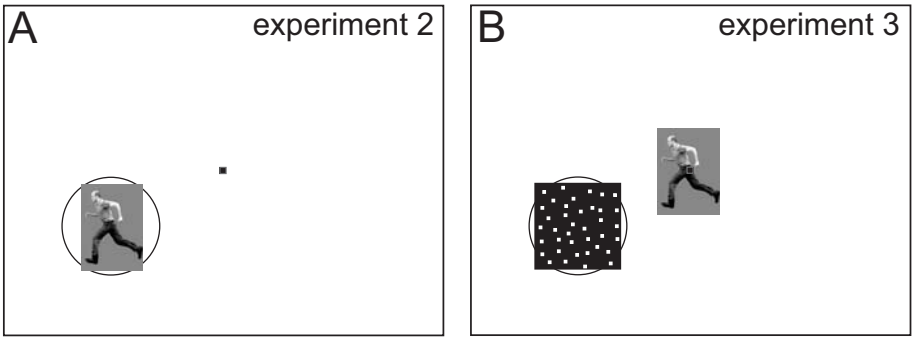

Figure 2

Schematic representation of the stimulus presentation for experiments 2 and 3. The monkey fixated a red dot (here shown as dark grey) in the middle of a computer screen with a black background in a darkened room. The receptive field of an MT cell is indicated by the circle. In experiment 2 (A), stimuli were presented in the middle of the receptive field. In experiment 3 (B), white dynamic dots were presented inside the receptive field simultaneously with a picture at the fixation point.

Pictures were presented for 500 ms with an interstimulus interval of 250 ms for most recordings, although in some recordings the presentation duration was longer (up to 1 sec). Additionally, some cells were presented with human pictures (with and without implied motion) that were flickering on and off at 10 or 20 Hz during the 500 ms stimulus presentation. This flicker stimulus was used to increase the base-line firing rate of the MT/MST cells during the presentation of the stimulus, which could increase the possibility to find modulatory effects.

Experiment 3: stimulus presentation
In the third experiment, grey scale pictures were presented foveally, while a dynamic random dot pattern (RDP, 500 white dots with a limited lifetime of 10 ms, with a pixel size of 0.2° by 0.2°, against a black background) was presented at the receptive field (Figure 2B). Both stimuli were presented for 500 ms with 250 ms inter stimulus interval. Pictures were 8.5° by 11.5° in most recordings, but were downsized to 4.25° by 5.75° for 8 units with near foveal receptive fields, to prevent overlap of the pictures with receptive fields. The RDP was optimized for the receptive field size. Pictures depicted humans and monkeys with implied motion or without implied motion, all profiled leftwards or rightwards (Figure 1C). Since the pictures were not presented within the receptive fields, control stimuli for low-level visual features (the bars and scrambled stimuli of experiment 1 and 2) were unnecessary.

Data analysis
Data of the reverse correlation recordings was analyzed as described previously (Borghuis *et al.*, 2003). The preferred direction was defined as the direction with maximum correlation, and the non preferred direction is defined as the direction opposite to the preferred direction. Furthermore for each cell we calculated the direction index (DI):

DI = 1-(relative probability in null direction/relative probability in preferred direction) (1)

Latency was established as the centre of a 5 ms interval with the highest direction-selectivity index. Cells were divided into four groups according to their direction tuning: direction independent; upwards or downwards tuned; leftwards tuned (with 45° upwards or downwards deviation); and rightwards tuned (with 45° upwards or downwards deviation). Cells tuned for leftwards or rightwards motion were used to correlate implied motion direction preferences with real motion tuning.

Data from experiments 2 and 3 were analyzed identically. To establish the response latency, the mean firing rate during spontaneous activity

and its standard deviation were calculated for a 100 ms window before stimulus onset. The mean firing rate in a 25 ms windows at stimulus onset was calculated. This window shifted from 0 ms after onset onwards in steps of 1 ms. At the first window with a mean response higher than 3 times the standard deviation before stimulus onset, the latency was established as the middle of the window. For some cells this criterium was too high (10 MT and 12 MST units in the first experiment; 2 MT units in the second experiment). Their latency was set at 2 or 1 times the standard deviation. For 4 MT units and 7 MST units in experiment 2 and 1 MT unit in experiment 3, this criterium was still too high and their latency was set for further analysis as the average MT or MST latency of all other cells. Average firing rates were calculated over a 500 ms period after the response latency.

Results

Experiment 1: STS cell examples
We recorded responses from STSa cells while monkeys viewed the same implied motion stimuli (Figure 1A) that were used for MT/MST recordings as will be described in experiment 2 and 3. The aim of experiment 1 is to show that the stimuli we used to test implied motion responses in MT and MST did evoke the selective responses in STSa that have been described before for different stimuli (Barraclough *et al.*, 2006; Jellema *et al*., 2006). Another difference with those previous STSa studies is that we also included bar stimuli that serve as controls for low-level factors. For STS cells we used a tilted straight bar, while the tilted bars for the MT and MST cells had a side bar that diminishes a possible "falling" implied motion (Figure 1B), and that made the resemblance with the human figures even stronger. The number of recorded cells (n=14) was not high enough to reliably compare population responses to the stimuli used in this paper with the stimuli used by Barraclough *et al.* (2006). However, two STSa cells could be used as example cells to show that some STSa cells indeed responded selectively to the implied motion content of the pictures used in the current study. The first cell (Figure 3A) showed a distinct preference for sitting monkeys, regardless of the face direction. The average firing rate of this cell was 19 times higher for sitting monkeys (50.6 spikes/sec) than for walking monkeys (2.65 spikes/sec). A second cell (Figure 3B) showed a strong preference for humans running leftwards (average firing rate of 32.0 spikes/sec), but not rightwards (average firing rate of 14.5 spikes/sec), nor standing (average firing rate of 12.75 spikes/sec) (Figure 3B). Even though this cell responded (weakly) to tilted bars (average firing rate 22 spikes/sec for left and 20 spikes/sec for right), this response was not direction specific and much lower than the response to the preferred human picture.

The response preferences of both STSa cells were much higher than we will describe in the next paragraphs for MT and MST neurons, but were typical for the STSa cells reported earlier in a larger population of cells that were tested with similar implied motion stimuli (Barraclough *et al*., 2006). These example cells indicate that differences in responses to implied motion in MT and MST vs. responses recorded in STSa cells in a previous study cannot be attributed to differences in the stimulus sets that were used.

MT and MST cell characteristics
In total we recorded 137 MT and 26 MST single and multi units. In experiment 2 we recorded 40 MT single units and 14 MT multi units, as well as 13 MST single units and 9 MST multi units, with a non-flickering stimulus presentation. Additionally, 6 MT single units, 8 MT

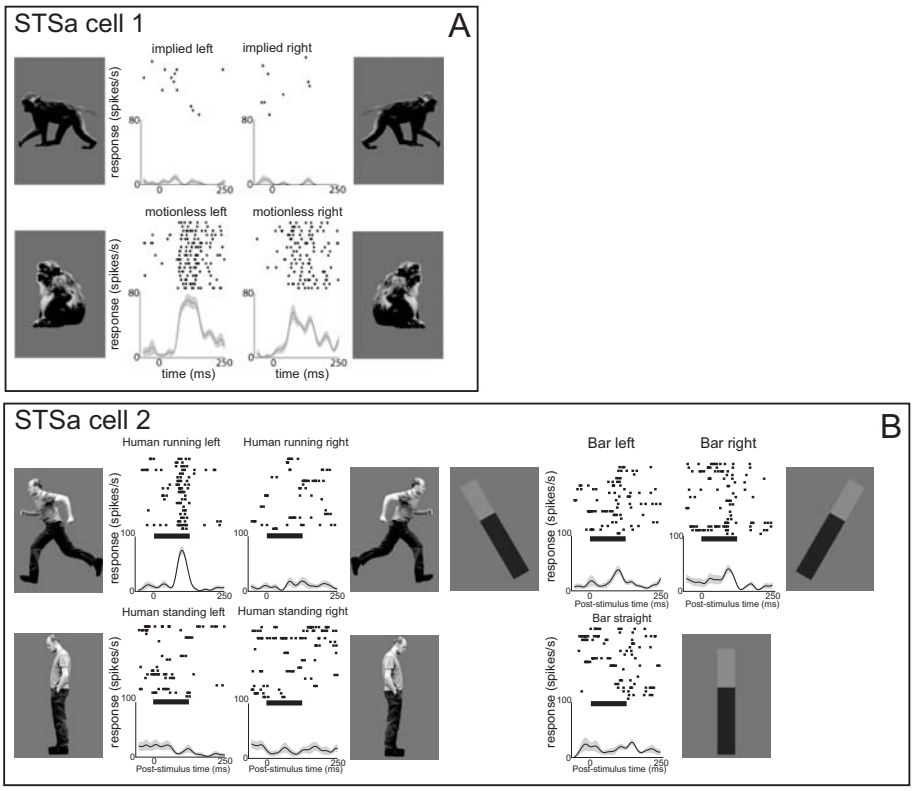

Figure 3
Responses from two example STS cells. Stimulus pictures are depicted left and right of the cells' corresponding response. Responses are shown as individual spike occurrence over time, across trials (top part of response panels), and as peri-stimulus time histograms (lower part of response panels). Picture presentation (onset at 0 ms, duration of 125 ms) is depicted as a black horizontal bar. One cell showed a preference for motionless monkey pictures, regardless of direction (A). A second cell had a distinct preference for rightwards human implied motion pictures, and barely responded to implied motionless pictures or implied motion towards the right, or to tilted and vertical bars.

multi units plus 4 MST single units were tested with stimuli flickering at 10 or 20 Hz. For experiment 3, 43 single units and 26 multi units were recorded in area MT. The whole population of MT units (n=137) had receptive fields at an average eccentricity of 9.6° ± 4.6 sd with an average diameter of 8.2° ± 2.9 sd. MST cells had much larger receptive fields that were often hard to identify precisely and could even extend to ipsilateral locations. Stimuli were presented at locations within the receptive field where the visual responses and motion selectivity were strongest (average eccentricity 7.3° ± 4.6 sd (n=26). Direction selectivity for real motion was obtained with a reverse correlation paradigm (Borghuis *et al*., 2003) containing 8 directions.

For each cell the DI was calculated. MT units (n = 137) had an average DI of 0.4 ± 0.3 sd at an average peak response latency of 59.1 ms ± 18.2 sd while MST units (n = 26) had an average DI of 0.7 ± 0.2 sd at an average peak response latency of 71.9 ms ± 13.4 sd.

Experiment 2: Responses to implied motion pictures in MT/MST receptive fields

In the second experiment, MT and MST neural activity was recorded during presentation of pictures inside the receptive field with and without implied motion as well as control pictures consisting of scrambled and bar stimuli (Figure 1B). It could be argued that the tilted bar as used in experiment 1, suggested a falling motion. Therefore, in experiment 2 we added a sidebar to make the bar more balanced. Also a control with scrambled pictures of humans with and without implied motion was added. To analyse the population and determine the temporal characteristics of the responses we constructed peri stimulus time histograms (PSTHs) (Figure 4) for the non-flickering conditions. The response of each neuron was segmented in 20 ms bins. The responses in Figure 4 were not normalized, which emphasizes responses from units with high firing rates. We also examined population PSTHs after normalization to the average response, and found similar results.

The PSTHs in Figure 4 showed a transient response with, averaged over all conditions, a peak response latency of 65.0 ms ± 16.6 sd for the MT units (non-flickering, n=54) and 64.6 ms ± 18.9 sd for the MST units (flickering, n=22). After this peak, the average response of MT neurons was sustained and higher than spontaneous activity until the end of the stimulus presentation, while the responses in MST dropped to or below spontaneous activity. We defined the sustained activity by calculating the average firing rate between

Figure 4 (next page)
Peri stimulus time histograms (PSTHs) for MT and MST units in experiment 2. The upper panels indicate the responses for implied motion or tilted bars (solid lines) and motionless pictures or vertical bars (dashed lines). The lower graphs indicate the response of implied motion or tilted bars in the preferred direction (solid lines) or non preferred direction (dashed line) of the cell. The numbers in the lower left corner of each graph indicate the number of cells. Stimulus onset is at 0 ms. Since for some cells stimuli were presented for periods longer than 500 ms, the PSTH is not shown past 500 ms (the stimulus end time for most units) and therefore the off response is not depicted.

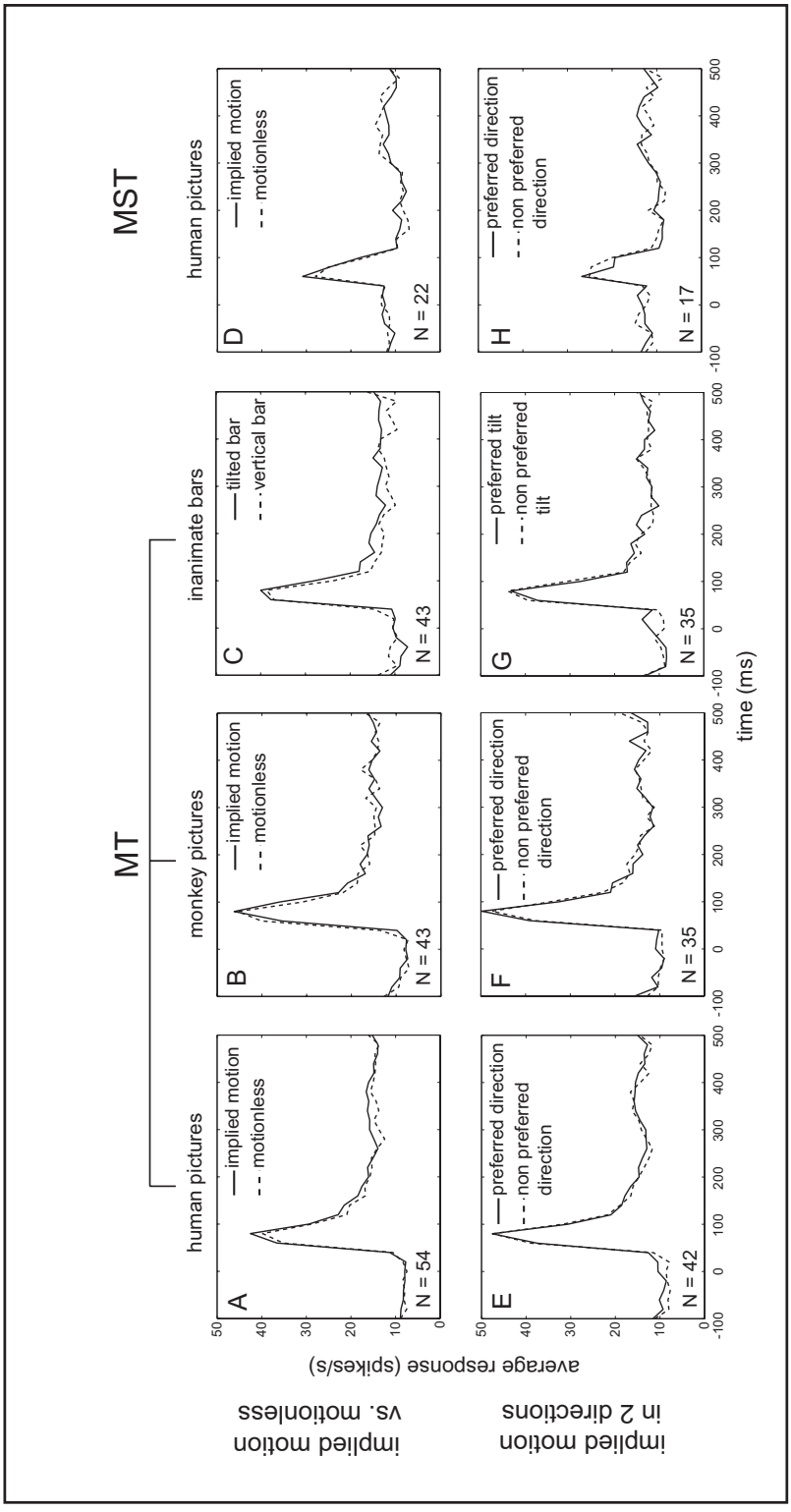
MT
MST
human pictures
monkey pictures
inanimate bars
human pictures
implied motion
motionless
tilted bar
vertical bar
implied motion
motionless
A
B
C
D
N = 54
N = 43
N = 43
N = 22
preferred direction
non preferred direction
preferred tilt
non preferred tilt
preferred direction
non preferred direction
E
F
G
H
N = 42
N = 35
N = 35
N = 17
implied motion in 2 directions
implied motion vs. motionless
average response (spikes/s)
time (ms)

200 and 400 msec after stimulus onset for each cell separately. The average firing rate of MT neurons was 7.9 spikes/s ± 7.1 sd during spontaneous activity and 15.1 spikes/s ± 16.8 sd during the sustained period. For MST neurons spontaneous activity was 11.0 spikes/s ± 6.5 sd while the sustained response was 10.0 spikes/s ± 7.8 sd. Spontaneous and sustained firing rates were compared in non-parametric tests and differed significantly for MT neurons (Wilcoxon signed rank test, $p = 0.001$), but not for MST neurons (Wilcoxon signed rank test, $p = 0.236$). This result agrees with recent macaque fMRI results that showed strong activation of static stimuli compared to only fixation in MT while no activation was observed in MST (Nelissen *et al*., 2006).

The results of figure 4 show that there were no clear differences between the different conditions, when comparing implied versus motionless pictures of humans in MT (Figure 4A) or MST (Figure 4D), and monkeys (Figure 4B) or bars (Figure 4C) in MT. Also no difference was found when comparing implied motion directions congruent or incongruent with the preferred direction (Figure 4, lower graphs). This preferred direction for real motion was determined from the motion reverse correlation experiments, and we only included units with a DI of at least 0.1 and preferred direction along the horizontal axis (± 45 degrees deviation). For the inanimate bars, preferred direction was defined as a tilt in the preferred motion direction, which corresponded to the off-balance tilt of human implied motion pictures.

Signal to noise levels for the different conditions were different. First of all, this is caused by different numbers of cells as indicated in the lower left corner of each graph. Furthermore, during tests that included monkey pictures and bars, the human pictures were presented three times more often than monkey or bar pictures. Additionally, since implied motion pictures were presented towards left or right direction whereas the implied motionless pictures were presented only from frontal angle, the implied motion pictures and tilted bars were presented 2 times more often than the motionless or vertical pictures. Not enough MST neurons were tested with monkey and bar stimuli to establish a reliable PSTH.

Although we did not find evidence for implied motion processing in areas MT and MST in the average PSTH plots of Figure 4, analysis of single units separately is necessary to exclude the possibility that a subset of neurons is modulated by motion implied in the pictures.

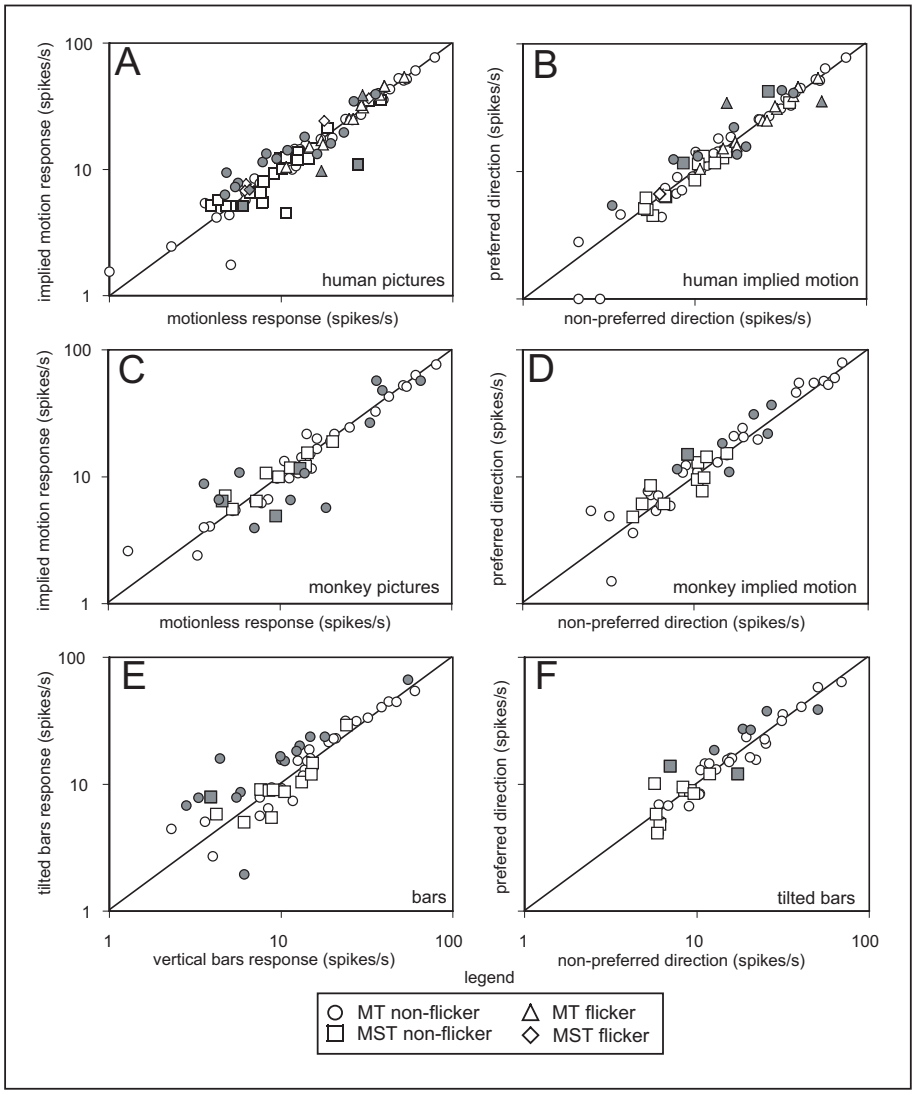

Figure 5
Comparison of MT and MST unit average activity induced by implied motion vs. motionless pictures or tilted versus vertical bars (left panels) and implied motion or tilted bars in preferred vs. non-preferred direction (right panels) in experiment 2. Each point represents the average responses from one unit. The diagonal line is the line of unity when the response to types of stimuli is equal. The difference in response was tested for significance for each cell separately using an ROC analysis with a permutation test. Cells with significantly different responses are indicated by filled symbols.

Experiment 2: cell-by-cell analysis

We analysed single units separately, first by comparing the responses to picture conditions of all MT and MST units averaged over 500 ms after the response latency. The response latency was calculated from the average response of a cell for all conditions and determined for each cell separately. The average responses are plotted in Figure 5 as scattergrams of implied motion versus motionless (Figure 5, graphs on the left) or preferred versus non preferred direction conditions (Figure 5, graphs on the right). If the responses for two conditions were equal the point falls on the line of unity that is indicated in each plot by the black diagonal line.

Response preferences were statistically tested by a non-parametric paired test (Wilcoxons). No significant difference was found between implied motion and motionless pictures for either human (not flickering and flickering in separate tests) (Figure 5A), monkey stimuli (Figure 5C), nor between tilted and vertical bars (Figure 5E) (Wilcoxons signed rank test p-values for all conditions > 0.05). Also no significant differences in response to preferred vs. non-preferred implied motion direction for both human (Figure 5B) and monkey (Figure5D) pictures or tilt (Figure 5F) was found (Wilcoxons signed rank test p values for all conditions > 0.05). A comparison of response strength of MST neurons in the non-flickering condition (indicated in Figure 5 with square symbols) between implied motion and motionless pictures, tilted and vertical bars as well as preferred vs. non-preferred direction did not reveal any significant differences (Wilcoxon p values for all conditions >> 0.05). Average responses for scrambled stimuli vs. all unscrambled stimuli for 49 MT and 26 MST units, did not differ significantly (Wilcoxon p values >> 0.05) (data not shown).

area	pictures	nr. of cells	average firing rate implied motion / motionless	average ROC values	% sig. cells for implied vs. non implied	average ROC value for sig. cells	average firing rate implied motion / motionless for sig. cells
MT	humans	54	1.29 ± 1.61	0.53 ± 0.09	25.9	0.59 ± 0.12	1.28 ± 0.3
	humans flicker	14	0.95 ± 0.24	0.52 ± 0.12	14.3	0.54 ± 0.3	0.99 ± 0.16
	monkeys	43	1.44 ± 2.61	0.48 ± 0.15	25.3	0.50 ± 0.28	1.13 ± 0.65
	bars	43	1.23 ± 0.57	0.6 ± 0.14	23.3	0.7 ± 0.13	1.68 ± 0.74
MST	humans	22	1.00 ± 0.2	0.51 ± 0.01	9.1	0.5 ± 0.19	0.96 ± 0.41
	humans flicker	4	1.18 ± 0.11	0.56 ± 0.04	0	-	-
	monkeys	12	1.11 ± 0.32	0.48 ± 0.1	25.0	0.46 ± 0.22	1.25 ± 0.62
	bars	12	1.06 ± 0.37	0.5 ± 0.1	8.3	0.67 (n=1)	2.03 (n=1)

Table 1

MT and MST cell numbers, and their responses to stimuli with and without implied motion or tilt are shown by the average firing rates, average ROC values for the whole population and for cells with a significant selectivity for particular conditions as established in the ROC analysis.

area	pictures	nr. of cells	average firing rate preferred / non preferred	average ROC values	% sig. cells for preferred vs. non preferred	average ROC value for sig. cells	average firing rate preferred / non preferred for sig. cells
MT	humans	42	1.08 ± 0.35	0.51 ± 0.09	14	0.57 ± 0.18	1.23 ± 0.34
	humans flicker	12	1.15 ± 0.46	0.49 ± 0.15	17	0.56 ± 0.44	1.06 ± 0.37
	monkeys	35	1.09 ± 0.33	0.56 ± 0.13	17	0.60 ± 0.24	1.14 ± 0.31
	bars	35	1.46 ± 2.89	0.51 ± 0.13	14	0.65 ± 0.23	1.30 ± 0.31
MST	humans	17	0.98 ± 0.32	0.53 ± 0.11	17	0.73 ± 0.07	0.98 ± 0.85
	humans flicker	1	1.03 (n=1)	0.54 (n=1)	0	-	-
	monkeys	11	1.11 ± 0.29	0.51 ± 0.12	9	0.77 (m=1)	1.63 (n=1)
	bars	11	1.09 ± 0.42	0.47 ± 0.15	29	0.56 ± 0.36	1.33 ± 0.9

Table 2
For MT and MST cells with a horizontal direction preference the number of involved cells, and their responses to stimuli with implied motion or tilt are shown by the average firing rates, average ROC values for the whole population and for cells with a significant selectivity for particular conditions as established in the ROC analysis.

Table 1 describes MT and MST cell numbers, the average ratio of firing rates for implied versus motionless pictures, as well as ROC values (see below) for the whole population and for cells with a significant selectivity for particular conditions as established in the ROC analysis. In table 1, responses to implied vs. motionless stimuli are shown. Additionally, in table 2, these values are given for implied motion in preferred vs. non preferred direction, for cells with a horizontal preferred direction for real motion.

For each cell we also applied a receiver operating characteristic (ROC) analysis (Green and Swets, 1966) which is more sensitive to difference. To assess the significance we used a permutation test (n=1000) (Britten *et al*., 1996). In our total MT population 26% (14 out of 54) of the units had significantly different responses for implied versus motionless human pictures in the non flickering condition. For this subgroup of cells the ratio of the average firing for human implied motion versus motionless pictures was, on average, 1.3, which corresponded to a difference of 2.2 spikes/sec. Response ratios and average response differences for implied vs. motionless pictures of significant cells were 1.13 with 0.19 spikes/sec and 1.68 with 5.55 spikes/sec for the monkey and the bar pictures respectively. This indicates that although a quarter of the MT cells responded significantly higher to either implied motion or implied motionless stimuli, the magnitude of this difference is very small. In MST the percentages of significant cells were lower compared to MT cells, except for the monkey condition. Again, the increase in average firing rate was very small.

We tested whether preferences of cells that showed significantly different responses were biased in the expected direction (column 7 in table 1). Under our definitions an ROC value > 0.5 means a higher response to implied versus motionless pictures. Because the average ROC values for the human pictures were above 0.5 for MT cells (but equal to 0.5 in MST cells), one might conclude that this small subset of MT neurons was significantly more responsive in the expected direction. However, as we will discuss later, we think this is due to low-level effects, as the bar stimuli show the same preference, but even stronger. Furthermore, this preference was not present for the monkey pictures in MT cells, and even opposite in MST cells.

We performed the same ROC analysis to determine whether responses were different for stimuli in the preferred direction versus non preferred direction (Table 2 and Figure 5B, D and F). This analysis was only performed on units with preferred directions for real motion along the horizontal axis (within $\pm$ 45 degrees) as determined with the reverse correlation paradigm. Additionally, 11% (10 out of 94) of all cells recorded in experiment 2, were selective for upwards or downwards motion, but were also significantly selective for either leftwards or rightwards implied motion for human pictures *(4 MT cells)*, flickering human pictures (1 MT cell and 1 MST cell), monkey pictures (2 MT cells) or for tilt direction of the bars (2 MT cells). These results show that a small percentage of MT and MST cells had a significant preference for implied motion in a specific direction, which did not always correspond to the preferred direction for real motion.

We examined whether MT neurons that were selective for tilted bars vs. vertical bars had the tendency towards a preference of implied motion vs. motionless pictures, by comparing the ROC values (Figure 6). Units with a preference for implied motion had a tendency to prefer tilted bars, as is indicated by the relatively high number of cells in the upper right quadrant, compared to the lower right quadrant in figure 6A. No trend was visible for monkey implied motion vs. bar stimulus (Figure 6B).

Figure 6 (next page)
ROC values for human and monkey implied motion and tilted bars were compared. For increasing selectivity for human implied motion vs. implied motionless pictures, selectivity for tilted bars vs. vertical bars increased as well (A). Cells with significantly different responses for either the human implied pictures or bar stimuli are indicated with filled symbols. No clear trend was observed for ROC values for response preferences to monkey pictures and bars (B). Implied motion preference for human pictures and monkey pictures was not consistent, 5 cells with a significant preference for human implied motion even had a significant preference for monkey motionless pictures (C).

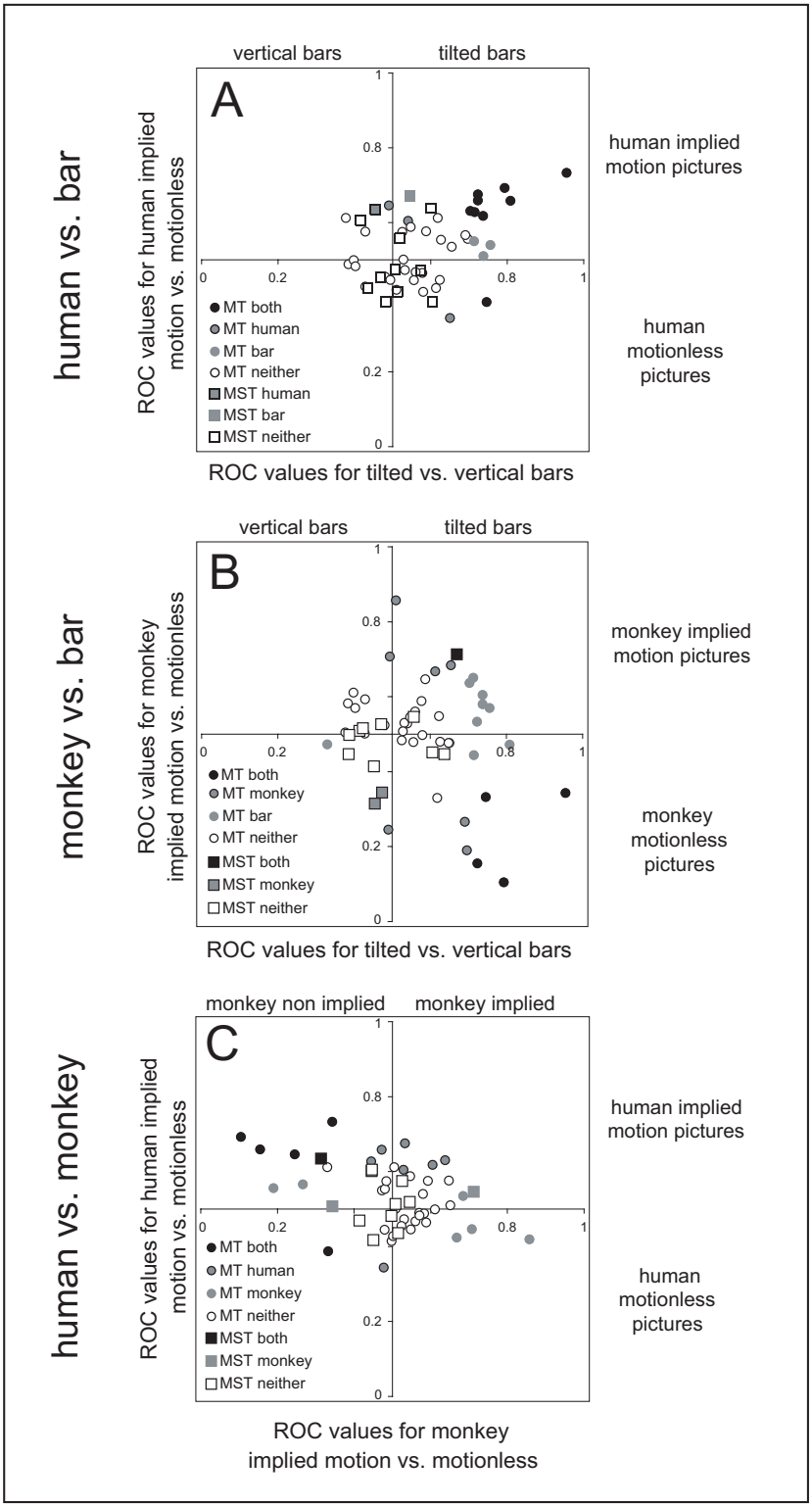
human vs. bar
vertical bars
tilted bars
A
ROC values for human implied motion vs. motionless
human implied motion pictures
human motionless pictures
MT both
MT human
MT bar
MT neither
MST human
MST bar
MST neither
ROC values for tilted vs. vertical bars
monkey vs. bar
vertical bars
tilted bars
B
ROC values for monkey implied motion vs. motionless
monkey implied motion pictures
monkey motionless pictures
MT both
MT monkey
MT bar
MT neither
MST both
MST monkey
MST neither
ROC values for tilted vs. vertical bars
human vs. monkey
monkey non implied
monkey implied
C
ROC values for human implied motion vs. motionless
human implied motion pictures
human motionless pictures
MT both
MT human
MT monkey
MT neither
MST both
MST monkey
MST neither
ROC values for monkey implied motion vs. motionless

For human implied motion vs. monkey implied motion, this trend may even be in the opposite direction, units with a significant preference for human implied motion had a significant preference for monkey pictures without implied motion, although units with a significant preference for either monkey or human pictures were much more scattered (Figure 6C). These results are an indication that preferences for implied vs. motionless human motion pictures could be caused by the same low-level stimulus features that were responsible for the tilted bar preference.

Experiment 3: Modulation by implied motion of MT responses to a dynamic noise pattern

To test whether viewing of implied motion has a modulatory effect on MT neuron responsiveness to real motion, human and monkey pictures with and without implied motion were presented foveally, while responses to dynamic noise patterns in the receptive field of MT neurons were recorded. With this experiment we directly tested the hypothesis that position and size invariant object recognition neurons as found in STSa cause this modulatory effect. A direct advantage of this experimental design was that low-level effects were excluded because the stimulus inside the receptive field was always the same dynamic noise pattern. Similar to figure 5 of experiment 1, we correlated the responses to implied and motionless pictures (Figure 7). Note that as the responses in this experiment were higher than in experiment 2, the axis in figure 7 were scaled higher than in figure 5. This increased response might be due to a higher response of MT cells to dynamic noise vs. static pictures, or might reflect a higher percentage of multi-units in the population (26% in experiment 2 vs. 33% in experiment 3). We found no significant differences between average responses (Wilcoxon p values >> 0.05) for implied versus motionless pictures of humans (Figure 7A) and monkeys (Figure 7B) and preferred versus non-preferred implied motion pictures (Figure 7E and F). In experiment 2 motionless pictures were not facing frontal like in experiment 1, but facing leftwards or rightwards. Also no significant difference (Wilcoxon p values >> 0.05) between face directions was found (Figure 7C and D)

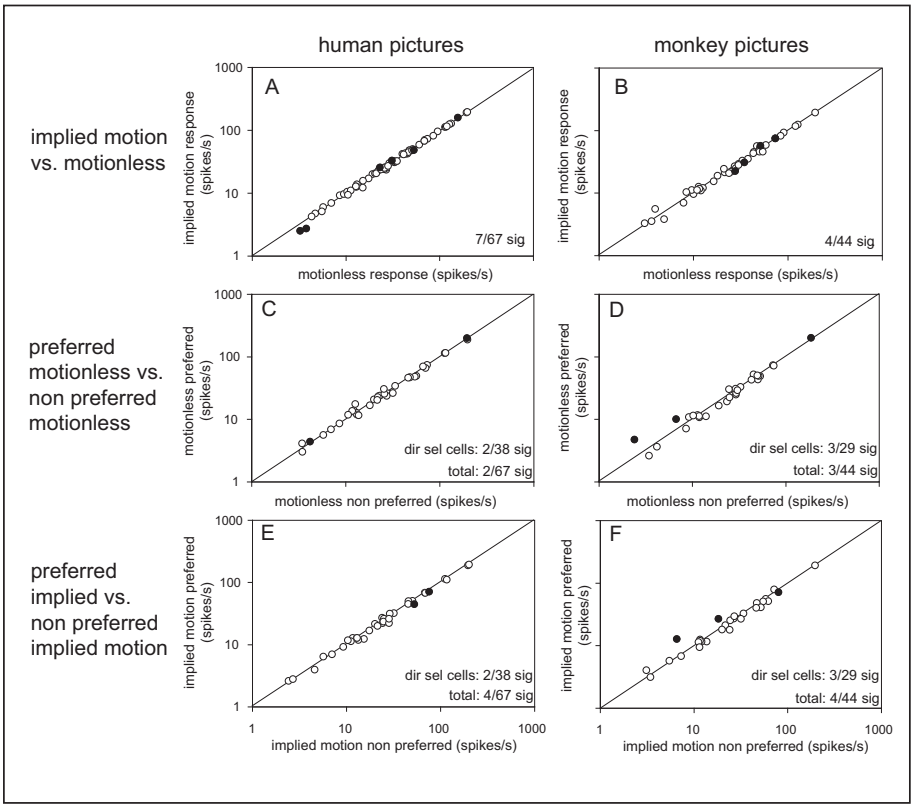

Figure 7
Comparison of MT unit activity induced by dynamic noise onset in the receptive field combined with picture stimuli at the fovea (experiment 3). Each dot represents average responses from one MT unit. The left panels represent responses to a combination of dynamic noise with pictures of humans with and without implied motion. The right panels shows the same for the monkey stimuli. Middle panels show responses to the combined presentation of dynamic noise with pictures of humans and monkeys without implied motion facing preferred and non-preferred direction. Lower panels show responses to simultaneous presentation of dynamic noise with pictures of humans and monkeys with implied motion in preferred and non-preferred direction. The numbers in the right lower corner of each graph indicate the number of significant cells out of the units that were horizontally directionally selective for real motion, and the number of significant units out of the number of total units that were tested for each condition.

pictures	pictures	nr. of cells	ratio average firing rate implied motion / motionless or preferred / non preferred	average ROC values	% sig. cells for preferred vs. non preferred	average ROC value for sig. cells	ratio average firing rate implied / motionless or preferred / non preferred for sig. cells
implied vs. non implied motion	humans	67	0.99 ± 0.07	0.49 ± 0.05	10	0.46 ± 0.12	0.93 ± 0.15
	monkeys	44	1.01 ± 0.12	0.49 ± 0.05	9	0.40 ± 0.16	0.97 ± 0.13
motionless (face direction)	humans	38	1.02 ± 0.11	0.51 ± 0.08	5	0.70 ± 0.03	1.05 ± 0.02
	monkeys	29	1.01 ± 0.23	0.51 ± 0.12	10	0.58 ± 0.30	1.54 ± 0.46
implied motion	humans	38	1.00 ± 0.08	0.48 ± 0.06	5	0.36 ± 0.01	0.90 ± 0.06
	monkeys	29	1.03 ± 0.24	0.51 ± 0.12	10	0.59 ± 0.27	1.45 ± 0.54

Table 3
MT cell numbers in experiment 3, and the modulation of their response to stimuli with and without implied motion or tilt are shown by the average firing rates, average ROC values for the whole population and for cells with a significant selectivity for particular conditions as established in the ROC analysis.

Similar to experiment 2, we determined ROC values for the different conditions (Table 3). The average ROC value over all units for implied versus motionless pictures was 0.49 (±0.05 sd, n=67) and 0.49 (± 0.08 sd, n=44) for human and monkey pictures, respectively. The percentage of cells with significantly different responses was 10% (7 out of 67), and 9% (4 out of 44), for human and monkey pictures, respectively. The average ROC value of significantly different units for implied versus motionless pictures was 0.46 (±0.12 sd, n=7) and 0.40 (± 0.16 sd, n=4) for human and monkey pictures, respectively. Average response ratios and differences in average spike rate for implied motion vs. motionless pictures were 0.95 with 0.17 spikes/ sec for human pictures, and 0.97 with -0.03 spikes/sec for monkey pictures.

Cells with a horizontal preference for real motion, as established with the reverse correlation paradigm, were tested for differences between implied motion in the preferred and non preferred direction. The average ROC values over all units for preferred versus non-preferred were 0.48 (± 0.06 sd, n=38) and 0.51 (± 0.12, n=29) for human and monkey pictures, respectively. For cells with a significant difference, average ROC values were 0.36 (± 0.01 sd, n=2) and 0.59 (± 0.27, n=3).

Since the motionless pictures in experiment 3 had a horizontal gaze direction (Figure 1C), responses to these pictures were also compared over preferred and non-preferred viewing direction. The average ROC values for preferred versus non-preferred were 0.51 (± 0.08 sd, n=38) and 0.51 (± 0.12, n=29). For cells with a significant difference, average ROC values were 0.70 (± 0.03 sd, n=2) and 0.58 (± 0.3, n=3).

These results show that the response to dynamic noise of only a very small percentage of MT cells (10% for human pictures and 9% for monkey pictures) was selectively modulated by either implied motion or motionless stimuli. Additionally, a small percentage of MT cells had a significant preference for implied motion in a particular direction, or face direction (5% for human pictures, 10% for monkey pictures). These percentages were too low to establish whether the preferred direction for implied motion or face direction corresponded to the preferred direction for real motion.

Discussion

In this study we have tried to find evidence for animate implied motion processing in cortical areas MT and MST of macaque monkeys. Modulatory input by pictorial content, that is recognized as a moving organism or object could be, in principle, integrated at the level where normally real motion is processed. This type of integration of different modalities could be formed by association. Since normally snapshots of moving objects are associated with motion, pictorial information could modulate low-level motion areas.

There are several other reasons why modulatory effects in areas MT and MST were to be expected. First of all, several human fMRI experiments showed significantly different BOLD activations in the human MT complex when comparing responses to pictures with humans, animals or objects moving versus pictures of humans, animals or objects standing still (Kourtzi & Kanwisher., 2000; Senior *et al*., 2000). Secondly, single cell recordings in monkeys have shown specific neurons in the STS that respond selectively to different degrees of implied motion (Barraclough *et al*., 2006; Jellema *et al*., 2006). Finally, modulatory input to MT and MST not related to motion itself, has been shown in numerous macaque single cell studies, for instance modulation by working memory (Bisley *et al*., 2004; Zaksas and Pasternak, 2005) and attention (Treue and Maunsell, 1996; Treue and Martinez Trujillo, 1999; Treue and Maunsell, 1999; Recanzone and Wurtz, 2000; Martinez-Trujillo and Treue, 2002; Cook and Maunsell, 2004; Maunsell and Treue, 2006).

However, in our study we did not find strong evidence for implied motion processing in macaque areas MT and MST. In experiment 2, we presented stimuli in the receptive fields of MT and MST cells. At the population level, cells did not respond differently to pictures of humans or monkeys when they are articulated, compared to non-articulated versions of the same subjects. A proportion of the cells showed a significant, differential response, but the actual difference in firing rate for these cells was very low, only a few spikes per second. Additionally, cells that were significantly selective for human implied motion versus motionless pictures also tended to have larger differences for the control bar stimuli. This suggests that the effects that were found may be attributable to low-level differences in the stimulus, for instance orientation and position of the stimulus. Furthermore, cells that were significantly responsive to monkeys with or without implied motion, had no consistent preference for either implied or motionless stimuli. More importantly, preferences for human and monkey implied motion were not consistent, cells selective for human implied motion, might even prefer monkey pictures without implied motion over monkey pictures with implied motion. This is in

contrast with human fMRI results (Kourtzi and Kanwisher, 2000) that show activation within area MT+ by implied motion expressed by both human and animal agents, and indicates that the response to human implied motion is not a response to the implied motion content of the stimuli, but more likely reflects responses to low-level visual features.

It is already known for a long time that MT neurons can respond selectively to static bars (Albright, 1984). Our results show that in addition to a transient response to stimulus onset, MT neurons had highly significant sustained responses above spontaneous activity for the static images. Since MST neurons did not have this sustained response, it can probably not be explained by small eye movements that cause motion on the retina. Also in a recent fMRI study in monkeys it has been shown that area MT has a differential response to static images compared to fixation only, while MST has not (Nelissen *et al*., 2006). In this respect it is even rather surprising that we do not find very large differences in responses for the different pictures, especially for our control stimuli. The small differences that we find can probably be attributed to low-level differences. This is supported by our result that the cells with the largest response differences for implied motion, also show larger differences for our control stimuli. However, we cannot exclude that the small differences in response that we find are also related to implied motion or that these low-level effects exactly counteract an implied motion signal. On the other hand, also for the previous human fMRI studies (Kourtzi & Kanwisher., 2000; Senior *et al*., 2000) it can not be excluded that low-level differences in the images (partly) cause the differences that were reported. It may also be that the tilted bars form a basic feature that underlies implied motion recognition, similarly as two dots and a stripe placed at correct locations within a circle may form critical features to which face recognition cells in inferior temporal cortex respond (Kobatake & Tanaka, 1994). However, although most observers will probably report that they perceive two dots and a stripe within a circle as a “smiley” face, we think that the abstract bars used in this study will not be so readily recognized as a running man in naive observers. Furthermore, implied motion may come in many more forms than there are face variations and therefore may be harder to reduce to simple features. More importantly, this explanation cannot explain the lack of a response to monkey implied motion in MT and MST.

In a third experiment we removed low-level effects by placing the stimuli at the fovea and always the same dynamic random dot pattern inside the receptive field. Even though the pictures were not presented within the receptive fields, it might still be possible that modulatory effects outside of the classical receptive field influence the response

(Allman *et al*., 1985a, 1985b; Tanaka *et al*., 1986; Xiao *et al*., 1995). Furthermore, presentation of the pictures on the fovea ensured that the monkey saw the picture content clearly. In this experiment we found a small percentage (about 10%) of cells that could be selectively modulated by the stimulus content, again with a very low difference in actual firing frequencies. In our opinion these effects were so small that it puts strong doubts to the hypothesis that implied motion signals are fed back to area MT from position and size invariant neurons that code implied motion as found in STSa. Additionally, these weak activations and low cell numbers may not be enough to explain the fMRI activation in MT+ that was found in human studies (Kourtzi & Kanwisher., 2000; Senior *et al*., 2000). Especially not, since the cells that did have a significant selective response on average had a ROC value below 0.5, which indicated a preference for motionless stimuli instead of implied motion stimuli.

A direct comparison between human fMRI experiments and our single unit recordings is difficult, since it has been shown that BOLD signal correlates more with local field potentials (incoming signals) than direct neural activation (Logothetis & Pfeuffer, 2004). Another obvious reason for the different findings in human fMRI studies and our single unit recordings in MT and MST, is differences in location and function between cortical areas involved in object and motion processing in human versus rhesus macaques. Although homologues of cortical areas MT and MST have been suggested (Morrone *et al*., 2000; Dukelow *et al*., 2001; Peuskens *et al*., 2001; Huk *et al*., 2002; Goossens *et al*., 2006), there are also several clear differences in function and location when motion an object sensitive cortical regions are compared of humans and monkeys are directly compared (VanDuffel *et al*., 2002; Orban *et al*., 2003; Nelissen *et al*., 2006). Recent evidence from fMRI in macaque monkeys suggests that combining object and motion information may mainly occur in areas FST and a newly defined area LST (Nelissen *et al*., 2006). These two areas would be strong candidates for implied motion processing. Since these areas are located near area MT, they could have been part of human MT and its satellites that were shown to have implied motion activation in previous human fMRI studies.

An area that is known to be activated by implied motion is STSa, as was shown in this study and others (Barraclough *et al*., 2006; Jellema *et al*., 2006). Most cells in this area also respond to moving random dots (unpublished observations). However, the properties of cells in this area are very diverse and complex. About 60% of the cells in this area that respond to static images of human figures are sensitive to the degree of articulation of the figure. This is much more than the 25% or less that we found for MT and MST neurons. However, in STSa about half of the cells responds preferentially to implied motion,

while the other half responds preferentially to motionless stimuli (Barraclough *et al*., 2006). Based on these results one would not expect a differential response for implied motion pictures versus motionless pictures in an fMRI experiment. Furthermore, properties of these cells in STSs are often more complex, for instance the response can depend on head direction and whether the figure is a human or monkey subject. Cells selective for static images of articulated figures were more likely to respond to movies of walking subjects (Barraclough *et al*., 2006), but typically there is no correlation with responses for implied motion and response to moving random dot patterns (unpublished observations). Therefore, it is not very plausible that cells as found in STSa of monkeys are related to the implied motion activation that was found in human fMRI experiments.

Implied motion activation in human and monkey MT and MST has been shown using inanimate Glass patterns (Krekelberg *et al.*, 2003, Krekelberg *et al*., 2005). This type of stimulus is ambiguous in direction and indicates the path of motion. This type of motion-from-dynamic-structure implied motion can evoke MT and MST responses, whereas our results show that there is no evidence for animate implied motion processing in macaque area MT and MST. This suggests that Glass patterns and (animate) implied motion in photographs are different classes of implied motion and are processed by different neural structures.

Several arguments could be given, why we were not able to show evidence for implied motion activity in areas MT and MST. First of all, although our search stimulus consisted of both moving random dot patterns and the static images that we used in this study, we cannot completely exclude the possibility that our sample was biased. Also we may not have covered every subregion of MT and MST. However, we searched extensively for implied motion responsive neurons, as we recorded from several locations and in two different animals, for one animal even in two hemispheres. Second, it could be argued that our stimuli did not convey a strong signal for implied motion, that monkeys were not able to recognize or interpret these pictures, that monkeys did not perceive implied motion or that the monkeys were not paying attention to the pictures because their task was only to fixate the fixation dot. In our opinion all these arguments are not valid since we found strong differential activities to the same stimuli in STSa cells while monkeys perform the same task. Furthermore, the same stimuli have been shown to elicit differential responses in human evoked potential recordings (Lorteije *et al*., 2006), and the stimuli are very similar to the type of stimuli that were used in the human fMRI study of Kourtzi and Kanwisher (2001). Furthermore, there is a plethora of studies showing that Rhesus macaque monkeys can interpret the content of pictures depicted on a computer screen

as observed from their behaviour. Also many studies have shown differential neural activation in object recognition areas for different pictures in monkey fMRI or single unit recording studies.

Our results show that MT and MST cells may respond selectively to low-level stimulus features within pictures with and without implied motion. However, even though STSa cells may respond to the implied motion content within a static picture, we have not found conclusive evidence for implied motion processing in macaque areas MT and MST.

CHAPTER 5

VISUAL FEATURES UNDERLYING THE IMPLIED MOTION RESPONSE IN HUMAN MIDDLE TEMPORAL CORTEX

Abstract

Viewing static snapshots of humans, animals and objects in motion evokes a higher fMRI BOLD response in human area MT+ than pictures of the same agents at rest. Since area MT+ is traditionally known for its vital role in processing real motion, it was concluded that this area also responded to the motion implied by the figures in the photographs. However, these pictures may not only have differed in the presence or absence of implied motion, but also in low-level visual features such as size, position and form of the agent expressing motion. These low-level features could also be responsible for differences in BOLD signal of MT+. To investigate the degree in which the response to implied motion in MT+ can be attributed to implied motion or low-level visual features, we conducted two combined experiments. In the first experiment, we recorded activation to pictures of humans with and without implied motion. We compared this to activation elicited by abstract forms (bars). The abstract bars could be tilted or vertical to resemble the form of the human implied motion or motionless motion pictures, respectively. These abstract forms did not convey implied motion information and mainly differed in size and tilt. In the second experiment we took an opposite approach and used a large variety of pictures of monkeys at different positions, with different sizes and in completely different natural environments. The main factor that differed in these monkey pictures was the implied motion information, and we assumed that on average low-level factors were equal. If activation in MT+ for implied motion versus motionless pictures was not only due to low-level factors, we expected to find a difference in activation for the monkey pictures and differences in activation that were larger for the human than for the abstract pictures. The BOLD response in area MT+ to human figures with implied motion was significantly higher than the response to human figures without implied motion, which is in accordance with previous human fMRI studies of Kourtzi and Kanwisher (2000) and Senior *et al*. (2000). However, the difference of activation in MT+ for tilted vs. vertical bars was also highly significant. Furthermore, no difference between implied and motionless pictures was found for the BOLD response in MT+ for the large set of diverse monkey photographs. No cortical areas were found that responded to implied motion in human and monkey pictures but not to size and form features of the abstract bars. Our results indicate that low-level stimulus features play an important role in activation differences for implied motion vs. motionless. This puts strong doubts to the claims of previous studies that animate implied motion is processed in human MT+.

Introduction

We readily recognize whether an animal, person or object within a photograph was moving or standing motionless at the moment the photograph was taken. Photographers, painters, sculptures and cartoonist can successfully convey motion information, even though no real motion may be present in their work. Orientation, body posture and articulation of the limbs of an animal or person may provide static form information that enables us to identify this implied motion. Freyd (Freyd, 1983) found that implied motion within a static image may even distort the spatial memory of observers, as they extrapolate the remembered position of a person towards the direction of the motion implied in the picture. These results suggest an interaction of visual form processing with motion or spatial position processing. In this study, we recorded cortical activity while human participants viewed pictures with and without implied motion. The implied motion pictures depicted humans and monkeys that were moving when the photograph was taken. The motion that was implied by these pictures was clearly recognizable by the body posture and position of the limbs, and had a distinct, unambiguous direction. The pictures that did not convey implied motion, were motionless, depicted monkeys and humans that were not moving when the photograph was taken.

To investigate whether a common neural substrate for real and implied motion processing existed, two fMRI studies were performed (Kourtzi & Kanwisher, 2000; Senior *et al.*, 2000). Both compared fMRI BOLD responses to pictures with implied motion (e.g., a running athlete or a cup falling off a table) with BOLD responses to pictures of the same objects, but motionless (e.g., standing athlete, houses or a cup on the table) in human observers. To locate motion processing areas, either contracting and expanding rings vs. static rings, or movie clips of a moving objects vs. static pictures of these objects without implied motion were used. Both studies found that the middle temporal region (MT+) showed a higher BOLD activation to both real motion compared to static stimuli, and to implied motion pictures, compared to pictures without implied motion. These results suggest that area MT+ processes both real and implied motion. Furthermore, when coherent firing in this area is disrupted by application of transcranial magnetic stimulation, the mental extrapolation of the location of an object implying motion disappears (Senior *et al.*, 2002), indicating the functional necessity of MT+ for implied motion perception.

It is well established that the primary function of the MT+ complex is to analyze the direction and speed of object motion in the visual world, as shown by a plethora of single-cell studies in monkeys (Britten *et al.*, 1992; Pack *et al.*, 2006) and imaging studies in humans (Sunaert

et al., 1999; Tootell *et al*., 1995b). Therefore, the finding that implied motion processing also occurs in this area was surprising, since such complex form processing is thought to occur along the ventral pathway, whereas MT+ is part of the dorsal pathway (Ungerleider & Mishkin, 1982). EEG recordings revealed that the response to implied motion from motion sensitive cortex was significantly delayed compared to its response to real motion (Lorteije *et al.*, 2006). This delay indicates that implied motion information may be processed along a longer route than real motion, probably via the ventral visual stream and is then projected onto dorsal motion sensitive cortex, which may be MT+.

However, even though it seems appropriate that integration of real and implied motion processing occurs in a dorsal motion area like human MT+, neither fMRI experiment provides conclusive evidence that the BOLD activation within MT+ can be attributed solely to the presence of implied motion within the pictures. Pictures with implied motion not only differ from their motionless counterparts by the presence vs. absence of implied motion, but also by several low-level visual features. First of all, an animate agent expressing implied motion has a different body expression as its motionless counterpart, e.g., with outstretched limbs vs. limbs against the body. This body expression enlarges the visual area occupied by the agent. From single cell recordings in macaque we know that MT cells have relatively small receptive fields. Roughly speaking the diameter of the receptive field is equal to 0.8 x the eccentricity (Maunsell & Van Essen, 1983). If human MT cells have similar receptive field sizes, an increase in occupied area would also lead to an increase of the number of MT+ neurons whose receptive field overlaps with the covered area. The second important low-level factor that differs between implied motion and motionless figures is that agents expressing implied motion can be oriented differently than their motionless counterparts, and because of their articulation often contain more differently oriented features. Especially for human agents, body posture during movement is more tilted compared to the vertical orientation of a standing person, and since legs and arms are more outstretched, more differently oriented features are in the picture. Single unit recordings have revealed that cells in macaque area MT are orientation selective for static bars (Albright, 1984). This means that during a block of implied motion stimuli more cells are activated than in a block of motionless stimuli. Orientation differences between pictures with and without implied motion may thus contribute to differences in BOLD activation.

We recorded differences in BOLD activation for implied and motionless stimuli in MT+ with a design that is very similar to the previous study by Kourtzi and Kanwisher (2000). However, in addition to a repetition of the experiment of Kourtzi and Kanwisher, we designed two types

of stimulus sets to explicitly control for low-level factors. These stimulus sets were presented within a single experiment. However, based on their different approach on low-level controls, we will address them here as individual experiments. In the first experiment we recorded activation to pictures depicting human figures with vs. without implied motion, and compared this to activation by pictures depicting abstract forms (bars). The configuration of the forms closely matches the human figures with respect to size, average luminance, covered space and orientation. However, these forms do not convey implied motion. In the second experiment we used an orthogonal approach, by presenting a large number of very different pictures of monkeys in motion or standing/sitting still with different sizes, positions, orientations, etc. The monkey pictures showed the animals in their natural environment instead of a grey background and therefore the content of the pictures varied even more drastically with respect to low-level features. Our assumption is that with this very large variety in low-level factors, the main difference between the monkey pictures is implied motion information and, on average, differences in low-level factors are cancelled out.

The fMRI BOLD response in area MT+ was significantly stronger for human pictures with implied motion vs. without implied motion, but also for tilted bars vs. vertical bars. BOLD responses in MT+ to monkey pictures with implied motion did not significantly differ from BOLD responses to monkey pictures without implied motion. These results indicate that differences in MT+ activation between stimuli with and without implied motion can be, at least partly, attributed to low-level stimulus features such as size and orientation. Additionally, cortical areas that responded significantly different to monkeys and humans with vs. without implied motion, and responded equally to the size and tilt differences of abstract forms, were not found.

Methods

Subjects
Eight healthy subjects (5 male, 3 female; mean ± SD age, 24.8 ± 6.1 years) who were recruited from the staff and students of Utrecht University, participated in the experiment. All subjects were right handed and had normal or corrected to normal vision. A history of neurological illness resulted in exclusion from the experiment, as did metal implants. All subjects gave informed consent for participation (approved by the Human Ethics Committee of the University Medical Center Utrecht).

Scanning protocol
All images were obtained with a Philips Achieva 3T MRI scanner (Philips Medical Systems, Best, the Netherlands) with a Quasar Dual gradient set. The head was held in place with padding. Functional scans were acquired in sagittal orientation, and structural scans were acquired in transverse orientation, from the same section of the brain. For functional scans, a navigated 3D-PRESTO pulse sequence (Ramsey *et al.*, 1998; van Gelderen *et al.*, 1995) was used with following parameters: TR=21.75 ms (time between 2 subsequent RF pulses); effective TE=32.4 ms; FOV(anterior-posterior, inferior-superior, right-left)= 224*256*128 mm; flip angle=10 degrees; matrix: 56*64*32 slices; voxel size 4 mm isotropic; 8 channel head coil; SENSE factors=2.0 (left-right) and 1.8 (anterior-posterior). The total acquisition time per volume was 500.3 ms. Immediately after functional scans, an additional PRESTO scan of the same volume of brain tissue was acquired with a high flip-angle (27 degrees, FA27) for the image co-registration routine (see below). Finally, a T1 weighted structural image was acquired.

Task design
The fMRI design used a PC, a rear projection screen and a video-projector system for presentation. All stimuli were projected on a grey background. All events were time-locked to the fMRI scans. Instructions were given verbally, prior to the start of the experiment. Subjects were requested to fixate on a red dot (visual angle) in the centre of the screen for the entire duration of the experiment.

Implied Motion Experiment
We used a block design and experimental design that was similar to the study of Kourtzi *et al*., (2000). The implied motion experiment consisted of seven conditions which included blocks of pictures of humans that implied motion, pictures of humans that did not imply motion, abstract figures that roughly resembled the surface of the human pictures with implied motion, abstract figures resembling the surface of the human pictures without implied motion and pictures of

monkeys that implied motion, pictures of monkeys that did not imply motion (Figure 1). All subjects were presented with human, monkey and abstract bar pictures, except for one subject that only performed in the conditions with monkeys and humans.

A new picture was presented every 1000 ms (2 scans) for a duration of 300 ms. In the 700 ms in between the pictures, only the red fixation dot was displayed. After the experiment, participants reported that they had clearly perceived the picture content and recognized the presence or absence of implied motion in the human and monkey conditions at these presentation durations. Twenty pictures were presented in each block. In addition, there was a rest condition in which only the red fixation dot was displayed on the screen for a duration of 20 s. There were 21 blocks per scanning session (3 blocks per condition), and 3 scanning sessions in total.

The pictures of humans with and without implied motion consisted of digitized grey-scale pictures of three different human agents on a grey background (height of 350 pixels, 13.2° visual angle), either running towards the left or right (implied motion), or standing still at left or right profile view (motionless). The pictures of two agents were repeated three times during each block, the picture of one agent was repeated four times during each block. The luminance of the implied motion figures was corrected to match the luminance of their corresponding motionless pictures. We were unable to measure the absolute luminance of the pictures inside the scanner. However, the relative luminance between the conditions, as established outside the scanner, would have remained similar.

Abstract pictures consisted of either a single vertical bar (height of 13.2° visual angle) that resembled a human agent that was standing still (motionless), or a combination of two tilted bars that resembled either a human agent running to the left, or a human agent running to the right (implied motion). The vertical bar was repeated twenty times during each block, the pictures of the tilted bars were repeated ten times during each block (ten left and ten right). Since the luminance of the three human agents varied (between agents, but not between implied and motionless conditions), luminance of the bars was also varied across a middle, a slightly lighter shade and a slightly darker shade. As with the human pictures, the relative luminance of tilted and vertical bars was matched.

The pictures of monkeys with and without implied motion consisted of digitized colour photographs (250 x 350 pixels, 9.4° x 13.2° visual angle) of monkeys in their natural surroundings. The set contained forty pictures that implied motion, and forty pictures that did not imply motion. The pictures of each set were repeated in random order during each new block.

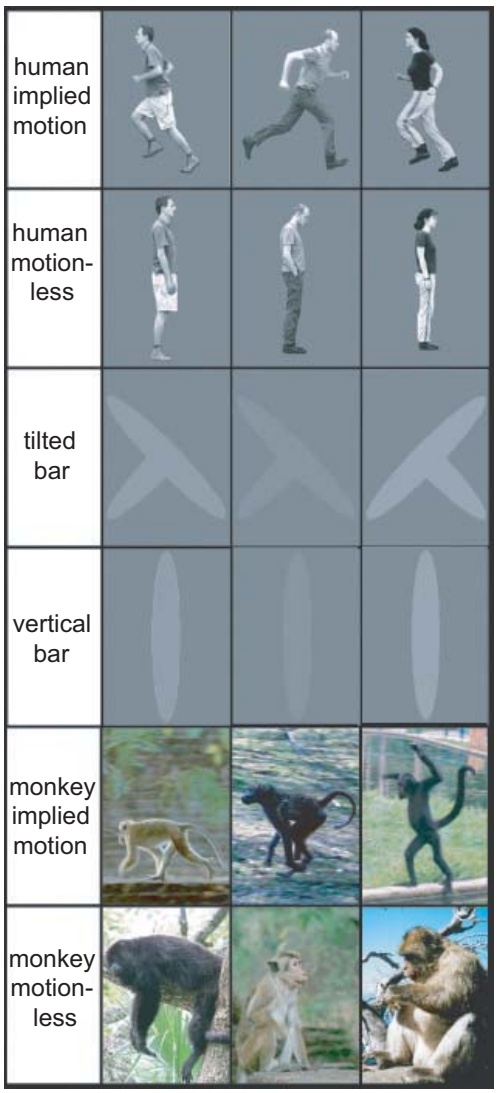

Figure 1:
Pictures containing human figures with and without implied motion, tilted and vertical bars, and pictures of monkeys with and without implied motion were used in this study. Three different human agents and three bars with varying luminance were used in this study. Both human pictures and tilted bars could be facing left and right direction. A stimulus set of 40 monkey pictures with and 40 without implied motion were presented. Three examples are given for each condition.

Motion Mapper
The task for mapping motion sensitive areas consisted of the presentation of random dot patterns that were intermittently displayed for 1000 ms, with a pause of 300 ms during which only the fixation dot was visible. The random dot patterns were either moving to the left or right (10°/s), or were static. Blocks of moving random dot patterns were alternated with static random dot patterns. Each block lasted 26 second, and there were 18 blocks in total. 934 scans were acquired in a single session during the entire motion mapping experiment.

Analysis
The fMRI time series data were preprocessed using SPM2 (http://www.fil.ion.ucl.ac.uk/spm/spm2.html). Functional scans were realigned (without reslicing) to the first scan to correct for slight movements of the head and were then coregistered to the FA27 volume. The T1-weighted anatomical image was also coregistered to the FA27 volume, using full affine transformations (no reslicing). The anatomical T1-weighted image was normalized to MNI space (Montreal Neurological Institute) (Collins *et al.*, 1994). The same normalization parameters were applied to the functional scans, which were then resliced at 4 x 4 x 4 mm. Finally, the normalized functional scans were smoothed with a 8-mm (FWHM) Gaussian kernel.

Statistical analysis of fMRI scans was done with custom-written programs in IDL (Research Systems Inc. Boulder, USA). Data for each subject were submitted to a linear multiple regression analysis. The factor matrix for the implied motion experiment contained six factors for stimulus related changes in BOLD-signal during the six conditions in which pictures were shown (the rest condition was used as a reference). Low frequency noise was modeled with additional factors the mean signal intensity of each scan, and 18 discrete cosine functions forming a high pass filter with a cut-off at $7.14*10^{-3}$ Hz to correct for low frequency scanner and physiological artifacts. All events in the design-matrix were convolved with a predefined haemodynamic response function (Friston *et al.*, 1995). For the voxel based analysis, the t-statistics of the relevant contrasts (implied vs. motionless monkey, implied vs. motionless human, and implied vs. motionless abstract) were calculated for every voxel. The effects of these contrasts over the entire group were calculated using the normalized t-volumes (Worsley, 1994). Bonferroni correction for the number of tests for all brain voxels resulted in a critical z-value of 4.66 for each voxel.

For the ROI based approach, the motion mapping experiment was used. Motion sensitive areas were located by contrasting activation between the presentation of static and moving random dot patterns.

MT+ was defined for all individual subjects as the motion sensitive activation in the ascending limb of the superior temporal sulcus. The predefined MT+ area was used in the region of interest analysis of the implied motion task. In all subjects the average regression coefficients of all conditions were calculated in area MT+. Differences between the implied and motionless stimuli were tested using a paired samples t-test.

Results

Robust MT+ activation was detected in seven subjects during the motion mapping task (data of the motion mapping experiment in one subject were lost due to erroneous task recordings). The comparison of activation in the MT+ between implied and motionless stimuli revealed no difference for pictures of monkeys ($t6=1.218$; $p=0.269$). However, for human as well as abstract pictures there was more activation in MT+ during implied motion pictures, than during motionless motion pictures ($t6=4.65$; $p=0.003$ for human pictures, $t5=4.34$; $p=0.007$ for abstract pictures) (Figure 2).

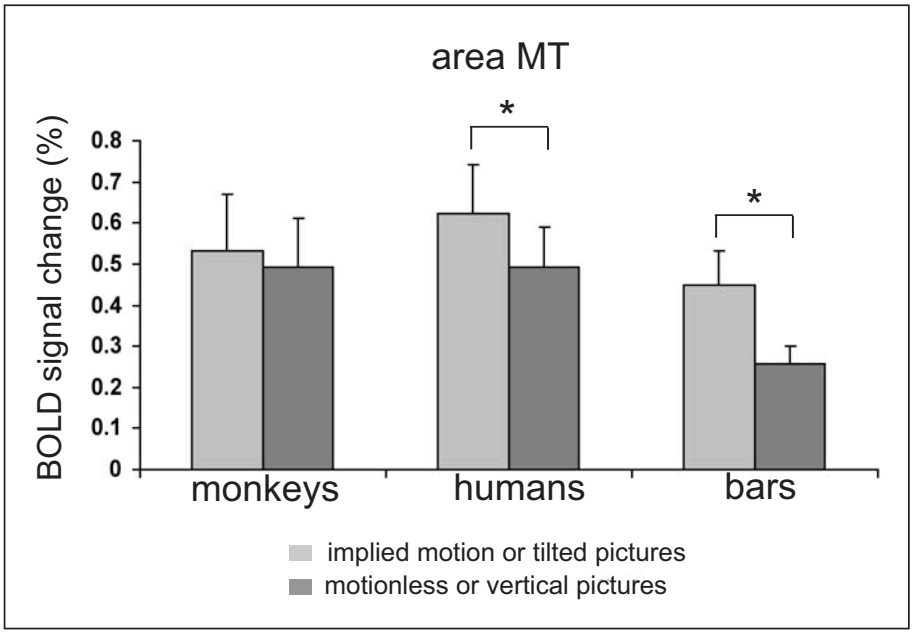

Figure 2:
Average signal in MT+ during the six conditions relative to passive fixation. MT+ was defined individually, using the motion mapping paradigm. Bars indicate standard errors, asterisks show significant differences.

The voxel based comparison between implied and motionless pictures of humans and abstract figures revealed increased activation during implied motion stimuli in several areas including Brodmann area 17 and 18 in early visual cortex, MT+ in the middle temporal/occipital region, and parts of the inferior and superior parietal lobe. Differences between implied and motionless pictures of monkeys were nearly entirely restricted to relative increases during implied motion stimuli in areas in the parietal lobe (Figure 3, Talairach x, y and z coordinates; 42, -79, 22 for the left parietal lobe, and -30, -79, 91 for the right parietal lobe). Testing the signal difference between implied motion and motionless pictures of humans and between tilted and vertical abstract bars in these parietal areas also revealed a significant difference for abstract bars ($t6=2.82$; $p=0.026$), but not for human pictures ($t7=0.81$; $p=0.447$) (Figure 4).

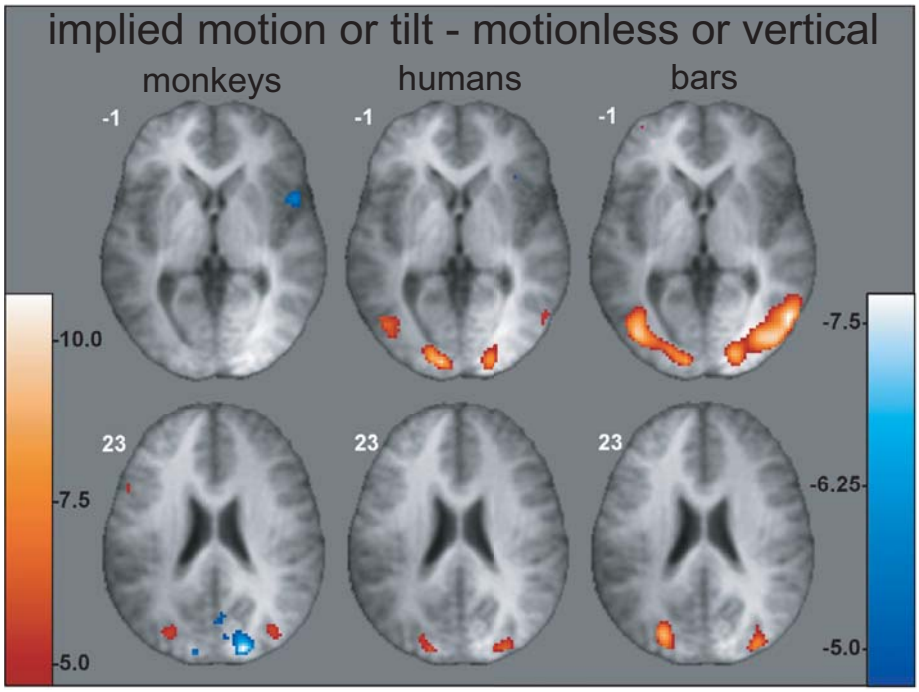

Figure 3:
Results of the contrast between implied and motionless stimuli for monkey, human, and abstract pictures. Significant voxels were thresholded at $p<0.05$ (corrected), and superimposed on the averaged anatomical scan. MNI z-coordinates are displayed in white on the top left of each slice.

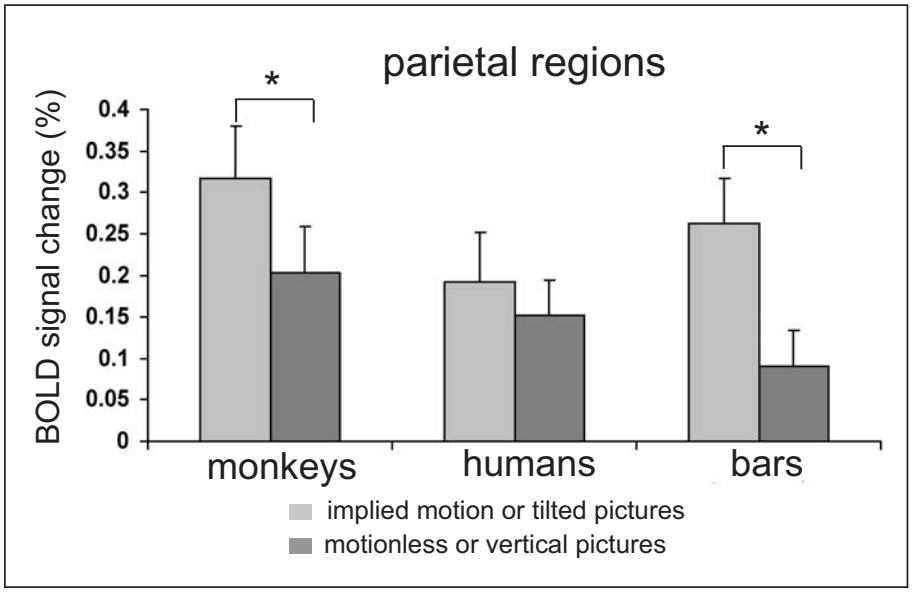

Figure 4:
Average signal during the six conditions relative to passive fixation in parietal areas that were significantly more active during implied motion pictures of monkeys, than motionless pictures of monkeys. Bars indicate standard errors.

Discussion

The fMRI BOLD response was recorded in human subjects, while they viewed pictures with and without implied motion. The first type of pictures consisted of human figures that were either running leftwards or rightwards, or standing still leftwards and rightwards. To control for low-level visual features between the human implied motion and motionless figures, pictures of bars were presented. These bars could be tilted, to represent the implied motion condition, or they could be tilted to represent the motionless human figures. As the human implied and motionless figures, the tilted and vertical bars differed in size and orientation, but unlike the human pictures they both did not contain any implied motion information. A third stimulus type consisted of a large variety of pictures depicting monkeys at several different sizes, forms and positions and depicted at very different backgrounds. These pictures could be divided into a set with implied motion, and a set without implied motion. We assumed that on average the low-level differences between these large sets of pictures would be roughly equal, and that the implied motion content was the main difference between these sets.

Our data show, that activation of area MT+ was significantly higher for pictures of running humans compared to responses to standing humans. This implied motion activation was not observed for monkey pictures. However, activation was also higher while viewing tilted bars than while viewing vertical bars. These results suggest that the implied motion activation that was evoked by the human figures may be for a large part attributed to responses to low-level visual features, likely predominantly size and orientation.

The effect of size on MT responses can be explained by the number of receptive fields that the stimulus covers. A larger stimulus will fall within more receptive fields, thus evoke a response of more MT neurons. Even though the total (background) picture size was equal for all stimuli, the size of the human implied motion figures and tilted bars covered a larger portion within the pictures. These outstretched areas may evoke a higher MT response than the grey, featureless background.

Area MT neurons are orientation selective for static bars, as has been shown by single cell recordings (Albright, 1984). This does not necessary imply that MT neurons are more selective to tilted orientation than to vertical orientation. However, human pictures with implied motion and tilted bars contain parts that are not in the same position for all implied motion or tilted stimuli, e.g., legs and sidebars. In the vertical bars and the motionless human pictures, less different degrees of orientation are present, thus evoking a response from a smaller orientation selective group of neurons.

The effect of these low-level features may even have been enhanced by the stimulus presentation. Pictures were presented for 300 ms, with a 700 ms interval. Part of the visual field that was empty or grey in one picture, may be occupied by part of a human body or tilted in the next picture. Since the human motionless pictures and the vertical bars occupied a smaller area with a similar orientation for the different figures, these local contrast changes and changes in orientation will occur less for these motionless and vertical pictures.

For the monkey pictures, these low-level features were assumed to be statistically equal in both conditions. Therefore, the lack of an implied motion activation due to the monkey pictures is consistent with the hypothesis that the “implied motion” response in area MT mainly reflects low-level visual features.

Orientational, size or positional features may also have contributed to the implied motion activations that were found in previous fMRI (Kourtzi & Kanwisher 2000; Senior *et al.,* 2000). In these previous studies an explicit control for these low-level effects was not presented. Additionally, presentation rates were even faster in these studies (300 ms on, 500 ms off for Kourtzi and Kanwisher and 250 ms on 250 ms off for Senior *et al*), which may have made the effect of local contrast reversals and different local orientations in these studies even larger. Our implied motion figures resembled the stimuli that were used in the study by Kourtzi and Kanwisher, who also used cut-out figures of humans set against a homogenous background, and pictures of animals within a natural setting (or other more complex scenes). Interestingly, in their study BOLD activation in implied motion figures was not only increased in the human condition, but also in the animal condition. However, the difference in response for animal pictures was also much smaller and barely significant compared to the human pictures.

The higher implied motion response in Kourtzi and Kanwishers’ animal pictures may have two explanations. Firstly, in favour of evidence for low-level effects, neither their nor our study can rule out that animal and monkey pictures on average did not differ slightly in low-level features between implied motion and implied motionless pictures. Unlike Kourtzi and Kanwishers’ animal pictures, our monkey pictures experiment did not evoke a significantly different response for the implied motion and motionless condition. This may be because our monkey stimulus set of 40 different pictures per condition could have averaged out more low-level differences than Kourtzi and Kanwishers smaller set of 20 different pictures. Secondly, in favour of implied motion signals, these differences may reflect a true response to the implied motion content of the pictures. According to this last hypothesis, our results show that both low-level and implied motion

processing occur within the same area. However, we would have expected a difference in activation for the monkey condition in our study. Additionally, since the human pictures differed in both implied motion content and in low-level features, whereas the bars only differed in low-level features, we would have expected the response difference in the human condition to be larger than the response difference for the bar condition. This does not seem to be the case, because the difference in response to tilted vs. vertical bars even seems to be stronger than the difference in response to human figures with and without implied motion. Furthermore, the bar stimuli clearly activate a much larger area of visual cortex. However in absolute terms the activation of the human figures was larger than the bars, which could be the result of more local contrast difference in the human figures, also because three different human figures were used, and only one standard set of bar stimuli. Also, we cannot exclude the possibility that a ceiling effect, or other non-linearity, caused less difference for the human figures. Additionally, participants may have associated the bar figures with the implied motion figures, thus adding an implied motion component to the tilted bars. Even though associations between real motion and abstract forms have been suggested before (Schlack & Albright 2006), it seems hardly likely that the associated form evokes a stronger contrast response that the original implied motion. It may also be that the tilted bars form a basic feature that underlies implied motion recognition, similarly as two dots and a stripe placed at correct locations within a circle may form critical features to which face recognition cells in inferior temporal cortex respond (Kobatake & Tanaka, 1994). However, although most observers will probably report that they perceive two dots and a stripe within a circle as a “smiley” face, we think that the abstract bars used in this study will not be so readily recognized as a running man in naive observers. Furthermore, implied motion may come in many more forms than there are face variations and therefore may be harder to reduce to simple features. More importantly, this explanation cannot explain the lack of a response to monkey implied motion in areas responsive to human implied motion as MT+.

The main conclusion we can draw from all this reasoning, is that our study clearly shows that in human MT+ low-level effects can play a major role in activation differences for implied and motionless pictures, which puts strong doubts to the conclusion of the previous studies (Kourtzi and Kanwisher, 2000; Senior *et al*., 2000) that implied motion activates human MT+. Even though Senior and colleagues tested implied motion with a different group of stimuli (e.g., an arm pushing a cup from a table instead of whole bodies), the same low-level features that were present in our and in Kourtzi and Kanwishers’ study, could also have affected responses found in that study.

Besides area MT+, we also compared responses to all conditions in other cortical areas. No area was found that responded exclusively to the implied motion content of the human and/or monkey pictures, but not to the low-level features within the bar stimuli. Regions in the superior temporal sulcus (STS) that were homologue to areas that respond to human body postures in the macaque monkey (Barraclough *et al*., 2006, Jellema *et al*., 2006), did not show a strong response to the implied motion, vs. motionless stimuli. This is not completely surprising, as both cells with a preference for implied motion stimuli, and cells with a preference for motionless stimuli have been found in these regions (Barraclough *et al.,* 2006). Thus, the net difference in activation between implied and motionless conditions, as recorded by fMRI, could be close to nil. Interestingly, parietal areas do respond significantly stronger to the monkey pictures with implied motion compared to monkey pictures without implied motion. However, these areas were not activated significantly stronger by human figures with vs. without implied motion, but they did respond stronger to tilted vs. vertical bars. Therefore, this area does not seem to be involved in implied motion processing, although it remains unclear to which features of the images it does respond.

Size, tilt and curvature and apparent rotation or reversal due to stimulus presentation may partly underlie the difference in area MT+ BOLD response between pictures with implied motion and pictures without implied motion, in this and previous studies. However, responses to these low-level visual features may mask a response to implied motion. In this case, separate neural populations sensitive to either implied motion or low-level stimulus features would be mixed within the same area. To identify such areas, responses to implied motion and motionless pictures without differences in low-level stimulus features should be recorded. Although some visual features are easily corrected for (such as size), a perfectly control stimulus for animate implied motion and motionless stimulus seems to be close to an Utopia, as implied motion is made up from these differences. However, implied motion as expressed by inanimate Glass patterns may convey implied motion information for which low-level features are controlled. Glass patterns consist of a collection of randomly placed pairs of dots, all oriented along a common path. They contain no coherent motion, are ambiguous in motion direction and do not convey pictorial information but suggest a path of motion. This motion-from-dynamic-structure stimulus may form a different class of implied motion than the (animate) picture implied motion that was used in this study. These implied motion classes may be processed by other neural structures. Glass patterns evoke an implied motion response in both monkey and human area MT (Krekelberg *et al*., 2003; Krekelberg *et al*., 2005). Such perfect control for low-level features is not possible for our animate implied motion.

Another way of locating cortical areas with neural subpopulations responsive to implied motion per se, would be by using an adaptation paradigm (Krekelberg *et al.*, 2006). For instance, after adapting subjects with real motion, responses to implied motion may be reduced, while responses to low-level stimulus features may be unchanged. Thus, areas consisting of separate neural populations responsive to implied motion or low-level stimulus features would show a reduced BOLD response to implied motion after adaptation, whereas activation in areas that are only sensitive to low-level stimulus features would remain unchanged. Recent EEG data reveal that such implied motion adaptation by real motion even is direction dependent (Lorteije *et al*, in press), which would facilitate functional identification of true implied motion sensitive areas. Additionally, low-level responses and implied motion responses may occur as separate processes within the same neurons. The implied motion response might then be separated from low-level responses by regarding the temporal properties of both activations. This would require fMRI scans at extremely high temporal resolution, or different techniques such as MEG, EEG, or extracellular recordings.

The results of the current study indicate that differences in MT+ activation between stimuli with and without animate implied motion can be, at least partly, attributed to low-level stimulus features such as size and orientation. Additionally, cortical areas that responded significantly different to monkeys and humans with vs. without implied motion, and responded equally to the size and tilt differences of abstract forms, were not found.

GENERAL DISCUSSION

In this thesis, the (cortical) processing of real and implied motion was examined. The temporal, spatial and functional properties, which were established in the previous chapters, will be discussed here.

Temporal properties of real and implied motion responses

The viewing of real motion and that of implied motion evokes cortical responses in humans that can be recorded using EEG. Since EEG has a very high temporal resolution, this technique is very suitable to perform a detailed comparison of response latencies to a range of different stimuli. Real motion typically evokes a negative peak around 150 to 200 ms after motion onset, which is often referred to as the N2 peak (Bach & Hoffmann, 2000; Bach & Ullrich, 1994; Heinrich *et al.*, 2004; Hoffmann *et al.*, 2001; Kubova *et al.*, 1995; Muller *et al.*, 2004; Probst *et al.*, 1993). In Chapter 1, the evoked potential to implied motion was compared with evoked potentials to real motion. The implied motion response was defined as the difference in potential between responses to static pictures with implied motion and responses to static pictures without implied motion. This subtraction eliminated responses to features that both types of stimuli have in common, such as face recognition or picture onset, and therefore mainly reflects the response to implied motion. The response to implied motion was significant during two time periods, first as an early positive peak that occurred around 80 to 100 ms after stimulus onset, and secondly as a late positive peak, which was maximal around 280 to 300 ms. The early response was thought to arise from early visual areas as a response to low-level stimulus differences between pictures. This was suggested by its location, the influence of stimulus intensity, and because low-level responses have been shown to occur at that latency (Arakawa *et al.*, 2000; Busch *et al.*, 2004; Johannes *et al.*, 1995; Kenemans *et al.*, 2000). The late response was thought to mainly reflect implied motion processing, which was confirmed by data presented in Chapter 2 that will be discussed later.

Source localisation revealed that this late implied motion response arose from cortical areas that were also involved in the processing of real motion. However, response latencies of these areas to real motion were roughly 120 ms faster than the latency of the (late) response to implied motion. Thus, temporal properties of real and implied motion processing indicate that implied motion information arrives in dorsal motion sensitive cortex later, and therefore probably via a longer route, than real motion. The ventral visual stream has an important functional role in processing (animate) object information. Therefore, implied motion may be processed along the ventral pathway leading towards inferior temporal cortex, and from there may be

projected via the STS onto dorsal motion areas, whereas (direction dependent) processing of real motion occurs mainly along the dorsal pathway.

Integration of real and implied motion

The response to implied motion in Chapter 1 seemed to arise from motion sensitive cortex. This suggestion concurred with results from earlier fMRI studies in humans, which found that motion sensitive area MT+ was activated by both real motion and motion implied in photographs (Kourtzi and Kanwisher, 2000; Senior *et al*., 2000). However, neither the source localization in Chapter 1, nor the fMRI results allowed us to conclude whether the same cells within this area were involved in both real and implied motion processing. This was investigated in Chapter 2 in an evoked potential study that used an adaptation paradigm. Responses to implied motion (the difference potential of responses to pictures with and without implied motion) after adaptation to a static or moving pattern were compared. These results showed that the amplitudes of both the positive peak around 100 ms (P100) and the positive peak around 280 ms (P280) could be modulated by the preceding adaptation. However, only the P280 could be modulated by real motion adaptation in a direction dependent manner, whereas the P100 was modulated by motion regardless of the direction. Since the pictures that were tested were identical for both adaptation directions, this direction specific adaptation strongly indicates that the P280 does not reflect responses to low-level visual features, but instead reflects implied motion processing. These results strongly indicate that the neural structure that underlies the P280 is involved in processing of both real and implied motion. Furthermore, the results show that these neurons are direction selective for both real and implied motion, which suggests that real and implied motion information are integrated at this stage. This integration may have important functional benefits. In natural scenes, a moving animate figure expresses both form cues (implied motion) and real motion cues. The extra activation of motion areas by implied motion would make the viewer more susceptible to the motion of the moving figure, which is especially relevant when the background is also moving. Think for example about a hare running through waving grass on a windy day. Integration of real and implied motion may cause the moving animal to jump out of the background motion. Furthermore, we often get an intermittent view of a continuous action due to distractions such as occluding objects or blinking of the eyes. To be still able to infer the course of the action in such situations, it would be extremely useful if the fragmented images of body postures expressing motion, would somehow contribute to the action representation and the perceived motion. This integration may also form the base for representational momentum effects that occur when observers view pictures with animate implied motion, as

have been described for instance by Freyd (1983, see general introduction). A comparison of processing of implied biological motion and social attention cues in individuals with Autistic Spectrum Disorder (ASD) and typical individuals suggested that processing of implied biological motion and the projection onto motion processing cortex may occur involuntary (or automatic) in typical people, but that this involuntary process is compromised in people with ASD (Jellema *et al.*, in revision).

Interestingly, the response to real motion is recorded as a negative peak, while implied motion evokes a positive peak. This could have three reasons. Firstly, it could indicate that real and implied motion are processed in different areas. This explanation was contradicted by the source localisation and direction specific adaptation. Secondly, it could indicate that real motion activates these areas, whereas implied motion has an inhibitory effect. This explanation is also contradicted by the direction specific adaptation effect that was found, as adaptation with real motion would probably enhance an inhibitory effect of implied motion with the same direction, whereas in our results this implied motion peak was reduced. However, this explanation cannot be completely ruled out. Thirdly, the difference in polarity could indicate that the input this area receives comes from different cortical areas. This last explanation is in agreement with the dorsal pathway input for real motion and ventral projection for implied motion.

Dorsal and ventral motion processing areas

Interestingly, in addition to a dorsal/ventral divergence for real and implied motion processing, real motion processing itself also seems divided along dorsal and ventral areas, as is discussed in Chapter 3. The dorsal areas are mainly involved in processing direction selective motion with both high and low speeds (which may be processed by separate neural populations), whereas the ventral areas are less direction dependent and are tuned to much lower speeds. This ventral motion pathway may be involved in processing structure from motion, but may also be involved in implied motion processing. However, although these areas may be involved in early stages of implied motion processing, they are not likely to reflect the delayed response to implied motion that was found in the evoked potential studies (Chapters 1 and 2). This delayed response could be adapted by real motion in a directionally dependent manner. Whereas the ventral motion sensitive areas were not strongly direction selective, responses in dorsal motion processing areas were highly direction dependent. Dorsal areas are therefore a much better candidate for a neural structure underlying the implied motion response.

No evidence for implied motion processing from single-cell studies in macaque area MT and MST

Human fMRI studies have revealed the involvement of area MT+ in motion processing (Sunaert *et al*., 1999; Tootell *et al.*, 1995a). Since this area is responsive to both real and implied motion, the integration of real and implied motion that was found in Chapter 2, may well take place in this area. Responses of single cells in MT and MST that are both part of the MT+ complex, to implied motion were recorded in two experiments, which are discussed in Chapter 4. Such extracellular recordings could in principle provide further insight into implied motion processing, for example, by providing the percentage of MT and MST cells that are responsive to implied motion, or by comparing tuning curves for real and implied motion direction, or by providing latencies of single cells to both motion types. Additionally, extracellular recordings could establish whether implied motion modulates responses to real motion in MT and MST neurons and if so, whether implied motion information can only modulate neural responses within the receptive field or whether it is a more global modulation that is affecting neural responses even when implied motion information is outside the receptive field. In the first experiment, pictures of humans and monkeys, with and without implied motion, were presented within the receptive field of MT and MST cells. Additionally, abstract forms were presented to control for differences in size and orientation of the human implied motion vs. motionless pictures. On population level, MT and MST did not respond differently to pictures of humans and monkeys with implied motion compared to pictures without implied motion. Individual cells could have a preference for human figures with implied motion vs. without implied motion, but this preference was not correlated with a preference for monkeys with implied motion, but instead corresponded to a preference for tilted abstract forms. This strongly indicates that the preference for human implied motion could be explained by low-level visual differences between pictures with and without implied motion, most notably stimulus orientation, as MT cells have been shown to be orientation selective (Albright, 1984). These responses to low-level features may contaminate an implied motion response supplied by higher order form processing pathways. To eliminate these low-level effects, in a second experiment, responses of MT cells to dynamic noise patterns in the receptive field were recorded while pictures of monkeys and humans with and without implied motion were presented outside the receptive field, on the fovea. Since STS neurons that are selective for implied motion have much larger receptive fields than MT cells, it can be argued that a projection from STS onto MT may be independent of the location of the receptive fields of MT cells. However, no convincing evidence for modulation of MT cell responses by implied motion information was found.

However, Krekelberg and colleagues did find responses to motion implied by Glass patterns in monkey and human MT and MST (Krekelberg *et al.*, 2003; Krekelberg *et al.*, 2005). Glass patterns consist of dot pairs that are organized in a global form (e.g., circle) to indicate a path of motion that is ambiguous in direction. This type of motion-from-dynamic-structure implied motion can evoke MT and MST responses, whereas our results show no evidence for modulation of MT and MST responses by animate implied motion in the macaque. This suggests that Glass patterns and (animate) implied motion in photographs are different classes of implied motion that are processed by different neural structures.

Visual features underlying an "implied motion" response

The adaptation-EEG experiment (Chapter 2) and the single-cell data (Chapter 4) seem to provide different (mutually exclusive) perspectives on the role of MT+ in implied motion processing. Whereas the adaptation EEG suggests that dorsal motion areas which may be MT+ are involved in both implied and real motion processing, the macaque cell studies suggested that MT and MST neurons are mainly involved in real motion processing and not in implied motion processing. To further examine this issue, and also to determine to what extent low-level features of the stimuli can explain the 'implied motion' response, a human fMRI study was performed, which is discussed in Chapter 5. Subjects were presented with human figures with and without implied motion, as well as abstract forms that controlled for low-level visual features such as size and orientation that differed between the implied motion and motionless conditions. These stimuli had also been used in the extracellular recordings. Additionally, a large variety of pictures of monkeys at different positions, with different sizes and in completely different natural environments were presented. The main factor that is different in these monkey pictures is the implied motion information, while on average low-level factors were assumed to be equal. The BOLD response in area MT+ to human figures with implied motion was significantly higher than the response to human figures without implied motion. However, no difference in BOLD signal in MT+ between implied motion and motionless pictures was found for monkey photographs. MT+ activation due to the tilted vs. vertical bars differed significantly. The human implied motion effect and the size of the abstract form difference were similar in size. These results are in accordance with the results found in the extracellular recordings in macaques, and indicate that responses to implied motion vs. motionless pictures in area MT and MST may be largely attributed to low-level stimulus features.

It could be argued that monkey and human participants may have associated the bar figures with the implied motion figures, thus adding an implied motion component to the tilted bars. Even though associations between real motion and abstract forms have been suggested before (Schlack & Albright 2006), it seems hardly likely that the associated form evokes an equal or even stronger contrast response than the original implied motion, as was found in both humans and monkeys. Furthermore, an association with human and bar forms cannot explain the lack of a selective response to monkey pictures with and without implied motion.

It may also be that the tilted bars form a basic feature that underlies implied motion recognition, similarly as two dots and a stripe placed at correct locations within a circle may form critical features to which face recognition cells in inferior temporal cortex respond (Kobatake & Tanaka, 1994). However, although most observers will probably report that they perceive two dots and a stripe within a circle as a "smiley" face, in my opinion the abstract bars used in this study will not be so readily recognized as a running man by naive observers. Furthermore, implied motion may come in many more forms than there are face variations and therefore may be harder to reduce to simple features. More importantly, also this explanation cannot explain the lack of a response to motion implied by monkey pictures in human and macaque MT/MST. A future study could use the same adaptation paradigm as used in Chapter 2 to test whether responses to these abstract forms could also evoke a direction dependent response from motion sensitive areas.

Identification of neural structures integrating real and implied motion
Cortical areas that responded exclusively to implied motion expressed by human and monkey pictures, but not by size and form features of the abstract forms were not found in the fMRI study that was discussed in Chapter 5. The lack of fMRI activation by implied motion processing in temporal and STS regions that are known for their single cell preferences to implied motion and human forms can be easily explained. Since cells in such regions may be selective to either implied motion, or motionless stimuli (see Chapter 5 and Jellema and Perrett, 2003; Barraclough *et al*., 2006), the population response that is recorded with fMRI may show no preference for either. Furthermore, direction preference for random dot motion and implied motion direction do not seem to be correlated in this area (unpublished data).

The neural structure(s) underlying the integration of real and implied motion processing that was found in Chapter 2 remained unidentified in the fMRI data. It is unlikely that the response to implied motion and the integration of real and implied motion that were recorded

with EEG occurred within these STS areas. Firstly, because EEG records population responses and these are not different for stimuli with and without implied motion in areas STS. Secondly, responses to random dot motion and implied motion do not seem to be correlated in this area.

It could be argued that the responses to implied motion as found in the evoked potential study that was discussed in Chapter 1, may also reflect low-level differences. However, direction dependent adaptation of the P280 component that was discussed in Chapter 2 strongly indicates that this response was not due to low-level visual features, but to implied motion per se. Furthermore, it could be that implied motion responses as recorded by fMRI were contaminated by responses to low-level features. An area that responds fast to low-level features and has a later response to implied motion, will add both responses in an fMRI signal. Using techniques with higher temporal resolution, such as extracellular recordings and EEG, these responses can be recorded as separate responses across time. Alternatively, two populations of neurons could be mixed within the same area, one population that is sensitive to implied motion, and one sensitive to low-level features. These two populations would add up in an fMRI study, and also in an EEG study if their latencies are similar. Extracellular recordings would be able to discriminate between these populations. Alternatively, an adaptation paradigm as used in Chapter 2 could be used to separate responses of these populations.

The experiments described in this thesis have not been able to identify the locus of integration of real and implied motion, even though from Chapter 2 it could be concluded that such a site exists. Our extracellular recordings suggest that this does not occur in area MT or MST. Recently Nelissen and colleagues defined cortical areas in macaque monkeys rostrally of MT/MST, that like MT/MST responded to real motion in inanimate dot patterns, but seem to specialize in action related movement (Nelissen *et al.*, 2006). These areas included the lower superior temporal (LST) region, the fundus superior temporal (FST) region and the middle of the superior temporal polysensory region (STPm). All three are located near the MT/MST complex and may therefore be part of the human MT/MST complex, which was activated by implied motion in previous fMRI studies (Kourtzi & Kanwisher, 2000; Senior *et al*., 2000). These three cortical areas would be possible candidates in future single cell studies for finding areas that integrate real and implied motion.

Concluding remarks

Real and implied motion processing were studied in humans and macaque monkeys. Temporal properties and processing pathways for both types of motion are discussed. Most importantly, evidence is shown for integration of real and implied motion. This integration could very well cause the sense of motion that we perceive while viewing static representations of motion that may be present in sculptures, paintings and photographs. Furthermore, this process may enable us to distinguish movement of an animal or person against a moving background, to track a moving person or object when the movement is intermittent due to occluding objects or eye blinks. In the end, implied motion processing may help us to increase motion sensitivity, because object information is added to the available real motion information. Furthermore, the studies described in this thesis have shed more light on how the brain integrates information from two totally different modalities.

REFERENCES

Albright, T. D. (1984). Direction and orientation selectivity of neurons in visual area MT of the macaque. *J Neurophysiol, 52*(6), 1106-1130.

Allison, T., Puce, A., & McCarthy, G. (2000). Social perception from visual cues: Role of the STS region. *Trends Cogn Sci, 4*(7), 267-278.

Allman, J., Miezin, F., & McGuinness, E. (1985a). Direction- and velocity-specific responses from beyond the classical receptive field in the middle temporal visual area (MT). *Perception, 14*(2), 105-126.

Allman, J., Miezin, F., & McGuinness, E. (1985b). Stimulus specific responses from beyond the classical receptive field: Neurophysiological mechanisms for local-global comparisons in visual neurons. *Annu Rev Neurosci*, *8*, 407-430.

Amano, K., Nishida, S., & Takeda, T. (2006). Meg responses correlated with the visual perception of velocity change. *Vision Res, 46*(3), 336-345.

Amorim, M. A., Lang, W., Lindinger, G., Mayer, D., Deecke, L., & Berthoz, A. (2000). Modulation of spatial orientation processing by mental imagery instructions: A meg study of representational momentum. *J Cogn Neurosci, 12*(4), 569-582.

Anderson, S. J., & Burr, D. C. (1985). Spatial and temporal selectivity of the human motion detection system. *Vision Res, 25*(8), 1147-1154.

Andreassi, J. L., & Juszczak, N. M. (1982). Hemispheric sex differences in response to apparently moving stimuli as indicated by visual evoked potentials. *Int J Neurosci, 17*(2), 83-91.

Arakawa, K., Tobimatsu, S., Kurita-Tashima, S., Nakayama, M., Kira, J. I., & Kato, M. (2000). Effects of stimulus orientation on spatial frequency function of the visual evoked potential. *Exp Brain Res, 131*(1), 121-125.

Bach, M., & Hoffmann, M. B. (2000). Visual motion detection in man is governed by non-retinal mechanisms. *Vision Res, 40*(18), 2379-2385.

Bach, M., & Ullrich, D. (1994). Motion adaptation governs the shape of motion evoked cortical potentials. *Vision Res, 34*(12), 1541-1547.

Barraclough, N. E., Xiao, D., Oram, M. W., & Perrett, D. I. (2006). Chapter 7 the sensitivity of primate STS neurons to walking sequences and to the degree of articulation in static images. *Prog Brain Res, 154*, 135-148.

Berg, P., & Scherg, M. (1994). Besa version 2.0 handbook, munich: Megis.

Bisley, J. W., Zaksas, D., Droll, J. A., & Pasternak, T. (2004). Activity of neurons in cortical area MT during a memory for motion task. *J Neurophysiol, 91*(1), 286-300.

Borghuis, B. G., Perge, J. A., Vajda, I., van Wezel, R. J., van de Grind, W. A., & Lankheet, M. J. (2003). The motion reverse correlation (mrc) method: A linear systems approach in the motion domain. *J Neurosci Methods, 123*(2), 153-166.

Britten, K. H., & Newsome, W. T. (1998). Tuning bandwidths for near-threshold stimuli in area MT. *J Neurophysiol, 80*(2), 762-770.

Britten, K. H., Newsome, W. T., Shadlen, M. N., Celebrini, S., & Movshon, J. A. (1996). A relationship between behavioral choice and the visual responses of neurons in macaque MT. *Vis Neurosci, 13*(1), 87-100.

Britten, K. H., Shadlen, M. N., Newsome, W. T., & Movshon, J. A. (1992). The analysis of visual motion: A comparison of neuronal and psychophysical performance. *J Neurosci, 12*(12), 4745-4765.

Britten, K. H., Shadlen, M. N., Newsome, W. T., & Movshon, J. A. (1993). Responses of neurons in macaque MT to stochastic motion signals. *Vis Neurosci, 10*(6), 1157-1169.

Busch, N. A., Debener, S., Kranczioch, C., Engel, A. K., & Herrmann, C. S. (2004). Size matters: Effects of stimulus size, duration and eccentricity on the visual gamma band response. *Clin Neurophysiol, 115*(8), 1810-1820.

Churchland, M. M., Priebe, N. J., & Lisberger, S. G. (2005). Comparison of the spatial limits on direction selectivity in visual areas MT and V1. *J Neurophysiol, 93*(3), 1235-1245.

Collins, D. L., Neelin, P., Peters, T. M., & Evans, A. C. (1994). Automatic 3d intersubject registration of mr volumetric data in standardized talairach space. *J Comput Assist Tomogr, 18*(2), 192-205.

Cook, E. P., & Maunsell, J. H. (2004). Attentional modulation of motion integration of individual neurons in the middle temporal visual area. *J Neurosci, 24*(36), 7964-7977.

Curran, W., & Benton, C. P. (2006). Test stimulus characteristics determine the perceived speed of the dynamic motion aftereffect. *Vision Res, 46*(19), 3284-3290.

DeAngelis, G. C., Cumming, B. G., & Newsome, W. T. (1998). Cortical area MT and the perception of stereoscopic depth. *Nature, 394*(6694), 677-680.

DeAngelis, G. C., & Newsome, W. T. (1999). Organization of disparity-selective neurons in macaque area MT. *J Neurosci, 19*(4), 1398-1415.

DeAngelis, G. C., & Uka, T. (2003). Coding of horizontal disparity and velocity by MT neurons in the alert macaque. *J Neurophysiol, 89*(2), 1094-1111.

Desimone, R., & Ungerleider, L. G. (1986). Multiple visual areas in the caudal superior temporal sulcus of the macaque. *J Comp Neurol, 248*(2), 164-189.

DeYoe, E. A., & Van Essen, D. C. (1988). Concurrent processing streams in monkey visual cortex. *Trends Neurosci, 11*(5), 219-226.

Di Russo, F., Martinez, A., Sereno, M. I., Pitzalis, S., & Hillyard, S. A. (2001). Cortical sources of the early components of the visual evoked potential. *Human Brain Mapping, 15*, 95-111.

Downs, E., & Jenkins, S. J. (1996). Effects of grade and conditions of motion on children's interpretation of implied motion in pictures. *Percept Mot Skills, 83*(3 Pt 2), 1289-1290.

Duffy, C. J., & Wurtz, R. H. (1991). Sensitivity of MST neurons to optic flow stimuli. I. A continuum of response selectivity to large-field stimuli. *J Neurophysiol, 65*(6), 1329-1345.

Dukelow, S. P., DeSouza, J. F., Culham, J. C., van den Berg, A. V., Menon, R. S., & Vilis, T. (2001). Distinguishing subregions of the human MT+ complex using visual fields and pursuit eye movements. *J Neurophysiol, 86*(4), 1991-2000.

ffytche, D. H., Howseman, A., Edwards, R., Sandeman, D. R., & Zeki, S. (2000). Human area v5 and motion in the ipsilateral visual field. *Eur J Neurosci, 12*(8), 3015-3025.

Freyd, J. J. (1983). The mental representation of movement when static stimuli are viewed. *Percept Psychophys, 33*(6), 575-581.

Freyd, J. J., & Finke, R. A. (1984). Representational momentum. *J. exp. psych: learning, mem. & cog.*(10), 126-132.

Friedman, S. L., & Stevenson, M. B. (1975). Developmental changes in the understanding of implied motion in two-dimensional pictures. *Child Dev, 46*(3), 773-778.

Friston, K. J., Frith, C. D., Turner, R., & Frackowiak, R. S. (1995). Characterizing evoked hemodynamics with fmri. *Neuroimage, 2*(2), 157-165.

Gegenfurtner, K. R., & Hawken, M. J. (1996). Interaction of motion and color in the visual pathways. *Trends Neurosci, 19*(9), 394-401.

Gegenfurtner, K. R., Kiper, D. C., & Levitt, J. B. (1997). Functional properties of neurons in macaque area v3. *J Neurophysiol, 77*(4), 1906-1923.

Georgeson, M. A. (1985). Inferring cortical organization from subjective visual patterns. *In: D.Rose & V.G. Dobson (Eds), Models of the visual cortex*, 223-232.

Goodale, M. A., & Milner, A. D. (1992). Separate visual pathways for perception and action. *Trends Neurosci, 15*(1), 20-25.

Goodale, M. A., Westwood, D. A., & Milner, A. D. (2004). Two distinct modes of control for object-directed action. *Prog Brain Res, 144*, 131-144.

Goossens, J., Dukelow, S. P., Menon, R. S., Vilis, T., & van den Berg, A. V. (2006). Representation of head-centric flow in the human motion complex. *J Neurosci, 26*(21), 5616-5627.

Graziano, M. S., Andersen, R. A., & Snowden, R. J. (1994). Tuning of MST neurons to spiral motions. *J Neurosci, 14*(1), 54-67.

Groh, J. M., Born, R. T., & Newsome, W. T. (1997). How is a sensory map read out? Effects of microstimulation in visual area MT on saccades and smooth pursuit eye movements. *J Neurosci, 17*(11), 4312-4330.

Haarmeier, T., & Thier, P. (1998). An electrophysiological correlate of visual motion awareness in man. *J Cogn Neurosci, 10*(4), 464-471.

Heinrich, S. P., & Bach, M. (2003). Adaptation characteristics of steady-state motion visual evoked potentials. *Clin Neurophysiol, 114*(7), 1359-1366.

Heinrich, S. P., van der Smagt, M. J., Bach, M., & Hoffmann, M. B. (2004). Electrophysiological evidence for independent speed channels in human motion processing. *J Vis, 4*(6), 469-475.

Hoffmann, M. B., Dorn, T. J., & Bach, M. (1999). Time course of motion adaptation: Motion-onset visual evoked potentials and subjective estimates. *Vision Res, 39*(3), 437-444.

Hoffmann, M. B., Unsold, A. S., & Bach, M. (2001). Directional tuning of human motion adaptation as reflected by the motion vep. *Vision Res, 41*(17), 2187-2194.

Hubbard, T. L. (2005). Representational momentum and related displacements in spatial memory: A review of the findings. *Psychon Bull Rev, 12*(5), 822-851.

Huk, A. C., Dougherty, R. F., & Heeger, D. J. (2002). Retinotopy and functional subdivision of human areas MT and MST. *J Neurosci, 22*(16), 7195-7205.

Huk, A. C., Ress, D., & Heeger, D. J. (2001). Neuronal basis of the motion aftereffect reconsidered. *Neuron, 32*(1), 161-172.

Itier, R. J., & Taylor, M. J. (2004a). N170 or n1? Spatiotemporal differences between object and face processing using erps. *Cereb Cortex, 14*(2), 132-142.

Itier, R. J., & Taylor, M. J. (2004b). Source analysis of the n170 to faces and objects. *Neuroreport, 15*(8), 1261-1265.

Jellema, T., Baker, C. I., Wicker, B., & Perrett, D. I. (2000). Neural representation for the perception of the intentionality of actions. *Brain Cogn, 44*(2), 280-302.

Jellema, T., Lorteije, J. A. M., van Schaffelaar, E., van Rijn, S., van 't Wout, M., de Haan, E. H. F., van Engeland, H. & Kemner, C. (under review). Failure to automate the processing of social cues in autism.

Jellema, T., & Perrett, D. I. (2003a). Cells in monkey STS responsive to articulated body motions and consequent static posture: A case of implied motion? *Neuropsychologia, 41*(13), 1728-1737.

Jellema, T., & Perrett, D. I. (2003b). Perceptual history influences neural responses to face and body postures. *J Cogn Neurosci, 15*(7), 961-971.

Jellema, T., & Perrett, D. I. (2006). Neural representations of perceived bodily actions using a categorical frame of reference. *Neuropsychologia, 44*(9), 1535-1546.

Johannes, S., Munte, T. F., Heinze, H. J., & Mangun, G. R. (1995). Luminance and spatial attention effects on early visual processing. *Brain Res Cogn Brain Res, 2*(3), 189-205.

Jonkman, L. M., Kenemans, J. L., Kemner, C., Verbaten, M. N., & van Engeland, H. (2004). Dipole source localization of event-related brain activity indicative of an early visual selective attention deficit in adhd children. *Clin Neurophysiol, 115*(7), 1537-1549.

Kemner, C., Jonkman, L. M., Kenemans, J. L., Bocker, K. B., Verbaten, M. N., & Van Engeland, H. (2004). Sources of auditory selective attention and the effects of methylphenidate in children with attention-deficit/ hyperactivity disorder. *Biol Psychiatry, 55*(7), 776-778.

Kenemans, J. L., Baas, J. M., Mangun, G. R., Lijffijt, M., & Verbaten, M. N. (2000). On the processing of spatial frequencies as revealed by evoked-potential source modeling. *Clin Neurophysiol, 111*(6), 1113-1123.

Kenemans, J. L., Lijffijt, M., Camfferman, G., & Verbaten, M. N. (2002). Split-second sequential selective activation in human secondary visual cortex. *J Cogn Neurosci, 14*(1), 48-61.

Kobatake, E., & Tanaka, K. (1994). Neuronal selectivities to complex object features in the ventral visual pathway of the macaque cerebral cortex. *J Neurophysiol, 71*(3), 856-867.

Kohn, A., & Movshon, J. A. (2003). Neuronal adaptation to visual motion in area MT of the macaque. *Neuron, 39*(4), 681-691.

Kourtzi, Z., & Kanwisher, N. (2000). Activation in human MT/MST by static images with implied motion. *J Cogn Neurosci, 12*(1), 48-55.

Krekelberg, B., Boynton, G. M., & van Wezel, R. J. (2006). Adaptation: From single cells to bold signals. *Trends Neurosci, 29*(5), 250-256.

Krekelberg, B., Dannenberg, S., Hoffmann, K. P., Bremmer, F., & Ross, J. (2003). Neural correlates of implied motion. *Nature, 424*(6949), 674-677.

Krekelberg, B., Vatakis, A., & Kourtzi, Z. (2005). Implied motion from form in the human visual cortex. *J Neurophysiol, 94*(6), 4373-4386.

Kubova, Z., Kuba, M., Spekreijse, H., & Blakemore, C. (1995). Contrast dependence of motion-onset and pattern-reversal evoked potentials. *Vision Res, 35*(2), 197-205.

Kulikowski, J. J. (1971). Effect of eye movements on the contrast sensitivity of spatio-temporal patterns. *Vision Res, 11*(3), 261-273.

Kulikowski, J. J., & Tolhurst, D. J. (1973). Psychophysical evidence for sustained and transient detectors in human vision. *J Physiol, 232*(1), 149-162.

Lagae, L., Maes, H., Raiguel, S., Xiao, D. K., & Orban, G. A. (1994). Responses of macaque STS neurons to optic flow components: A comparison of areas MT and MST. *J Neurophysiol, 71*(5), 1597-1626.

Levinson, E., & Sekuler, R. (1976). Adaptation alters perceived direction of motion. *Vision Res, 16*(7), 779-781.

Logothetis, N. K., Pauls, J., Augath, M., Trinath, T., & Oeltermann, A. (2001). Neurophysiological investigation of the basis of the fmri signal. *Nature, 412*(6843), 150-157.

Logothetis, N. K., & Pfeuffer, J. (2004). On the nature of the bold fmri contrast mechanism. *Magn Reson Imaging, 22*(10), 1517-1531.

Lorteije, J. A. M., Kenemans, J. L., Jellema, T., van der Lubbe, R. H. J., de Heer, F., & van Wezel, R. J. A. (2006). Delayed response to animate implied motion in human motion processing areas. *J Cogn Neurosci, 18*(2), 158-168.

Lorteije, J. A. M., Kenemans, J. L., Jellema, T., van der Lubbe, R. H. J., Lommers, M., & van Wezel, R. J. A. (in Press). Adaptation to real motion reveals direction selective interactions between real and implied motion processing. *J Cogn Neurosci*.

Malpeli, J. G. (1998). Measuring eye position with the double magnetic induction method. *J Neurosci Methods, 86*(1), 55-61.

Martinez-Trujillo, J., & Treue, S. (2002). Attentional modulation strength in cortical area MT depends on stimulus contrast. *Neuron, 35*(2), 365-370.

Mather, G., Verstraten, F., & Anstis, S. (1998). The motion after effect: A modern perspective. *Cambridge, Mass: MIT Press*.

Maunsell, J. H., & Van Essen, D. C. (1983). Functional properties of neurons in middle temporal visual area of the macaque monkey. I. Selectivity for stimulus direction, speed, and orientation. *J Neurophysiol, 49*(5), 1127-1147.

Maunsell, J. H. R., & Newsome, W. T. (1987). Visual processing in monkey extrastriate cortex. *Annu Rev Neurosci, 10*, 363-401.

Maunsell, J. H., & Treue, S. (2006). Feature-based attention in visual cortex. *Trends Neurosci, 29*(6), 317-322.

Mikami, A., Newsome, W. T., & Wurtz, R. H. (1986). Motion selectivity in macaque visual cortex. Ii. Spatiotemporal range of directional interactions in MT and V1. *J Neurophysiol, 55*(6), 1328-1339.

Milner, A. D., & Goodale, M. A. (1993). Visual pathways to perception and action. *Prog Brain Res, 95*, 317-337.

Morrone, M. C., Tosetti, M., Montanaro, D., Fiorentini, A., Cioni, G., & Burr, D. C. (2000). A cortical area that responds specifically to optic flow, revealed by fmri. *Nat Neurosci, 3*(12), 1322-1328.

Muller, R., Gopfert, E., Leineweber, M., & Greenlee, M. W. (2004). Effect of adaptation direction on the motion vep and perceived speed of drifting gratings. *Vision Res, 44*(20), 2381-2392.

Nelissen, K., Vanduffel, W., & Orban, G. A. (2006). Charting the lower superior temporal region, a new motion-sensitive region in monkey superior temporal sulcus. *J Neurosci, 26*(22), 5929-5947.

Niedeggen, M., & Wist, E. R. (1998). Motion evoked brain potentials parallel the consistency of coherent motion perception in humans. *Neurosci Lett, 246*(2), 61-64.

Orban, G. A., Fize, D., Peuskens, H., Denys, K., Nelissen, K., Sunaert, S., *et al*. (2003). Similarities and differences in motion processing between the human and macaque brain: Evidence from fmri. *Neuropsychologia, 41*(13), 1757-1768.

Pack, C. C., Conway, B. R., Born, R. T., & Livingstone, M. S. (2006). Spatiotemporal structure of nonlinear subunits in macaque visual cortex. *J Neurosci, 26*(3), 893-907.

Perge, J. A., Borghuis, B. G., Bours, R. J., Lankheet, M. J., & van Wezel, R. J. (2005a). Dynamics of directional selectivity in MT receptive field centre and surround. *Eur J Neurosci, 22*(8), 2049-2058.

Perge, J. A., Borghuis, B. G., Bours, R. J., Lankheet, M. J., & van Wezel, R. J. (2005b). Temporal dynamics of direction tuning in motion-sensitive macaque area MT. *J Neurophysiol, 93*(4), 2104-2116.

Perrett, D. I., Smith, P. A., Mistlin, A. J., Chitty, A. J., Head, A. S., Potter, D. D., et al. (1985). Visual analysis of body movements by neurones in the temporal cortex of the macaque monkey: A preliminary report. *Behav Brain Res, 16*(2 3), 153-170.

Peuskens, H., Sunaert, S., Dupont, P., Van Hecke, P., & Orban, G. A. (2001). Human brain regions involved in heading estimation. *J Neurosci, 21*(7), 2451-2461.

Probst, T., Plendl, H., Paulus, W., Wist, E. R., & Scherg, M. (1993). Identification of the visual motion area (area v5) in the human brain by dipole source analysis. *Exp Brain Res, 93*(2), 345-351.

Qian, N., & Andersen, R. A. (1994). Transparent motion perception as detection of unbalanced motion signals. Ii. Physiology. *J Neurosci, 14*(12), 7367-7380.

Ramsey, N. F., van den Brink, J. S., van Muiswinkel, A. M., Folkers, P. J., Moonen, C. T., Jansma, J. M., *et al*. (1998). Phase navigator correction in 3d fmri improves detection of brain activation: Quantitative assessment with a graded motor activation procedure. *Neuroimage, 8*(3), 240-248.

Recanzone, G. H., & Wurtz, R. H. (2000). Effects of attention on MT and MST neuronal activity during pursuit initiation. *J Neurophysiol, 83*(2), 777-790.

Reulen, J. P., & Bakker, L. (1982). The measurement of eye movement using double magnetic induction. *IEEE Trans Biomed Eng, 29*(11), 740-744.

Salzman, C. D., Murasugi, C. M., Britten, K. H., & Newsome, W. T. (1992). Microstimulation in visual area MT: Effects on direction discrimination performance. *J Neurosci, 12*(6), 2331-2355.

Scherg, M., & Picton, T. W. (1991). Separation and identification of event-related potential components by brain electric source analysis. *Electroencephalogr. Clin. Neurophysiol. Suppl., 42*, 24-37.

Schlack, A., & Albright, T. D. (2005). Associative learning in cortical visual area MT of macaque monkeys. *Society for Neuroscience conference abstract*.

Schlack, A., & Albright, T. D. (2006). Associative learning in cortical visual area MT of macaque monkeys. *Perception, 35*(11).

Schrater, P. R., & Simoncelli, E. P. (1998). Local velocity representation: Evidence from motion adaptation. *Vision Res, 38*(24), 3899-3912.

Senior, C., Barnes, J., Giampietro, V., Simmons, A., Bullmore, E. T., Brammer, M., et al. (2000). The functional neuroanatomy of implicit-motion perception or representational momentum. *Curr Biol, 10*(1), 16-22.

Senior, C., Ward, J., & David, A. S. (2002). Representational momentum and the brain: An investigation into the functional necessity of v5/MT. *Visual Cognition, 9*(1-2), 81-92.

Sereno, M. E., Trinath, T., Augath, M., & Logothetis, N. K. (2002). Three-dimensional shape representation in monkey cortex. *Neuron, 33*(4), 635-652.

Singh, K. D., Smith, A. T., & Greenlee, M. W. (2000). Spatiotemporal frequency and direction sensitivities of human visual areas measured using fmri. *Neuroimage, 12*(5), 550-564.

Smith, A. T., & Edgar, G. K. (1994). Antagonistic comparison of temporal frequency filter outputs as a basis for speed perception. *Vision Res, 34*(2), 253-265.

Smith, A. T., Wall, M. B., Williams, A. L., & Singh, K. D. (2006). Sensitivity to optic flow in human cortical areas MT and MST. *Eur J Neurosci, 23*(2), 561-569.

Sunaert, S., Van Hecke, P., Marchal, G., & Orban, G. A. (1999). Motion-responsive regions of the human brain. *Exp Brain Res, 127*(4), 355-370.

Tanaka, K., Hikosaka, K., Saito, H., Yukie, M., Fukada, Y., & Iwai, E. (1986). Analysis of local and wide-field movements in the superior temporal visual areas of the macaque monkey. *J Neurosci, 6*(1), 134-144.

Thompson, P. (1984). The coding of velocity of movement in the human visual system. *Vision Res, 24*(1), 41-45.

Tootell, R. B., Reppas, J. B., Dale, A. M., Look, R. B., Sereno, M. I., Malach, R., *et al*. (1995a). Visual motion aftereffect in human cortical area MT revealed by functional magnetic resonance imaging. *Nature, 375*(6527), 139-141.

Tootell, R. B., Reppas, J. B., Kwong, K. K., Malach, R., Born, R. T., Brady, T. J., *et al*. (1995b). Functional analysis of human MT and related visual c ortical areas using magnetic resonance imaging. *J Neurosci, 15*(4), 3215-3230.

Treue, S., & Martinez Trujillo, J. C. (1999). Feature-based attention influences motion processing gain in macaque visual cortex. *Nature, 399*(6736), 575-579.

Treue, S., & Maunsell, J. H. (1996). Attentional modulation of visual motion processing in cortical areas MT and MST. *Nature, 382*(6591), 539-541.

Treue, S., & Maunsell, J. H. (1999). Effects of attention on the processing of motion in macaque middle temporal and medial superior temporal visual cortical areas. *J Neurosci, 19*(17), 7591-7602.

Ungerleider, L. G., & Mishkin, M. (1982). Two cortical visual systems. *Analysis of visual behavior (Ingle, D.J., Goodale M.A. & Mansfield R.J.W., eds)*, 549-586.

Urgesi, C., Moro, V., Candidi, M., & Aglioti, S. M. (2006). Mapping implied body actions in the human motor system. *J Neurosci, 26*(30), 7942-7949.

van Boxtel, J. J., van Ee, R., & Erkelens, C. J. (2006). A single motion system explains human speed perception. *J. Cogn. Neurosc., in press*.

van de Grind, W. A., van der Smagt, M. J., & Verstraten, F. A. (2004). Storage for free: A surprising property of a simple gain-control model of motion aftereffects. *Vision Res, 44*(19), 2269-2284.

van de Grind, W. A., van Hof, P., van der Smagt, M. J., & Verstraten, F. A. (2001). Slow and fast visual motion channels have independent binocular-rivalry stages. *Proc Biol Sci, 268*(1465), 437-443.

van der Smagt, M. J., Verstraten, F. A., & van de Grind, W. A. (1999). A new transparent motion aftereffect. *Nat Neurosci, 2*(7), 595-596.

van Gelderen, P., Ramsey, N. F., Liu, G., Duyn, J. H., Frank, J. A., Weinberger, D. R., *et al*. (1995). Three-dimensional functional magnetic resonance imaging of human brain on a clinical 1.5-t scanner. *Proc Natl Acad Sci U S A, 92*(15), 6906-6910.

van Wezel, R. J., & Britten, K. H. (2002a). Multiple uses of visual motion. The case for stability in sensory cortex. *Neuroscience, 111*(4), 739-759.

Van Wezel, R. J. A., & Britten, K. H. (2002b). Motion adaptation in area MT. *J Neurophysiol, 88*(6), 3469-3476.

Vanduffel, W., Fize, D., Peuskens, H., Denys, K., Sunaert, S., Todd, J. T., *et al*. (2002). Extracting 3d from motion: Differences in human and monkey intraparietal cortex. *Science, 298*(5592), 413-415.

Verstraten, F. A. J., van der Smagt, M. J., Fredericksen, R. E., & van de Grind, W. A. (1999). Integration after adaptation to transparent motion: Static and dynamic test patterns result in different aftereffect directions. *Vision Res, 39*(4), 803-810.

Verstraten, F. A. J., van der Smagt, M. J., & van de Grind, W. A. (1998). Aftereffect of high-speed motion. *Perception, 27*(9), 1055-1066.

Worsley, K. J. (1994). Local maxima and the expected euler characteristic of excursion sets of chi square, f and t fields. *Advances in applied probability*, 13-42.

Xiao, D. K., Marcar, V. L., Raiguel, S. E., & Orban, G. A. (1997). Selectivity of macaque MT/v5 neurons for surface orientation in depth specified by motion. *Eur J Neurosci, 9*(5), 956-964.

Xiao, D. K., Raiguel, S., Marcar, V., Koenderink, J., & Orban, G. A. (1995). Spatial heterogeneity of inhibitory surrounds in the middle temporal visual area. *Proceedings of the National Academy of Sciences of the United States of America, 92*(24), 11303-11306.

Zaksas, D., & Pasternak, T. (2005). Area MT neurons respond to visual motion distant from their receptive fields. *J Neurophysiol, 94*(6), 4156-4167.

Zeki, S. (1993). A vision of the brain.

Zeki, S. M. (1974). Functional organization of a visual area in the posterior bank of the superior temporal sulcus of the rhesus monkey. *J Physiol, 236*(3), 549-573.

Zeki, S. M. (1978). Uniformity and diversity of structure and function in rhesus monkey prestriate visual cortex. *J Physiol, 277*, 273-290.

Verwerking van echte en geïmpliceerde beweging

(Nederlandse samenvatting)

Wanneer we een foto van een persoon zien, herkennen de meeste van ons of de persoon op de foto rende terwijl de foto gemaakt werd of dat deze persoon stil stond of zat of lag. De foto bevat echter geen echte beweging, alleen beweging geïmpliceerd door de houding van de persoon. Fotograven, schilders, beeldhouwers en andere kunstenaars zijn zeer succesvol in het overbrengen van een gevoel van dynamiek met deze geïmpliceerde beweging, ook al is hun werk statisch. Een voorbeeld hiervan is het beeld op de voorkant van dit proefschrift. Hoewel het beeld zowel in realiteit als op de foto niet beweegt, zullen de meeste mensen het toch direct als een rennend paard met amazone herkennen en misschien zelfs een gevoel van dynamiek ervaren. In dit proefschrift wordt de verwerking van geïmpliceerde beweging door de hersenen bestudeerd en vergeleken met de verwerking van echte beweging. Door het vergelijken van beide processen en door te onderzoeken of, hoe en waarom integratie van beiden plaats vind, kunnen we een beter beeld krijgen van hoe een “gevoel” van beweging ontstaat na het zien van geïmpliceerde beweging in statische beelden. Daarnaast leren we meer over hoe informatie van verschillende (visuele) modaliteiten in onze hersenen gecombineerd worden.

Studies van Senior en zijn collega’s (2000) en van Kourtzi en Kanwisher (2000), waarbij hersenactiviteit werd gemeten m.b.v. fMRI, suggereren dat het zien van foto’s met geïmpliceerde beweging (bijvoorbeeld een hardloper of een kopje dat van een tafel valt) een sterkere activiteit veroorzaakt in specifieke dorsale hersengebieden in vergelijking met het zien van foto’s van dezelfde personen of voorwerpen zonder geïmpliceerde beweging (zittend persoon of kopje op de tafel). Vooral in de hersengebieden rondom de “middle temporal” cortex (MT) was deze verhoogde activiteit zeer duidelijk. Dit was een wonderlijke vondst. De dorsale visuele gebieden en met name MT staan erom bekend dat ze voornamelijk betrokken zijn bij het verwerken van echte beweging, terwijl van de statische vorminformatie die in de foto’s aanwezig was gedacht werd dat deze in de ventrale visuele gebieden verwerkt werden. Figuur 1 van de Engelstalige introductie illustreert hoe visuele informatie enigszins gescheiden verwerkt wordt door een ventraal pad (ook wel “wat” pad of “perceptueel” pad genoemd) en een dorsaal pad (ook wel “waar” pad of “actie” pad genoemd). Hoewel een activering van deze dorsale bewegingsgevoelige gebieden het “bewegingsgevoel” bij het zien van geïmpliceerde beweging kan verklaren, roept dit de vraag op hoe de statische vorminformatie in deze dorsale gebieden terecht kan komen.

Vertraagde respons op geïmpliceerde beweging

Hersenactiviteit kan behalve spatieel (waar) ook temporeel (wanneer) bekeken worden. Met een elektro-encefalogram (EEG) kan hersenactiviteit in de tijd heel nauwkeurig gemeten worden. Door het meten van een EEG op verschillende plekken op de scalp kan m.b.v. een bronmodel ook bepaald worden welk deel van de hersenen verantwoordelijk is voor de activering. Hoewel een bronlokalisatie van een EEG signaal spatieel niet zo nauwkeurig is als een fMRI meting, kan met deze bepaling wel vrij nauwkeurig bepaald worden of twee responsies uit hetzelfde hersengebied stammen of juist uit andere gebieden. In hoofdstuk 1 werd de EEG respons van mensen op geïmpliceerde beweging gemeten. Hiervoor werd zowel de respons op foto's met geïmpliceerde beweging (rennende mensen) als zonder geïmpliceerde beweging gemeten (stilstaande mensen). Het verschil in respons op deze foto's werd gedefinieerd als geïmpliceerde bewegingsresponse. Door de respons op stilstaande mensen af te trekken van de respons op rennende mensen worden namelijk responsies op gemeenschappelijke aspecten van de foto's (zoals bijvoorbeeld gezichten) verwijderd en blijft voornamelijk de respons op de aanwezigheid van geïmpliceerde beweging over. De respons op geïmpliceerde beweging bleek maximaal te zijn rond 300 ms na aanvang van de stimulus. Bronlocalisatie liet zien dat deze respons uit een dorsaal gebied kwam dat ook een response op echte beweging gaf. De respons op echte beweging was echter zo'n 100 ms sneller dan de respons op geïmpliceerde beweging. Hieruit kan geconcludeerd worden dat de geïmpliceerde bewegingsinformatie via een langer traject de dorsale bewegingsgevoelige gebieden bereikt dan echte beweging. Dit is in overeenstemming met een verwerking van geïmpliceerde beweging ventrale visuele gebieden die vervolgens projecteren op dorsale gebieden. Deze projectie zou via de superiore temporale sulcus (STS) kunnen lopen, die een verbinding tussen dorsale en ventrale (temporale) gebieden vormt. Deze route is langer dan het verwerkingspad van echte beweging via de dorsale gebieden, hetgeen in overeenstemming zou kunnen zijn met de latere respons op geïmpliceerde beweging.

Interacties tussen echte en geïmpliceerde beweging

Hoewel zowel uit de bronlocalisaties van het eerste hoofdstuk en uit de fMRI studies van Kourtzi en Kanwisher (2000) en van Senior et al (2000) blijkt dat echte en geïmpliceerde beweging in een gemeenschappelijk hersengebied (mogelijk MT) verwerkt worden, hoeft dat niet te betekenen dat dezelfde neuronen in dat gebied betrokken zijn bij het verwerken van beide typen bewegingen. Het zou ook kunnen dat in dat gebied minstens twee verschillende populaties neuronen aanwezig zijn, een groep voor echte beweging en een

groep voor geïmpliceerde beweging. Ook zouden deze twee groepen wel in aparte gebiedjes kunnen liggen, maar zo dicht bij elkaar dat ze niet te onderscheiden zijn. Om dit te onderzoeken werd een EEG experiment uitgevoerd dat in hoofdstuk 2 beschreven wordt. Het onderzoek was gedeeltelijk identiek aan de EEG metingen die in hoofdstuk 1 beschreven worden, maar had een belangrijke toevoeging. Net als in hoofdstuk 1 werd de EEG gemeten terwijl vrijwilligers foto's van mensen met en zonder geïmpliceerde beweging zagen, maar nu werd elke foto voorafgegaan aan een korte periode waarin een patroon werd gepresenteerd. Dit patroon kon naar links of naar rechts bewegen, of stilstaan. De voorafgaande beweging had als doel om bewegingsgevoelige neuronen te adapteren, oftewel minder gevoelig te maken. Het is bekend dat na adaptatie met echte beweging, de EEG respons op beweging vervolgens verminderd is. Indien echte en geïmpliceerde beweging (gedeeltelijk) door dezelfde neuronen worden verwerkt, kan verwacht worden dat adaptatie met echte beweging ook een modulatie van de geïmpliceerde bewegingsrespons zou geven. Dit blijkt ook zo te zijn. Na adaptatie met echte beweging is de respons op geïmpliceerde beweging (dus het verschil in respons op foto's met en zonder geïmpliceerde beweging) rond 300 ms na stimulus aanvang verminderd vergeleken met de respons op geïmpliceerde beweging voorafgegaan door een statisch patroon. Dit adaptatie effect bleek ook nog eens richtingsafhankelijk te zijn. Wanneer de echte en geïmpliceerde beweging in dezelfde richting waren, was de vermindering van de respons op geïmpliceerde beweging groter dan wanneer de echte en geïmpliceerde beweging in tegenovergestelde richting waren. Dit is volledig in overeenstemming met het richtingsafhankelijke adaptatie effect dat al eerder gevonden was voor echte beweging, ook daarbij was de adaptatie sterker wanneer zowel de voorafgaande als de test beweging in dezelfde richting waren. Dit experiment is een sterke indicatie dat echte en geïmpliceerde beweging deels door dezelfde neuronen verwerkt worden en dat de interactie tussen deze twee typen beweging richtingsafhankelijk is.

Corticale paden voor verwerking van echte beweging

Voor inzicht in de verwerking van geïmpliceerde beweging, is het van belang om een goed beeld te hebben van de verwerking van echte beweging. Hoewel algemeen aangenomen wordt dat beweging grotendeels via het dorsale visuele pad wordt verwerkt, zijn er aanwijzingen dat dit proces onderverdeeld is in twee kanalen: een kanaal voor snelle beweging en een kanaal voor langzame beweging. Om deze twee kanalen van elkaar te scheiden, werd in hoofdstuk 3 wederom gebruikt gemaakt van bewegingsadaptatie in een EEG experiment. Dit keer werd niet alleen van een richtingsafhankelijk adaptatie effect gebruik gemaakt, maar ook van een snelheidsafhankelijk effect. Er werd zowel met een hoge als met een

langzame snelheid geadapteerd en getest. De adaptatie was maximaal wanneer zowel de richting als de snelheid van de adaptatie en de test overeen kwamen. Dit geeft aan dat er minstens twee populaties bewegingsgevoelige neuronen zijn (die voor twee kanalen kunnen staan), een populatie voor verwerking van beweging met lage snelheid en een populatie voor beweging met hoge snelheid. Met behulp van bronlocalisatie werden de hersengebieden die verantwoordelijk waren voor de adaptatie effecten bepaald. Hieruit bleek dat het adaptatie effect kon worden verdeeld in een richtingsafhankelijke en een richtingsonafhankelijke adaptatie. De richtingsafhankelijke adaptatie kwam voor beide snelheden voort uit eenzelfde dorsaal hersengebied. Voor de richtingsonafhankelijke adaptatie bleken echter verschillende hersengebieden voor beide snelheden betrokken te zijn. De relatieve locaties van de activeringen gaven aan dat snelle beweging via het dorsale visuele pad verwerkt wordt, terwijl langzame beweging zowel door het dorsale als via het ventrale pad verwerkt wordt. De dorsale verwerking lijkt richtingsafhankelijk te zijn, terwijl de ventrale verwerking richtingsonafhankelijk is. Langzame beweging en geïmpliceerde beweging zouden dus deels hetzelfde ventrale pad kunnen volgen. Het is echter wel onwaarschijnlijk dat de respons op geïmpliceerde beweging die in hoofdstukken 1 en 2 genoemd werd van deze ventrale gebieden afkomstig is, aangezien de geïmpliceerde bewegingsrespons richtingsafhankelijk is (als aangetoond met adaptatie) terwijl de ventrale echte bewegingsgebieden dat niet zijn. De dorsale bewegingsgevoelige gebieden zijn een veel betere kandidaat voor de locatie van de integratie tussen echte en geïmpliceerde beweging.

Geen bewijs voor verwerking van geïmpliceerde beweging in MT en MST

Op basis van de bronlocaties uit de eerste 3 hoofdstukken en de fMRI resultaten van Kourtzi en Kanwisher (2000) en van Senior et al (2000), lijkt de beweginsgevoelige “middle temporal” (MT) cortex samen met de nabijgelegen “medial superior temporal” (MST) cortex een goede kandidaat voor de integratie van echte en geïmpliceerde beweging. Om de verwerking van geïmpliceerde beweging en integratie van echte en geïmpliceerde beweging op cel niveau te meten, werd in hoofdtuk 4 in twee experimenten bij MT en MST cellen van wakkere rhesus makaken (*Macaca mulatta*) het voorkomen van actiepotentialen (vuurfrequentie) gemeten. Allereerst werd de vuurfrequentie van cellen gemeten terwijl foto’s met en zonder geïmpliceerde beweging in het receptieve veld van deze cellen (het stukje van het gezichtsveld waarin de cel gevoelig is) werden getoond. Hoewel een aantal cellen een lichte voorkeur had voor foto’s van rennende mensen boven foto’s van stilstaande, bleek deze trend afwezig voor foto’s van apen met en zonder geïmpliceerde beweging. Bovendien leek de

voorkeur voor de rennende mensen verklaard te kunnen worden door verschillen in laag visuele aspecten, zoals oriëntatie en grootte van de stimulus en niet zozeer door de geïmpliceerde beweging.

In een tweede experiment werd getest of geïmpliceerde beweging de respons op echte beweging kan moduleren. Hiervoor werden de foto's in het midden van het gezichtsveld op de fovea aangeboden, terwijl in het receptieve veld van de cel een dynamisch ruis patroon aangeboden werd. Dit patroon lijkt een beetje op de sneeuw van een televisie met kapotte antenne of kabel. Hoewel het geen coherente beweging bevat, heeft zo'n ruispatroon wel veel incoherente beweging waar MT en MST cellen goed op reageren. Er bleek echter geen aanwijzing te zijn voor modulatie van de respons van MT en MST cellen op echte beweging door het aanbieden van geïmpliceerde beweging op de fovea.

Op grond van deze resultaten lijken MT en MST niet de corticale gebieden te zijn waarin integratie van echte en geïmpliceerde beweging plaats vind. Om dit bij mensen te toetsen en om te zoeken naar gebieden die verantwoordelijk kunnen zijn voor de respons op geïmpliceerde beweging en de integratie van de twee bewegingstypen, werd een humaan fMRI onderzoek uitgevoerd dat is beschreven in hoofdstuk 5. De fMRI resultaten voor MT en MST kwamen sterk overeen met de celresponsies die in hoofdstuk 4 gevonden waren. Wederom was er een voorkeur voor foto's met vs. zonder geïmpliceerde beweging, maar leek deze voorkeur verklaard te worden door verschillen in laag visuele aspecten, zoals oriëntatie en stimulus grootte. Een zoektocht naar activeringen op uitsluitend geïmpliceerde beweging en niet op stimulus grootte en oriëntatie leverde geen hersengebieden op. Dit hoeft niet perse te betekenen dat er geen populatie van cellen bestaat die uitsluitend op echte en geïmpliceerde beweging reageert. Het kan zijn dat deze cellen zo dicht bij andere cellen liggen, die wel gevoelig zijn voor oriëntatie en grootte, zodat alleen hun gezamenlijk respons op zowel geïmpliceerde beweging en laag visuele aspecten gemeten word. Ook kan het zijn dat deze cellen zowel op geïmpliceerde beweging en echte beweging alsook op laag visuele aspecten reageren, maar op verschillende tijden. Aangezien fMRI een lage temporele resolutie heeft, zouden deze responsies niet van elkaar te onderscheiden zijn. Om deze mogelijke hersengebieden op te sporen zou in de toekomst gebruik gemaakt kunnen worden van een adaptatie paradigma of van een techniek met zowel hoge spatiele als temporele resolutie. Deze argumenten gaan echter niet voor MT en MST op, aangezien in hoofdstuk 4 de responsies van veel cellen gescheiden konden worden van de responsies van andere cellen en aangezien deze metingen met een zeer hoge temporele resolutie gemeten waren en geen verschillen tussen laag visuele aspecten en geïmpliceerde beweging in de tijd lieten zien.

Tot slot

In dit proefschrift werd de (corticale) verwerking van echte en geïmpliceerde beweging onderzocht. Uit EEG metingen blijkt dat echte en geïmpliceerde beweging in de cortex worden geïntegreerd. Aangezien de respons van de cellen die hieraan ten grondslag liggen op geïmpliceerde beweging vertraagd is ten opzichte van de respons op echte beweging, is dit een sterke aanwijzing dat geïmpliceerde beweging via het ventrale visuele pad wordt verwerkt en vervolgens op dorsale bewegingsgevoelige gebieden wordt geprojecteerd. Echte beweging wordt voornamelijk via de dorsale route verwerkt, hetgeen een snellere respons zou kunnen verklaren. Echter, ook langzame beweging wordt deels via het ventrale pad verwerkt. Deze verwerking is echter sterk minder richtingsafhankelijk dan de dorsale verwerking en het is daarom niet waarschijnlijk dat de richtingspecifieke integratie van echte en geïmpliceerde beweging in ventrale gebieden gebeurt, maar meer waarschijnlijk in de dorsale bewegingsgevoelige gebieden. Hoewel MT en MST voor de hand liggende kandidaten zijn voor deze integratie, blijkt de respons op geïmpliceerde beweging in deze gebieden verklaard te kunnen worden door laag visuele verschillen tussen de foto's en niet met geïmpliceerde beweging zelf. Met humane fMRI werd geen locatie gevonden waar deze integratie plaats vindt.

De integratie van echte en geïmpliceerde beweging zoals aangetoond met EEG, is een goede verklaring voor het gevoel van beweging dat wij kunnen ervaren wanneer we een foto, schilderij of beeld met geïmpliceerde beweging aanschouwen. Hoewel we dit gevoel misschien zeer waarderen, lijkt dit vanuit evolutionair standpunt niet erg belangrijk te zijn. Toch kan perceptie van geïmpliceerde beweging en met name de integratie ervan met echte beweging veel overlevingsvoordeel opleveren. Het zou ertoe kunnen leiden dat bewegingsgevoelige neuronen extra gevoelig worden voor de beweging van een mens of dier t.o.v. bewegingen in de omgeving, waardoor bijvoorbeeld een rennende muis tussen de beweging van waaiende losse bladeren extra opvalt. Ook kan geïmpliceerde beweging helpen bij het visueel volgen van een rennend dier, wanneer het beeld wordt onderbroken door obstakels zoals bomen of door oogknipperingen.

Dankwoord / Acknowledgements

Veel mensen hebben in meer of mindere mate bijgedragen aan dit proefschrift, waarvoor ik zeer dankbaar ben. Allereerst mijn co-promoter Richard van Wezel die als dagelijkse begeleider altijd klaar stond met hulp en advies, en bovendien ook nog van het Nest een aangename en levendige werkomgeving wist te maken. Dankjewel Ries. Ook Tjeerd Jellema had als co-promoter altijd tijd voor wijze raad en een leuk gesprek, zij het over een wat grotere geografische afstand. De biologie/psychologie discussies waar de werkbesprekingen met ons drieën vaak in uitmondden, waren zeer vermakelijk maar ook verrassend verfrissend en zinvol. Ook beide promotoren Bert van den Berg en Leon Kenemans ben ik zeer dankbaar voor hun bijdragen. Ik heb groot respect voor de wijze waarop jullie oog voor detail kunnen houden in het toch wel zeer uitlopende werk van jullie promovendi, zeker wanneer zo'n promovenda een poster of artikel opstuurt met als aanhef: "ik weet dat het kort dag is, maar dit moet eigenlijk vandaag nog weg..."

Maarten van der Smagt beschouw ik als een officieuze derde co-promoter. Onze samenwerking was niet alleen heel nuttig (zie hoofdstuk 3), maar ook erg leuk. Ik kom zeker nog eens langs voor een wedstrijdje electrodes plakken. Dank ook zeker voor degene die me het electrodes plakken en de algehele EEG techniek in de eerste plaats heeft geleerd, Rob van der Lubbe. Hoewel ik aanvankelijk wat gespannen je commentaar op manuscripten tegemoet zag vanwege je vermogen de zwakke plekken exact op te sporen, bleek al snel dat dit kritische commentaar de stukken flink ten goede kwam.

Aangezien ik de meeste tijd met de neurobiologen heb doogebracht, lijkt het me toepasselijk deze collega's het eerst te bedanken. Jacob en Andre waren zeer leuke Nest-kamergenoten waarbij de gespreksonderwerpen nooit op leken te raken. Jacob droeg bovendien ook veel bij aan de extracellulare metingen en niet alleen vanwege zijn "stimulerende" vermogen. Mathijs droeg als fMRI expert veel bij aan dit proefschrift en weet de paardenplaatjes in dit proefschrift vast ook zeer te waarderen. Zeer belangrijk waren ook de stage en scriptie studenten; Alexander werkte als mijn eerste stage student aan oogbewegingen en ik vind het erg leuk hem nu weer als collega in Rotterdam te hebben, Frederiek en Marjolein blonken uit in het EEG onderzoek en psychofysica en waren bijzonder gezellig om mee samen te werken, Neeltje schreef misschien wel de allerbeste scriptie die ik ooit gelezen heb en Chris heeft enkele mooie psychofysica experimenten opgezet en is nu goed op weg als aio. Lonneke was niet alleen een bijzonder leuke collega met een onverzettelijke missie om eenzame collega's aan het lunchen te krijgen, ze is ook een supergoede vriendin. Roger maakte het laatste halve jaar in het

Kruyt erg gezellig, hoewel de plantachtigen op onze kamer daar misschien anders over dachten. Wim van de Grind en Martin Lankheet gaven regelmatig advies op manuscripten, data, onderzoeksvoorstellen en andere belangwekkende zaken in het (wetenschappelijke) leven. Rob `vrije-wil-bestaat-niet´ Peters en Frank `check-recheck-double-check´ Bretschneider hebben sinds mijn eerste stage jaren geleden altijd goede raad gegeven, waarvoor ik ze zeer dankbaar ben. Mieke, Ildiko, Bart en Janos gaven het goede voorbeeld als succesvolle promovendi. Jan, Michiel, Ervin, Anna, Jaap, Douwe, Ger-Jan en Erik (bedankt voor de cursus: hoe wordt ik een succesvolle sollicitant?) zorgden voor gezelligheid in zowel Kruyt als Nest, samen met de vele studenten die bij de groep stage liepen, ik noem er een paar; Anneke, Michiel, Daan, Sigrid, Martijn, Marijn, Roxane, Tycho, Wouter, Joren, Miesje, Marieke, Annika, Nick en Helene, dankjulliewel.

De fysici die naar de lunchbesprekingen kwamen voor hun verfrissende input, met name Raymond, Casper, Tomas, Jeroen, Gijs, Allard en Elena.

Onmisbaar waren Theo, Henk, John en Hans voor het verzorgen van de dieren. Theo was daarnaast ook een geweldig luisterend oor met altijd wijze adviezen en nimmer schunnige poëzie (te laat, te laat....). Ed, Gerard, Wim Loos en de Robben zorgden voor een perfecte technische ondersteuning. Dank ook aan Miriam, Antje en Maartje voor het office managen.

Verder wil ik alle psychonomen bedanken, met name kamergenoten Jeroen duty-cycle Benjamins en Katinka; werkbesprekers Frans, Chris, Ignace, Susan, Marieke, Tobias en Tanja; Peter voor technische ondersteuning en verder Joke, Bas, Bjorn, Titia, Nisan, Hubert, Ilse, Helen, Christine, Ryota, Veronica, Leonie en Ans.

Ook de psycho-farmacologen ben ik dankbaar voor hun hulp en de leuke tijd die ik in het Went had, met name Annelies, Tineke, Elise, Joris, Judy, Koen, Gert, Marga, Marco, Berend en Ed.

Het Helmholtz instituut heeft gezorgd voor een aantal interessante cursussen, retraites en lezingen.

Dank ook aan de vele proefpersonen.

Dank aan Frits Kindt (fotografie), Jeroen Warnaar (fotografie en vormgeving), Alyanne de Haan (beeldverwerking) en Paul den Hertog (printpartners Ipskamp) zonder wie dit boekje een stuk minder mooi zou zijn.

Also many thanks to the people in David Perrett's lab in St. Andrews, especially to Dave himself, Nick Barraclough, Dengke Xiao and Mike Oram. I've had a great time in Scotland and have enjoyed our collaboration very much. While I've switched to English I'll also take the oppurtunity to thank my great Australian friends Carolyn and Jessica, but also Mark, the whole Springbett family and the Neuroscience lab, especially Lyn, Jenny and Sarah.

Verder wilde ik Gerard Borst en mijn nieuwe collega´s in Rotterdam bedanken. Het werkte heel motiverend om te weten dat ik na het afronden van dit proefschrift weer aan een nieuw uitdagend onderwerp in een leuke groep kon beginnen.

Hierbij wil ik ook graag mijn Nederlandse vrienden bedanken voor de lol en steun die ze al jaren geven. Kaa, Ak en Lilian voor alle koffie-ochtenden en vakantie avonturen, Marjelle en Floor voor de cultureel verantwoorde films, fitness en het bespreken van het aio leven, jullie zijn geweldig. Johan die altijd klaar stond om enge donkere kruipruimtes te trotseren. Pol en Mieke staan garant voor geweldige boswandelingen en geweldige maaltijden waarna minstens 5 balansdagen vereist zijn. Chris voor het delen van een sushi-verslaving. De IBB'ers voor een geweldige tijd, met name Rianneke, Aukje, Judith, Annet, Jeroen, Job, Staf, Monique en Demis. Geert en Jojee voor overzeese wijze postdoc raad. Olaf, voor een luisterend oor in de beginperiode van dit aio-pad. Jesse en Ingrid voor alweer een ellenlange vriendschap. Cor, voor alle liedjes en wijze lessen. Sarah Engels-Greer en Alexandra Flohr voor hun lessen en choreografieën waarin de samenwerking van geïmpliceerde en echte beweging in de dans heel inspirerend werkte. Ook dank aan mijn mededansers, met name de harde maandagavond kern: Wieke, Saskia, Britt, Laurien, Anne-Marit, Jeannette, Paula en Joke.

Mijn paranimfen, Annemieke en Jacob.

Frans, Anneke, Bas en Pebbles Warnaar/Kok.

Mijn vader en moeder (ookal heb ik me niet aan je matrix gehouden papa) en Annemieke, Chino, Indy, Marjoke, Max, Michel, Romy, Vera en Zoëy voor alle steun, liefde en plezier.

Mijn Jeroen Warnaar.

CURRICULUM VITAE

Jeannette Lorteije werd op 6 oktober 1977 geboren te Waalre. In 1996 behaalde zij haar VWO diploma op het St. Joris college in Eindhoven. Van 1996 tot en met 2001 studeerde zij biologie aan de Universiteit Utrecht. Tijdens haar studie liep zij stage bij de vakgroep Neuro-Ethologie (de huidige leerstoelgroep Functionele Neurobiologie) van de Universiteit Utrecht; bij het Konrad Lorenz Forschungsstelle (KLF) in Gruenau im Almtal in Oostenrijk; en bij de vakgroep Neuroscience aan de University of Western Australia (UWA) in Perth, Australië. Na haar afstuderen trad zij in 2002 in dienst als promovenda bij de vakgroep Functionele Neurobiologie van de faculteit biologie aan de Universiteit Utrecht, waarbij ze begeleid werd door dr. Richard van Wezel, dr. Tjeerd Jellema, prof. dr. Bert van den Berg en prof. dr. Leon Kenemans. Daarnaast was zij van januari 2006 tot juli 2006 aangesteld als onderzoeker bij dr. Maarten van der Smagt van de capaciteitsgroep Psychonomie bij de faculteit Sociale Wetenschappen van de Universiteit Utrecht. Sinds november 2006 is zij aangesteld als postdoc bij prof. dr. Gerard Borst van de afdeling Neurowetenschappen aan de Erasmus Universiteit te Rotterdam.

Publications

Articles

Lorteije, J.A.M., Bretschneider, F., Klaver, I., Peters, R.C.
Psychophysical test for bimodal integration of electroreception and photoreception in the catfish *Icatlurus nebulosus* LeS. Netherlands J. Zool., Volume 50, Number 3, 2000, pp. 389-400(12)

Lorteije, J. A. M., Kenemans, J. L., Jellema, T., van der Lubbe, R. H. J., de Heer, F., & van Wezel, R. J. A. (2006). Delayed response to animate implied motion in human motion processing areas. *J Cogn Neurosci, 18*(2), 158-168.

Lorteije, J. A. M., Kenemans, J. L., Jellema, T., van der Lubbe, R. H. J., Lommers, M., & van Wezel, R. J. A. (in Press). Adaptation to real motion reveals direction selective interactions between real and implied motion processing. *J Cogn Neurosci*.

Articles submitted for publication, or in preparation

Jellema, T., Lorteije, J., Van Schaffelaar, E., De Haan, E. H. F., Van Engeland, H. & Kemner, C. Failure to automate the processing of social cues in autism. Neuropsychologia (under revision).

Lorteije J.A.M., van Wezel R.J.A. & van der Smagt M.J. Disentangling neural structures for processing of high and low speed motion (submitted)

Lorteije J.A.M., Barraclough N.E., Jellema T., Duijnhouwer J., Xiao D.K., Lankheet M.J.M., Perrett D.I. & van Wezel R.J.A. No evidence for animate implied motion processing in macaque areas MT and MST (submitted)

Lorteije J.A.M., Raemaekers M. & van Wezel R.J.A. Visual features underlying the implied motion response in human middle temporal cortex (in preparation)

Conference proceedings, refereed abstracts

Jellema, T., Lorteije, J. A. M., Van Rijn, S., Van ‘t Wout, M., De Heer, F., De Haan, E. H. F., Van Schaffelaar, E., Kemner, C., Van Engeland, H. (2004). Failure to automate the semantic processing of social cues in autism. Perception, 33, 101 (Suppl.).

Lorteije, J.A.M., Bretschneider, F., Klaver, I., Peters, R.C.
Psychophysical test for bimodal integration of electroreception and photoreception in the catfish *Icatlurus nebulosus* LeS. Netherlands J. Zool., Volume 50, Number 3, 2000, pp. 389-400(12)

Lorteije, J. A. M., Kenemans, J. L., Jellema, T., Van der Lubbe, R. H. J., De Heer, F., Van Wezel, R. J. A. (2004). Temporal characteristics of neuronal sources for implied motion perception. Perception, 33, 100 (Suppl.).

Lorteije, J. A, M., Kenemans, J. L., Jellema, T., Van der Lubbe, R. H. J, Lommers, M., Van Wezel, R. J. A. (2005). Motion adaptation modulates implied motion processing. Society for Neuroscience.

Lorteije, J.A.M., van Wezel R.J.A., Lankheet M.J.M.(2002). Perception of eye positions. Perception, ECVP02 (Suppl.)